

Bioengineering approaches to emulate the stem cell niche

THÈSE N° 6502 (2015)

PRÉSENTÉE LE 6 FÉVRIER 2015

À LA FACULTÉ DES SCIENCES DE LA VIE

UNITÉ DU PROF. LUTOLF

PROGRAMME DOCTORAL EN BIOTECHNOLOGIE ET GÉNIE BIOLOGIQUE

ÉCOLE POLYTECHNIQUE FÉDÉRALE DE LAUSANNE

POUR L'OBTENTION DU GRADE DE DOCTEUR ÈS SCIENCES

PAR

Sylke HÖHNEL

acceptée sur proposition du jury:

Prof. A. Radenovic, présidente du jury

Prof. M. Lütolf, directeur de thèse

Prof. S. Méndez-Ferrer, rapporteur

Prof. O. M. Naveiras Torres-Quiroga, rapporteuse

Prof. C. Werner, rapporteur



ÉCOLE POLYTECHNIQUE
FÉDÉRALE DE LAUSANNE

Suisse
2015

"It always seems impossible until it's done."
Nelson Mandela

ACKNOWLEDGEMENTS

With great pleasure, I want to thank the many people who helped create this thesis.

It is difficult to overstate my gratitude to my thesis advisor Matthias Lutolf, who allowed me to learn and apply science in his laboratory, which has been a vibrant niche over the past five years. Thank you for your guidance, continuous support and pushing me to reach my goals.

To the members of my thesis jury, Carsten Werner and Simón Méndez-Ferrer for your help, insightful discussions as well as the privilege of your participation. And to Olaia Naveiras for being more than a committee member; thank you for your enthusiasm and encouraging input; you are a true inspiration.

To scientists and professionals who contributed their time, extraordinary work and expert advice: Miguel Garcia and Loïc Tauzin (Flow Cytometry Core Facility, EPFL), Jessica Sordet-Dessimoz and Gianni Mancini (Histology Core Facility, EPFL), Cyrille Hibert and Joffrey Pernollet (CMi, EPFL), Fernando Cortes Salazar and Andreas Lesch (LEPA, EPFL) and Mattia Marelli.

This road would have been only half as fun had it not been for the amazing people who shared it with me: Simone, Yoji, Lilia, Vincent, Adrian, Marlen, Massi, Mukul, Gena, Josefine, Vasco, Nicola, Evangelos, Yuya, Aline, Samy, Steffen, Marta, Kasia and Stefan.

A special thank you to Nikolce for always lending an ear to everyone (and their mother) and for being one of my proofreading b****es (buddies); to Laura for creating the best German compound words this world has ever seen (Stammzellnischinteraktionen) and to Andrea for your precious help and friendship.

To Nath for every second of practical and emotional support you gave me. Thank you for sharing my passions and dreams.

To Salim for being the best friend one could wish for and the most awesomest person in the whole wide world. Ares you are awesome too, especially when you tell Confucius jokes.

To my friends in Switzerland and abroad, who continue to keep me in their mind while I might be out of sight: Jo'an, Rosa, Toto, Marcus, Möbel, Manu, Tvisha, Philipp, Keks – thank you.

Last, and most importantly, I wish to thank my family. To my parents and grandparents, who raised me, taught me, supported me and loved me. To my sister, who has always been the person I look up to. To you I dedicate this thesis.

SUMMARY

Stem cells hold tremendous potential for clinical therapies. However, there remains significant need for better *ex vivo* culture and manipulation methods. On the one hand, many tissue-specific stem cells cannot be propagated without causing rapid deviations in cellular phenotype. On the other hand, outside of a developing organism, it remains very difficult to differentiate stem cells into mature functional cell types. Such protocols could for example be used to build more effective and predictive pre-clinical models that would reduce or even replace animal studies.

Manipulating stem cells *in vitro* in a controlled manner requires a thorough understanding of the complex cocktail of cell-extrinsic factors originating from the niche, and the cell-intrinsic signaling pathways that are triggered by stem cell-niche interactions. Many stem cell niches remain ill defined and little is known about how niche cues such as mechanical constraints and biochemical signals converge to regulate stem cell behavior. Since stem cell-niche interactions are often difficult to elucidate using *in vivo* models, this thesis explored a new generation of microsystems to emulate stem cell niches.

In the first part of this thesis, a customizable microarray platform was developed in order to systematically study how biochemical signals together with substrate stiffness regulate stem cell behavior. We thus screened combinations of 12 different proteins over three discrete substrate stiffnesses in order to study their effect on the adipogenic differentiation of CD105^{pos} CD146^{pos} human mesenchymal stem cells (MSCs). These cells and their differentiated progenies are of high therapeutic relevance for skeletal tissue regeneration and have also been implied as niche-modulating neighbors of hematopoietic stem cells (HSCs) in the bone marrow. Using a combinatorial *in vitro* niche screening approach, substrate stiffness was found to be the major determinant of the frequency of lipid accumulation in MSCs, while the lipid content was found to be strongly driven by the biochemical context.

To further understand how niche cells together with stem cells self-organize to form a functional tissue, three-dimensional (3D) organ-mimicking structures from spheroids of pluri- and multi-potent stem cells have been developed. These emerging systems, termed organoids, are expected to provide instrumental insights into tissue or organ development and could be of great use for disease-specific drug screenings and, in the future, to generate clinically transplantable tissues. Current protocols for organoid generation are tedious, highly inefficient and irreproducible. To address this problem, in the second part of this thesis a high-density poly(ethylene glycol) (PEG)-based hydrogel microarray of U-bottom wells was

developed. This system was used for the high-throughput aggregation of one or multiple cell types and to allow their long-term culture. In contrast to state-of-the-art microwell systems, U-bottom microwells offer highly reproducible cell aggregation, a natural shape to maintain spheroid morphologies and freedom of substrate choice to enable the use of hydrated matrices that enhance long-term cell survival. Furthermore, the fabrication in hydrated substrates enables the *in situ* manipulation of spheroids through biomolecule delivery through the gel network. This was demonstrated by conducting 3D co-cultures of the hematopoiesis-supportive cell line OP9 together with HSCs. The interaction of these two cell types was illustrated by the inhibitory effect of hematopoietic cells on the adipogenic differentiation of OP9 in spheroid cultures, termed here 'lipospheres'. Furthermore, using this approach, it was shown that primary human MSCs could be expanded from single cells as uniform spheroids, termed mesenspheres. The morphological appearance of mesenspheres, which is rapidly lost in direct co-cultures on conventional tissue culture plastic surfaces, could be preserved in this novel micro-engineered culture system.

Establishing meaningful *in vitro* co-culture models requires knowledge about the phenotypic identity of both stems and niche cells. While such markers are generally under investigation, they are often insufficient to define and isolate a desired cell population to homogeneity. Therefore, in the last part of this thesis, an alternative approach to identify putative niche candidate cells was developed. Specifically, SNAP-tag fusion proteins expressed on cellular membranes were targeted for the formation of covalent bonds between substrates that harbor the SNAP-tag substrate benzylguanine (BG). Immobilizing sufficient amounts of BG on cellular membranes is a mean to enabling cell-cell pairing as demonstrated by the covalent aggregation of microbeads carrying SNAP-tag and BG at high concentrations.

The artificial niche models developed in this study are broadly applicable to desired cellular systems in order to gain insight into the multifactorial composition and architectural organization of specific niches. The dissection and understanding of these microenvironmental regulators and integration into existing protocols is expected to advance stem cell biology by ultimately propagating stem cells *in vitro* for clinical applications.

Keywords: stem cell, niche, bone marrow, mesenchymal stem cell, hematopoietic stem cell, high-throughput, combinatorial screening, organoids, micro U-bottom, 3D, PEG, hydrogel, cell-pairing, SNAP-tag, benzylguanine

RÉSUMÉ

Un profond changement de paradigme va voir le jour dans le domaine biomédical grâce à l'utilisation sûre des cellules souches en thérapie cellulaire. Cependant, des efforts sont encore à fournir afin d'améliorer la culture et d'offrir un meilleur contrôle de ces cellules. En effet, la plupart des cellules souches spécifiques à un tissu donné ne peuvent, d'une part, pas être propagées sans une déviation conséquente du phénotype initial et sont, d'autre part, difficiles à différencier en types cellulaires fonctionnels et matures de manière homogène *in vitro*.

La manipulation contrôlée des cellules souches *ex vivo* demande une excellente connaissance de l'environnement complexe de facteurs extrinsèques ainsi que l'activation des cascades de signaux intrinsèques à la cellule, orchestrés par sa niche. Cette connaissance est très restreinte pour beaucoup de systèmes biologiques et que peu d'études ont tenté d'analyser l'impact des contraintes mécaniques et des signaux biochimiques sur le comportement de ces cellules. Etant donné que l'étude de ces interactions est souvent compliquée, voir impossible, en utilisant des modèles animaux, ce travail de doctorat présente une nouvelle génération de plateformes intégrées pouvant imiter le microenvironnement des cellules souches.

Dans la première partie de ce travail, une plateforme de microarray polyvalente a été développée pour étudier systématiquement l'effet de la combinaison de signaux biochimiques et mécaniques sur la régulation du comportement des cellules. Nous avons donc analysé l'effet de 12 protéines différentes en combinaison avec trois différentes rigidités de surface sur la différenciation de cellules souches mésenchymales (CSM) humaines CD105⁺ CD146⁺ en adipocytes. Ces cellules et leur descendance différenciée sont suggérées comme ayant un potentiel thérapeutique important pour la régénération des tissus squelettiques et étant les cellules principales composant la niche des cellules souches hématopoïétiques (CSH) dans la moelle osseuse. Nous avons pu alors observer que la rigidité de la surface est un facteur majeur influençant la fréquence d'accumulation de vésicules lipidiques dans les CSM, tandis que le contenu lipidique est influencé de manière significative par l'environnement biochimique.

Pour mieux comprendre comment les cellules de la niche se réorganisent avec les cellules souches pour former un tissu fonctionnel, une plateforme permettant la formation de structures tridimensionnelles ressemblant à des mini-organes à partir de cellules pluri- ou multipotentes a été développée. Ces structures, appelées organoïdes, sont suggérées comme cruciales pour mieux comprendre la physiologie des tissus ou organes, donnant ainsi un outil prédictif puissant pour les screening pharmacologiques et permettant la fabrication *in vitro* d'organes transplantables. Cependant, les protocoles actuels pour former ces organoïdes sont fastidieux,

inefficaces, et irreproductibles. Dans la deuxième partie de ce travail, nous avons donc développé une plateforme de micropuits en forme de U, à base d'hydrogel synthétique (poly(éthylène glycol), PEG) pour former et cultiver ces organoïdes de manière reproductible à haut débit. En comparaison avec les systèmes de micropuits conventionnels, notre plateforme offre une reproductibilité idéale de l'agrégation des cellules, une forme naturelle pour maintenir la morphologie de l'agrégat et le libre choix du substrat, comme des substrats hydratés, améliorant alors la viabilité des cellules sur le long terme. De plus, l'utilisation de substrats hydratés permet la manipulation des agrégats *in situ* par la perfusion locale de molécules à travers ces derniers. En choisissant de développer un système de co-culture tridimensionnelle de CSH en combinaison avec une lignée cellulaire supportant l'hématopoïèse, OP9, nous avons pu observer que l'interaction entre ces deux types cellulaires a un effet inhibiteur des CSH sur la différenciation adipeuse d'agrégats d'OP9. De plus, l'utilisation de cette plateforme nous a donné l'opportunité de croître des agrégats de cellules CSM primaires, appelés mésosphères, à partir d'une seule cellule. La morphologie d'origine de ces cellules, rapidement perdue conventionnellement, a donc pu être préservée avec cette nouvelle plateforme de culture.

L'établissement de systèmes de co-cultures robustes en 3D *in vitro* requiert une connaissance certaine de l'identité phénotypique des cellules souches d'intérêt ainsi que des cellules niches. Leur isolation respective en utilisant des marqueurs de surface est toujours imprécise et donne lieu à des populations très inhomogènes. Pour tenter d'améliorer ces protocoles d'isolation, nous avons développé, dans la dernière partie de ce travail, une approche alternative d'identification de potentielles cellules de la niche pour une certaine cellule souche. Nous avons utilisé la technologie des SNAP-tags en les exprimant à la surface des membranes cellulaires pour former une liaison covalente entre les cellules en contact. En immobilisant une quantité suffisante de substrat sur des billes artificielles en hydrogel, nous avons pu démontrer la possibilité de former des agrégats attachés de manière covalente.

Les modèles de niche artificiels développés dans le cadre de ce travail de doctorat sont facilement applicables à tout système biologique pour étudier l'organisation multifactorielle et architecturale de niches spécifiques. Nous sommes convaincu que l'étude systématique de ces régulateurs microenvironnementaux et l'intégration des protocoles existants sont la clé pour permettre la propagation des cellules d'intérêts *in vitro* ainsi que leur application en clinique.

Mots clés: cellules souches, niche, moelle osseuse, cellules souches mésenchymales et hématopoïétiques, haut-débit, screening combinatoire, organoïdes, micropuits en forme de U, 3D, poly(éthylène glycol), hydrogel, jumelage cellulaire, SNAP-tag, benzylguanine.

ZUSAMMENFASSUNG

Stammzellen bieten enormes Potential für klinische Therapien. Es besteht jedoch noch erheblicher Bedarf für *ex vivo* Kultur- und Manipulierungsmethoden. Einerseits können viele gewebespezifische Stammzellen nicht vermehrt werden ohne schnelle Abweichungen im Zellphänotyp zu verursachen. Andererseits ist es immer noch sehr schwierig Stammzellen außerhalb des sich entwickelnden Organismus in ausgereifte, funktionelle Zelltypen zu differenzieren. Solche Protokolle könnten zum Beispiel genutzt werden um effektivere und vorhersagbare vorklinische Modelle zu generieren, die Tierversuche reduzieren oder sogar gänzlich ersetzen könnten.

Stammzellen auf eine kontrollierte Art *in vitro* zu manipulieren erfordert ein tiefes Verständnis des komplexen Gemischs an zellextrinsischen Faktoren, die der Nische entstammen, und der zellintrinsischen Signalwege, die durch Interaktionen von Stammzellen mit ihrer Nische ausgelöst werden. Viele Stammzellnischen sind immer noch schlecht definiert und wenig ist darüber bekannt, wie Nischsignale wie mechanische Beiträge und biochemische Signale konvergieren, um das Stammzellverhalten zu regulieren. Da solche Interaktionen oft schwer mithilfe von *in vivo* Modellen zu entziffern sind, wurde in dieser Doktorarbeit eine neue Generation an Mikrosystemen erforscht, um Stammzellnischen nachzubilden.

Im ersten Teil dieser Doktorarbeit wurde eine modulierbare Mikroarrayplattform entwickelt um die systematische Studie biochemischer Signale zusammen mit Substratsteifheit auf Stammzellverhalten zu ermöglichen. Ein Screening von 12 verschiedenen Proteinkombinationen über drei diskrete Substratsteifheiten wurde durchgeführt, um deren Effekt auf die adipogene Differenzierung von CD105^{pos} CD146^{pos} humanen mesenchymalen Stammzellen zu untersuchen. Diese Zellen und ihre differenzierten Nachkommen haben hohe therapeutische Bedeutung für die skeletale Gewebe-regenerierung und wurden als nischformende Nachbarn von Blutstammzellen im Knochenmark impliziert. Die Substratsteifheit wurde als Hauptdeterminist der Häufigkeit von Lipidakkumulierung in MSCs identifiziert, wohingegen der Lipidgehalt stark vom biochemischen Kontext abhängig war.

Um weiter zu verstehen, wie sich Nischzellen zusammen mit Stammzellen auto-organisieren, um funktionelle Gewebe zu formen, wurden dreidimensionale (3D) organitierende Strukturen von Sphroiden aus pluri- und multipotenten Stammzellen entwickelt. Von diesen Systemen, Organoide genannt, erhofft sich, dass sie instrumentelle Einsicht in Gewebe- und Organentwicklung liefern, dass sie von großem Nutzen für gewebsspezifische Medikamentenscreens sein werden und um in Zukunft klinisch nutzbare, transplantierbare Gewebe herzustellen. Aktuelle Protokolle für Organoidherstellung sind arbeitsaufwändig, sehr ineffizient und nicht robust. Um diese Probleme anzugehen, wurde ein auf Poly(ethylenglycol) (PEG)-

basierender Mikroarray, bestehend aus rundbodenförmigen Vertiefungen, entwickelt. Dieses System wurde für die Hochdurchsatzaggregation einer oder mehrerer Zelltypen genutzt und um ihre Langzeitkultur zu ermöglichen. Im Gegensatz zu bisherigen Systemen bieten rundbodenförmige Mikrowells äußerst reproduzierbare Zellaggregation und gewährleisten durch eine natürliche Form robuste Spheroidmorphologie. Die freie Wahl von Substraten wie z.B. Hydrogelen, begünstigt dieses System ein Überleben der Aggregatkultur über längere Zeit. Außerdem ermöglicht eine Herstellung in hydratisierten Substraten die *in situ* Manipulierung der Spheroide durch Biomolekülversorgung durch das Gelnetzwerk. Dies wurde durch 3D-Kokulturen von hämatopoetisch-unterstützenden OP9 Zellen zusammen mit Blutstammzellen illustriert. Außerdem wurde mit dieser Methode gezeigt, dass primäre MSCs vermehrt werden konnten ausgehend von uniformen Spheroiden, genannt „Mesensphären“. Das morphologische Erscheinungsbild der Mesensphären, das sehr schnell in direkten Kokulturen in konventionellen Gewebekulturen auf Plastikoberflächen verloren geht, konnte in diesen neuartigen mikrotechnischen Kultursystemen bewahrt werden.

Die Etablierung bedeutungsvoller *in vitro* Kokulturmodelle erfordert das Wissen über die phänotypische Identität von sowohl Stamm- als auch Nischzellen. Da solche Marker generell noch erforscht werden, sind sie oft unzureichend um eine gewünschte homogene Zellpopulation zu definieren oder gar zu isolieren. Deshalb wurde im letzten Teil der Doktorarbeit eine alternative Methode zur Identifizierung möglicher Nischzellkandidaten entwickelt. Genauer gesagt wurde ein SNAP-tag Fusionsprotein auf Zellmembranen exprimiert und für die Bildung kovalenter Bindungen zwischen Substraten, die das SNAP-tag Substrat Benzylguanin (BG) beherbergen, eingesetzt. Die Immobilisierung ausreichender Mengen an BG auf Zellmembranen ist ein Mittel, um Zell-Zell Paarungen zu ermöglichen. Dies wurde durch die kovalente Aggregation von sphärischen Mikrogelen, die SNAP-tag und BG in hohen Konzentrationen tragen, demonstriert.

Künstliche Nischmodelle, wie sie in dieser Studie entwickelt wurden, sind weitläufig anwendbar, um Einsicht in die multifaktorielle Komposition und architektonische Organisation von spezifischen Nischen zu gewinnen. Die Erforschung dieser Mikromilieu-Regulatoren und deren Integration in existierende Protokolle soll Innovationen in der Stammzellbiologie fördern und schlussendlich die Produktion von Stammzellen *in vitro* für klinische Anwendungen ermöglichen.

Schlüsselwörter: Stammzelle, Nische, Knochenmark, Mesenchymale Stammzelle, hämatopoetische Stammzelle, Hochdurchsatz, kombinatorisches Screening, Organoide, Mikrorundboden, 3D, PEG, Hydrogel, Zellpaarung, SNAP-tag, Benzylguanin

SOMMARIO

Le cellule staminali hanno un enorme potenziale in ambito clinico. Tuttavia, vi è ancora la necessità di migliorarne le tecniche di manipolazione e coltura ex vivo. Da un lato, molte cellule staminali derivate da tessuti adulti non possono essere mantenute in coltura senza comprometterne il potenziale. D'altra parte rimane molto difficile differenziare artificialmente le cellule staminali in direzione di precisi fenotipi. Protocolli in grado di risolvere queste questioni potrebbero, ad esempio, essere utilizzati per sviluppare modelli pre-clinici più efficaci e predittivi che consentano di ridurre o addirittura sostituire gli studi sugli animali.

Una precisa manipolazione di cellule staminali in vitro richiede una conoscenza approfondita delle specifiche nicchie in cui le cellule staminali risiedono: sia il complesso di fattori estrinseci che la caratterizzano, sia le interazioni di tali fattori con le cellule ospitate. Ad oggi, molte specifiche nicchie sono scarsamente definite e poco si conosce delle loro caratteristiche meccaniche e biochimiche implicate nella regolazione del comportamento delle cellule staminali. Considerate le difficoltà nello studio dell'interazione tra le cellule staminali e la loro nicchia in vivo, questa tesi esplora una nuova generazione di microsistemi per emulare le nicchie stesse.

Nella prima parte di questa tesi è trattato lo sviluppo di una piattaforma di microarray per lo studio sistematico del comportamento delle cellule staminali in risposta a stimoli biochimici e meccanici. È stata studiata la differenziazione in adipociti di cellule staminali mesenchimali umane (MSC, CD105pos e CD146pos) in risposta a una delle nicchie artificiali ottenute combinando 12 proteine e 3 rigidità del substrato. Queste cellule e la loro progenie dispongono di un elevato valore terapeutico per la rigenerazione del tessuto scheletrico e per il loro ruolo nel complesso che forma la nicchia delle cellule staminali ematopoietiche (HSC). Dallo screening in vitro sono emersi due fatti rilevanti: la rigidità influenza l'accumulo di lipidi, mentre i segnali biochimici ne influenzano il contenuto.

Per studiare l'interazione tra le cellule formanti la nicchia e le cellule staminali ospitate, sono stati sviluppati degli sferoidi tridimensionali (3D) combinando cellule staminali pluri- e multi- potenti. Tali "organoidi" rappresentano un nuovo strumento per studiare lo sviluppo di tessuti e organi. Tuttavia, ad oggi, la produzione di organoidi richiede molto tempo ed è inefficiente e scarsamente riproducibile. Per risolvere questo problema, nella seconda parte di questa tesi è trattato lo sviluppo di array di cavità a fondo emisferico, utilizzati per aggregare rapidamente uno o più tipi di cellule e coltivare gli organoidi così ottenuti. Array a elevata densità di questi pozzetti sono stati prodotti utilizzando un idrogel a base di poli (etilene glicole)

(PEG). Rispetto al passato, la geometria emisferica e l'utilizzo d'idrogel portano a una maggiore riproducibilità ed efficienza di aggregazione, unitamente a migliori risultati nella coltura a lungo termine. Inoltre, l'utilizzo d'idrogel permette una manipolazione degli sferoidi mediante la presentazione di biomolecole incorporate nella rete polimerica del gel. Per dimostrare tale asserzione, cellule della linea OP9 e cellule staminali ematopoietiche (HSC) sono state aggregate come organoidi 3D (o "Liposfere") e le loro interazioni hanno dimostrato un'azione inibitoria da parte delle HSC sulla differenziazione adipogenica delle OP9. Inoltre, mediante quest'approccio, è stato dimostrato che cellule staminali mesenchimali umane primarie potrebbero vedere il loro potenziale aumentato se aggregate in sferoidi omogenei (o "Mesosfere"). L'aspetto morfologico delle mesosfere, perso rapidamente se coltivate mediante protocolli convenzionali, può essere conservato mediante l'utilizzo di questo nuovo sistema di cultura micro-ingegnerizzato.

Per realizzare un modello di co-cultura in vitro è necessario conoscere a fondo le identità fenotipiche delle cellule coinvolte, staminali o formanti la nicchia. Nonostante nuovi indicatori molecolari siano documentati di continuo, essi sono spesso insufficienti per definire e isolare popolazioni cellulari omogenee. Pertanto, nella parte finale di questa tesi è stato definito un approccio alternativo per identificare potenziali cellule formanti la nicchia di cellule staminali. Più precisamente, proteine del tipo SNAP-tag sono state espresse sulle membrane cellulari e sono state utilizzate per formare legami covalenti con benzil-guanina (BG). Mediante l'immobilizzazione di sufficienti quantità di BG sulle membrane cellulari è stato possibile unire due cellule, come dimostrato da specifici test condotti con microsferi caratterizzate da alte concentrazioni di SNAP-tag e BG.

I modelli artificiali di nicchie di cellule staminali sviluppati in questa tesi sono applicabili a svariati sistemi cellulari, al fine di estrapolarne sia la loro composizione multifattoriale, sia la specifica organizzazione architettonica che caratterizza le nicchie stesse. La dissezione e comprensione delle funzioni di tali regolatori del microambiente e la loro integrazione nei protocolli esistenti potrà rappresentare un importante avanzamento nello studio della biologia delle cellule staminali. Si tratta di un passo verso lo sviluppo di protocolli di espansione in vitro delle cellule staminali, per un futuro utilizzo delle stesse in campo clinico.

Parole Chiave: cellule staminali, nicchia, midollo osseo, cellule staminali mesenchimali, cellule staminali ematopoietiche, high-throughput screening combinatorio, organoidi, pozzetti a fondo emisferico, 3D, PEG, idrogel, accoppiamento cellulare, SNAP-tag, benzil-guanina

TABLE OF CONTENT

ACKNOWLEDGEMENTS	V
SUMMARY	VII
RÉSUMÉ	IX
ZUSAMMENFASSUNG	XI
SOMMARIO	XIII
CHAPTER I – INTRODUCTION	1
MOTIVATION AND OBJECTIVES	3
BACKGROUND	7
Stem cells and the holy grail of biology	7
Stem cell niche	8
Stem cell and tissue bioengineering	10
The hematopoietic stem cell niche	13
Niche cell fate and microenvironmental implications	16
Limiting factors for ex vivo hematopoietic niche assays	18
Therapeutic potential of MSCs	19
REFERENCES	21
CHAPTER II – MICROENVIRONMENTAL REGULATORS OF STEM CELL DIFFERENTIATION	27
ABSTRACT	30
INTRODUCTION	30
EXPERIMENTAL METHODS	33
RESULTS AND DISCUSSION	36
CONCLUSIONS	45
REFERENCES	46
CHAPTER III – HIGH-THROUGHPUT GENERATION AND MANIPULATION OF CELL SPHEROIDS	49
ABSTRACT	52
INTRODUCTION	52
EXPERIMENTAL METHODS	55
RESULTS	56
DISCUSSION	64
REFERENCES	66
CHAPTER IV – THREE-DIMENSIONAL IN VITRO BONE MARROW MODELS	69
ABSTRACT	72
INTRODUCTION	73
EXPERIMENTAL METHODS	75
RESULTS	79
DISCUSSION	87
CONCLUSIONS	89
REFERENCES	90

CHAPTER V – MANIPULATING CELL-CELL INTERACTIONS IN THE NICHE	93
ABSTRACT	96
INTRODUCTION	96
EXPERIMENTAL METHODS	98
RESULTS	100
DISCUSSION	108
CONCLUSIONS	110
REFERENCES	111
CHAPTER VI – DISCUSSION AND PERSPECTIVES	113
APPENDIX A	XVII
APPENDIX B	XXIII

CHAPTER I

INTRODUCTION

MOTIVATION

The identification of stem cells with their life-long ability to maintain tissue homeostasis has had significant impact on medical care. The hope of universally treating human diseases with stem cell therapy can be exemplified by the historical success of bone marrow transplantations in curing or extending the lifetime of patients with acquired or hereditary hematological malignancies [1]. However, despite the growing demand and numbers of performed hematopoietic stem cell (HSC) transplantations each year [2], many technical hurdles remain that impact effectiveness in current and future stem cell therapeutic applications. Among them, probably the most critical challenge, is obtaining enough numbers of stem cells to treat adult patients by either harvesting from clinically safe sources or expanding them from such sources where they may be scarce [6]. However, most, if not all, *in vitro* expansion methods for stem cells, compliant with good laboratory practice (GLP)/ good manufacturing practice (GMP), are associated with commitment, and therefore loss of long-term multipotency. The underlying reason is the lack of interactions with the niche that instruct the stem cell to undergo self-renewal divisions, just as they occur in the native cell microenvironment. It is therefore crucial to understand the intrinsic tissue-specific signaling to which a stem cell is exposed in order to maintain stemness during *ex vivo* processing. One can eventually further apply this knowledge to direct differentiation of a stem cell towards a target lineage at a given time and place. Finally, and by far not minder relevant, it is a major challenge to maintain the viability and safety of a graft and to be able to monitor and adequately react to the progress, positive or negative, of a stem cell transplantation. Altogether these tasks are not trivial and current cell culture techniques often lack the potential to address multiple components of such a complex cellular microenvironment. Therefore, it is becoming increasingly necessary for regenerative medicine to acquire a fundamental understanding of niche signaling mechanisms, niche components and the possibility to translate this knowledge to predictive cell culture tools that are efficient, practical and scalable.

The hematopoietic stem cell niche in this context can serve as a potent model system to investigate the complex interplay of niche components. Indeed, there already exists a large pool of biological knowledge based on its clinical relevance and application. Among such niche components investigated in murine bone marrow, multiple mesenchymal-like cell types (mesenchymal stem and progenitor cells, MSCs) have recently been demonstrated to participate in HSC maintenance, migration and homing to the bone marrow [7-9]. These niche cells have been defined by the expression of various markers (Nestin, Sca-1, ALCAM, Leptin

receptor). However, ambiguity in determining the overlap of these cell populations remains unresolved. Mechanistic studies using these niche cell populations are complicated by the lack of markers for their prospective isolation, their relative low abundance and the fact that these cells, similar to primary HSCs, cannot be reliably propagated *in vitro*. Conventional cell culture protocols result in rapid, uncontrolled differentiation with loss of their HSC-maintaining potential.

Hence, there is a crucial need for better tools to advance the study of the molecular and cellular composition and interactions of the bone marrow niche. Specifically, we focused on three major problems that arise from conventional cell culture methods that render them insufficient to explore complex niche biology. First, as long as sophisticated markers for MSCs are poorly defined, simpler and more reliable isolation methods for niche cells have to be developed. Second, the fate of niche cells is closely linked to the homing and maintenance of HSCs *in vivo* [10, 11]. Both the molecular composition as well as mechanical properties have been shown to influence stem cell differentiation [12, 13], yet there is a lack of tools to address multiple modulators simultaneously. Finally, there is no culture system available that can recreate the three-dimensional cellular arrangement of HSCs together with cells that maintain them. Altogether novel tools that are able to address these questions will contribute to better defining the components of the bone marrow niche and advancing our understanding of multifactorial microenvironmental signals within this system and others.

OBJECTIVES

Considering the before-mentioned limitations, the overall goal of this thesis is the development of innovative stem cell manipulation techniques. Their prospective integration into culture platforms enables the study of complex biological networks, as demonstrated here by the model of the bone-marrow niche.

Aim 1: To decouple biophysical and biochemical microenvironmental regulators of stem cell differentiation

Multifactorial cellular microarrays will be used to probe the effect of complex niche signals on adipogenic differentiation of mesenchymal stem cells.

Aim 2: To develop a hydrogel-based platform for the high-throughput generation and manipulation of cell spheroids

U-bottom microwell arrays will be fabricated which allow the clustering and long-term culture of one or more cell types.

Aim 3: To develop a three-dimensional *in vitro* bone marrow model

The above microwell system will be used to build a 3D co-culture system of HSCs and niche cells.

Aim 4: To engineer a novel tool to manipulate cell-cell interactions in the niche

A chemical approach will be employed to capture cell-cell interactions via formation of non-natural chemical bonds.

BACKGROUND

Stem cells and the holy grail of biology

A stem cell is defined by its two distinct functional properties: the ability to self-renew over extended periods of time and the ability to differentiate towards more specialized lineages. While stem cells have prominently featured in headlines in recent years, this fundamental notion is not new knowledge. As early as 1905, the existence of a cell with such characteristics was hypothesized and depicted for the hematopoietic system (Figure 1.1).

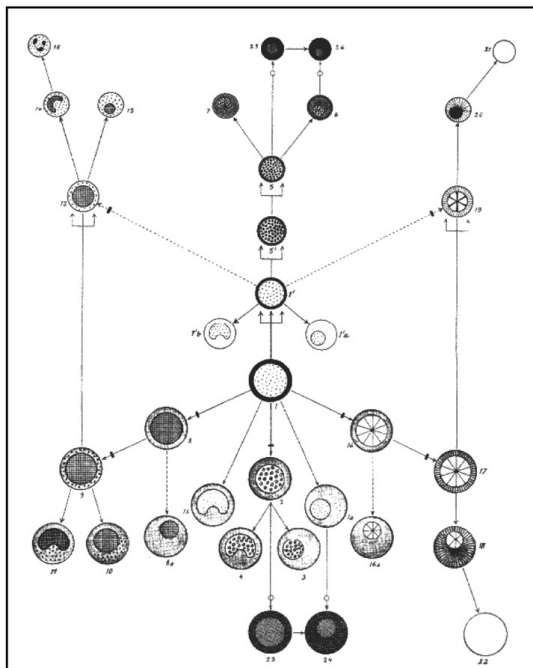


Figure 1. 1 Early blood stem cell research. Arthur Pappenheim's view of the hematopoietic lineage tree from 1905 [3]. Based on Paul Ehrlich's staining techniques to differentiate between different white blood lineages, the notion of a common precursor cell to the different blood cell types was born. The cell in the very center is referenced among other terms as "stem cell". Notably, Pappenheim's tree diagram of the blood cell system seems outstandingly clairvoyant.

In the 1930s, available experimental techniques fell short of providing evidence for the existence of a hematopoietic stem cell. It was nonetheless accurately described as a functional, less differentiated cell, residing in the bone marrow and susceptible to damage by radiation [14, 15]. In 1956 the first successful syngeneic bone-marrow transplant was performed by E. Donnall Thomas. Shortly after, in 1963, the true nature of hematopoietic stem cells (HSCs) as indefinitely self-renewing cells with multi-lineage differentiation capability was effectively proven in the mouse [16-18].

Since then, tissue-specific adult stem cells have been described in virtually every tissue of the human body: neural stem cells [19], satellite cells [20, 21], intestinal stem cells [22], epidermal stem cells [23], dental pulp stem cells [24], etc. These "multi-potent" cells are lineage-restricted and reside in the tissue to ensure its homeostasis and repair throughout life.

All tissue-specific stem cells are derived from pluripotent cells of the inner cell mass of a blastocyst as the human body develops. This process can be reproduced *in vitro* [25, 26]. Indeed, embryonic stem (ES) cells derived from this inner cell mass maintain their ability to self-renew *in vitro* and differentiate into cells of all three germ layers. These cells therefore constitute a promising platform to investigate developmental processes and to generate transplantable differentiated cells for regenerative medicine. Additionally, embryonic stem cells hold a distinct advantage over other tissue-specific stem cells: once ES cells are derived from the mammalian blastocyst, they can be easily propagated *in vitro* with rather little means and they harbor the ability to differentiate more readily than adult stem cells.

For all their potential, however, ES cells have raised the most prominent ethical debate of the last century considering their isolation procedure and have sparked great public interest and controversy. The generation of induced pluripotent stem (iPS) cells [27] circumvented the ethical issues tied to ES cell research. Nevertheless, standard iPS generation protocols lack GMP conformity, prompting the need for further advances, particularly to avoid genetic modification and tackle safety issues, which would insure a prominent future for iPS-derived cell therapies.

Where the body's own repair mechanisms fail, the use of *in vitro* conditioned stem cells holds big promises for medical treatments and cures. Stem cells are indeed the keystone to medicine's "holy grail" scenario: that in case of organ failure or loss, stem cells may be engineered to replace, repair and restore function to virtually any part of the body.

Stem cell niche

A stem cell does not function in isolation. Within a tissue, a stem cell is surrounded by a complex signaling machinery directing it to remain quiescent, to divide symmetrically or asymmetrically or to die. This concept of an all-instructive cellular microenvironment was first proposed by Schofield in 1978 [28]. Since then, our understanding of the different building blocks in this microenvironment has continuously increased. It has also been found that, although different in location and composition, mammalian stem cell niches share many general common features involving of soluble, physical and metabolic signals as well as cell-cell interactions (Figure 1. 2).

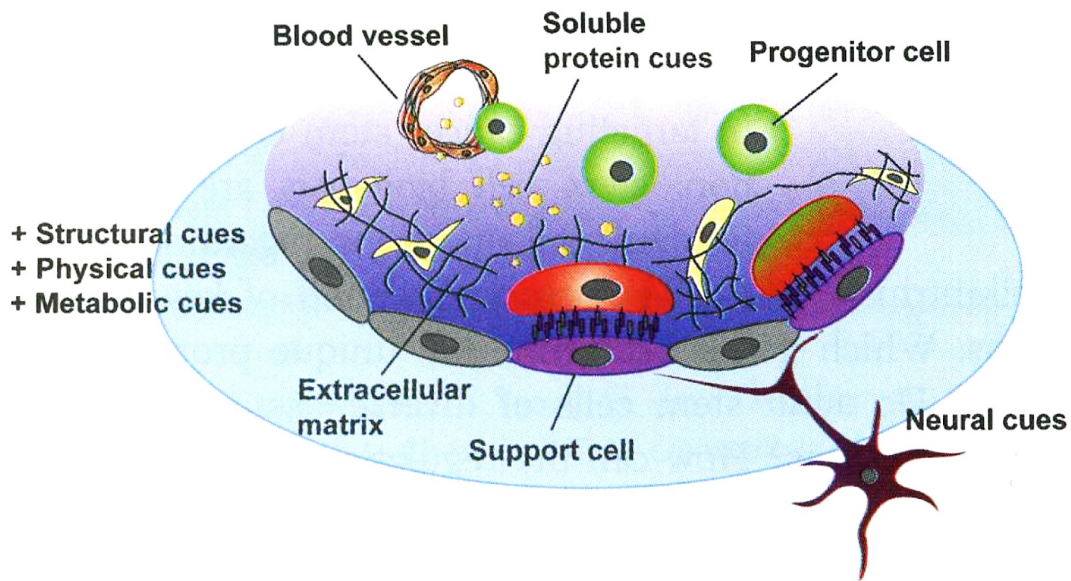


Figure 1. 2 The stem cell niche. A specific anatomic location that regulates and directs stem cell fate which comprises the complex interplay of physical signals, soluble signals, autocrine and paracrine signaling and physical and structural cues from neighboring cells and the surrounding extracellular matrix. Image from [5].

Classical cell culture techniques fail to recapitulate the physiological conditions of such multifactorial microenvironments. Indeed, polystyrene-based cell culture plates are hard, flat surfaces and make it nearly impossible to control the composition and mode of presentation of selected niche signals. Cells cultured on standard plastic platforms therefore experience entirely artificial and non-native environmental stimuli and cellular responses, making it extremely difficult for *in vivo* translation.

Given these significant limitations, the development of new technologies for improved culture, characterization and eventual expansion of stem cells is needed. These technologies need to be as versatile as the various stem cell niches in the body, acting a puzzle to select, assemble, combine and control the plethora of signal interactions found in the native stem cell niche. Given a discrete set of niche constituents, stem cells may therefore be supplied with an engineered microenvironment with the capacity to drive and fine-tune cellular responses to best mimic *in vivo* cellular processes. Such improved *in vitro* culture technologies would possess a highly predictive capability, which would stem the need for excessive, time- and cost-consuming *in vivo* experimentation.

Stem cell and tissue bioengineering

To understand stem cell behavior and to be able to manipulate their function at will, one must understand and manipulate the stem cell niche signals. The major questions can be summarized as follows:

- (i) Dissecting the microenvironmental cocktail: What signals are necessary to maintain or commit a stem cell?
- (ii) Identifying niche cells: Where do these signals come from?
- (iii) Role of niche architecture and organization: In what format do they need to be presented to the stem cell and how can we adapt this knowledge in a relevant culture system?

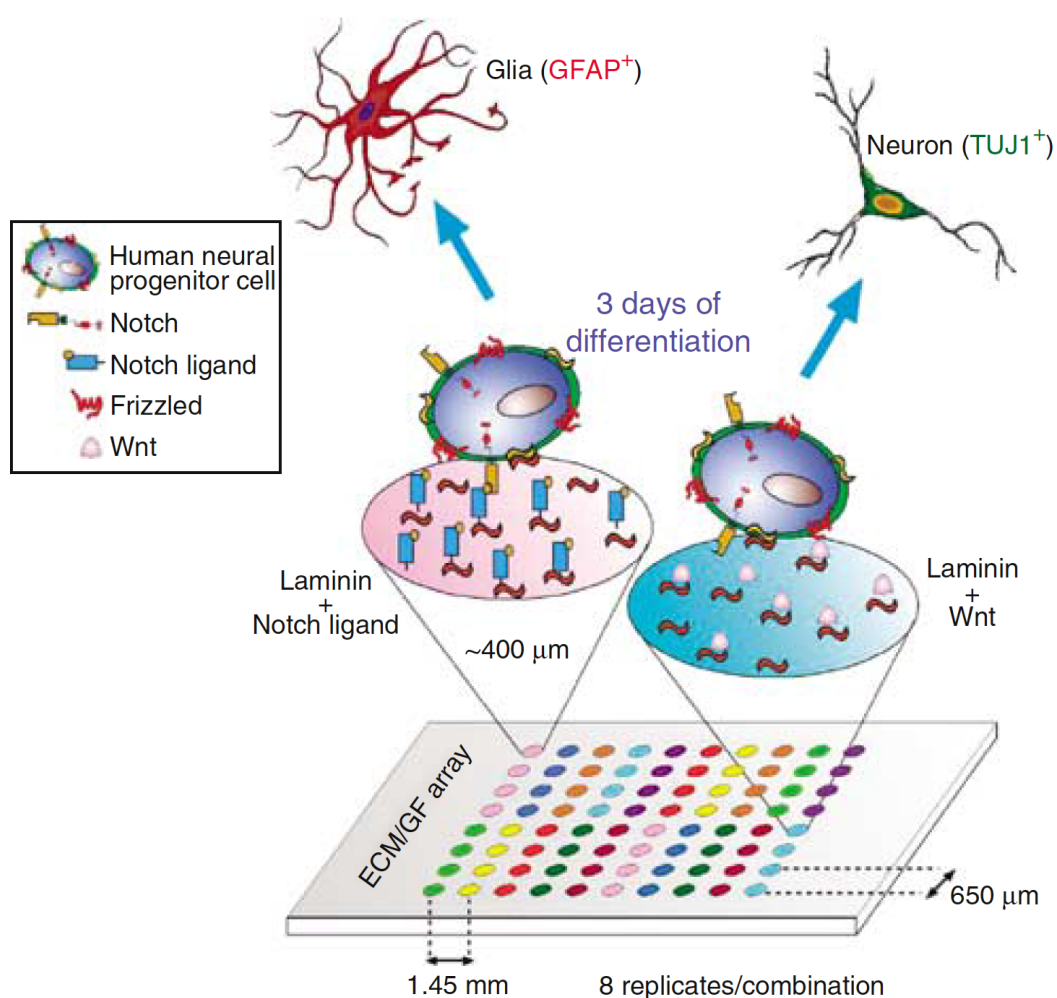


Figure 1. 3 Cellular microarrays. Schematic of early cellular microarrays based on the presentation of combinatorial molecular signals to given stem cells to direct their differentiation in vitro.

Because of the multifactorial nature of the stem cell niche, which was long hypothesized to exclusively harbor combinations of biochemical signals, cellular microarrays were developed to interrogate the effect of proteins on cell fate decisions (Figure 1.3). Mixtures of ECM components, morphogens and other signaling cues were immobilized to defined regions to which cells could attach and respond to. Such microarrays were employed for the parallel analysis of cell responses to combinatorial biochemical signals for a variety of stem and progenitor cell systems [12, 29, 30].

The emerging field of mechanobiology has however demonstrated that stem cells actively sense and respond not only to molecular cues of their microenvironment, but also to physical cues from the surrounding extracellular matrix (ECM) [13].

To integrate these findings into meaningful biological platforms, tunable synthetic biomaterials have been introduced that mimic more closely the properties of the native microenvironment. For example, artificial polymer-based matrices can be generated that recapitulate the molecular composition through covalent tethering of biomolecules and the mechanical properties in terms of stiffness, tensile strength and degradability through tuning of polymer backbone and content [31].

Thus combining cellular microarrays with biomaterial science is advantageous to better recapitulate the true nature of stem cells and how they respond to a given complex microenvironment *in vitro*.

In order to understand how and where niche signals are generated, many efforts have been made towards identifying the cellular constituents of the stem cell niche. For example, HSCs have been long associated to interact with osteoblasts at the endosteum, mesenchymal stem cells and with endothelial cells lining the sinusoids. Neural stem cells (NSCs) from the subventricular zone of the hippocampus and in the olfactory bulb are similarly located adjacent to endothelial cells. The Paneth cell has been identified as the niche cell for intestinal stem cells (ISCs), responsible for generating the Wnt signals responsible for ISC survival and maintenance. The identity of many niche cells remains unresolved often due to the fact that stem cells are extremely rare in number and difficult to identify.

To capture the 3D architecture and cellular complexity of a stem cell niche *in vitro*, miniature organoid models have recently been introduced and demonstrated to mimic aspects of tissue function. For example, embryoid bodies (EBs) formed by aggregation of embryonic stem cells (Figure 1.4 A-C), can self-organize to form three-dimensional (3D) physiological structures such as the optic cup, the adenophysis, thyroid follicles, inner ear sensory tissues and cerebral organoids (Figure 1.4 D-H) [32-36]. In one case, this kind of self-organization has

even been demonstrated for adult stem cells - the Lgr5-expressing intestinal stem cell, which is able to form all structures of the digestive tract including gastric and colon units (Figure 1.4I-K) [37-39]. While these “mini-organs” are most certainly interesting for predictive cell culture models, their low-throughput generation is currently limiting their application in larger screens.

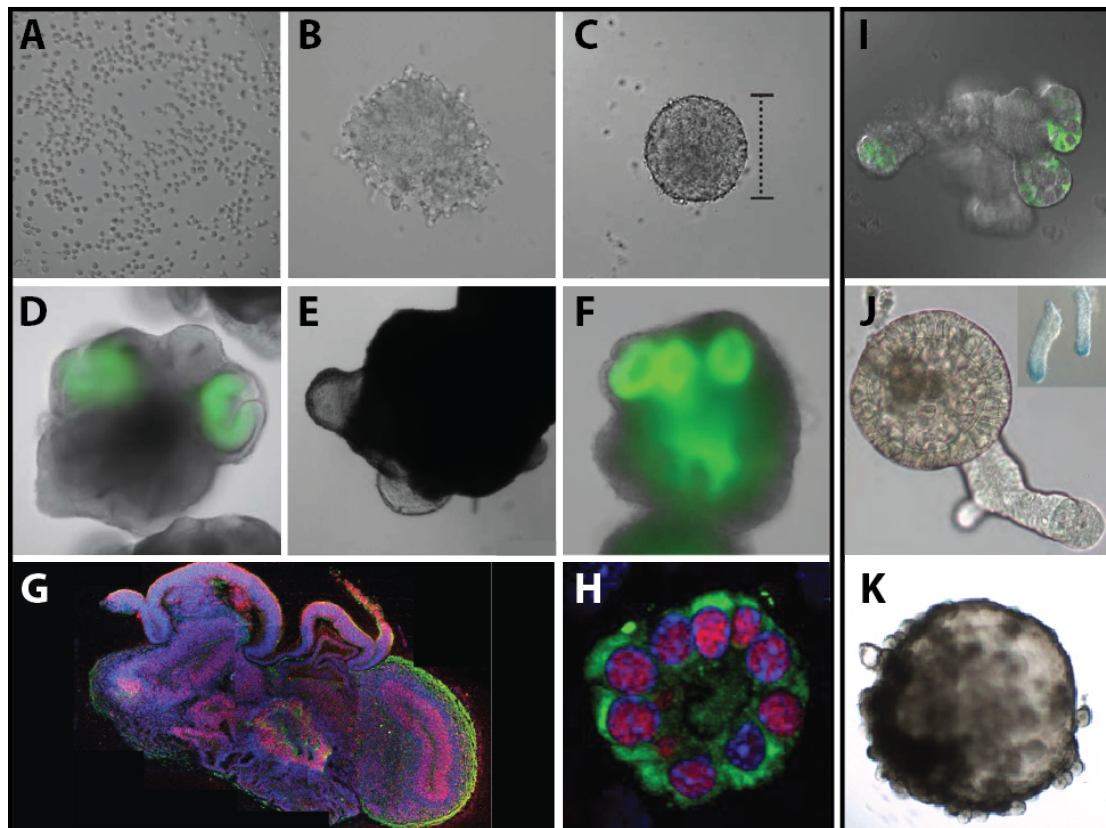


Figure 1. 4 Self-organizing organoids. Spheroids of pluripotent stem cells obtained through aggregation of e.g. embryonic stem cells (A-C) can self-organize to complex functional tissue structures such as (D) optic cup, (E) inner ear sensory tissue, (F) adenophysis, (G) cerebellar tissues and (H) thyroid tissues. In adult tissues, state-of-the-art self-organizing organoid structures have only been shown for the Lgr5-expressing intestinal stem cell, here forming (I) crypt-villi, (J) gastric and (K) colon three-dimensional microtissues. Image compiled from [32-39].

The hematopoietic stem cell niche

The research on the hematopoietic system over more than a century has made it one of the most well characterized and advanced stem cell systems known to date. The identification of discrete marker panels to refine and purify an HSC population laid the foundation for their prospective isolation to enable transplantation therapies. Yet knowledge acquired on the hematopoietic system thus far is mainly limited to the nature of HSCs *in vivo*. We now have a clear understanding of what markers define a primitive HSC and what soluble factors and cellular adhesions are upregulated and active in the hematopoietic niche *in vivo*. What remains unknown is how HSC function can be preserved during and after manipulation. Most HSCs quickly lose their multi-lineage potential once taken in culture. It is therefore necessary to define and detail the hematopoietic stem cell niche and how different parts of this system act in concert to obtain an *in vitro* and also clinically applicable system which can be controlled at will, *i.e.* to induce proliferation, retain function and exert function of a stem cell and its progeny at a given time and location.

The *Dexter culture* provided the first hematopoiesis-supportive *ex vivo* co-culture system of HSCs together with other bone marrow cells, proving the necessity for microenvironment-establishing niche cells [40]. However the question as to which specific cell type among the combination of fibroblasts, endothelial cells, adipocytes and osteoblasts truly constituted the HSC niche remained unclear.

Numerous stromal cell lines (*e.g.* MS5, S17, FBMD-1, OP9, AFT024) varying in their capacity to support early hematopoiesis and differentiation were proposed. [41-45] Yet, co-cultures with such cell lines generally demonstrated a loss or severe reduction of the long-term repopulating (LTR) ability of the cultured HSCs [46]. Further, *in vivo* counter-parts were not reported until a decade ago through the experimental evidence that mature osteoblasts influence HSC pool sizes [10, 47]. Yet it remained unclear whether the observed regulation was direct or indirect.

Subsequently, mesenchymal stem and progenitor cells (MSCs) with osteo-lineage potential were quickly hypothesized to partake in the HSC niche environment and multiple studies have focused on identifying the complex regulatory relationships between one or more definitive mesenchymal-like niche cell populations and HSCs in the bone marrow.

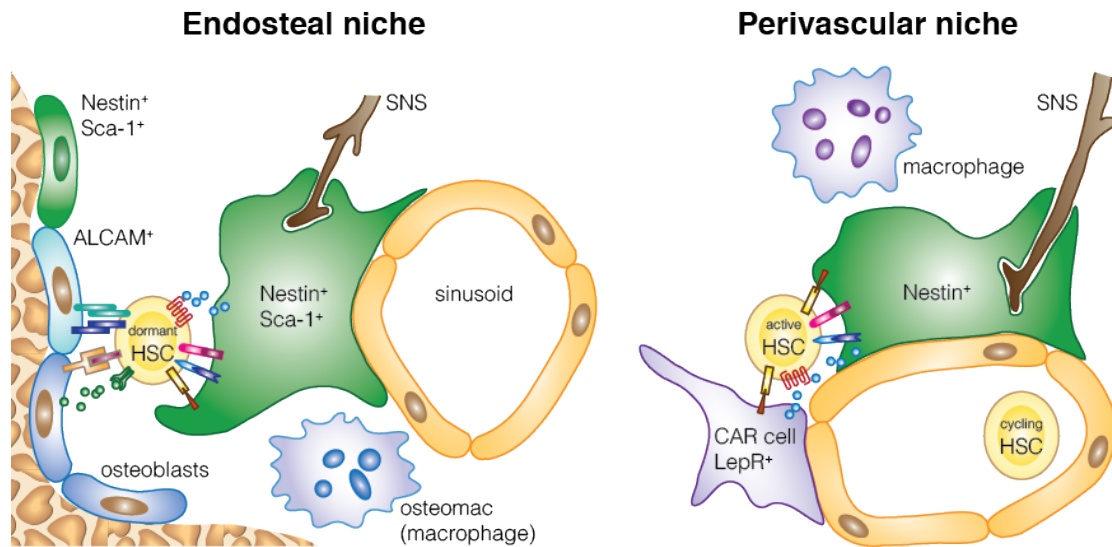


Figure 1. 5 A current view on the distinct HSC niches in the bone marrow. Current research proposes the existence of two locally distinct HSC niches close to the endosteum (endosteal niche) and surround sinusoids (perivascular niche). Niche cells expressing a variety of markers have been reported (Nestin, ALCAM, Sca-1, LepR, also refer to Table 1. 1). Adapted from [4]

Current data suggest the existence of two categorical niches for hematopoietic stem cells, an endosteal niche and a perivascular niche (Figure 1. 5). Each of these niches may not only be characterized by a distinct location but also by a specific composition of multiple cell types that contribute to a specialized function [48].

Most information on the local architecture and composition of the bone marrow has been gathered through histological sectioning and immunostaining of bone, made possible by the discovery of a simple two-color immunophenotypic signature of highly enriched HSCs [49]. In mouse as in human, most HSCs are found in the trabecular or spongy region of the bone marrow [50-52]. Yet the detailed location remains under investigation, as HSCs have been associated adjacent to sinusoid vessels. Also, part of the endosteal area is highly vascularized, yet sinusoids are more abundant at further distances away from the endosteum towards the center of the bone marrow [53, 54]. Immediately after transplantation into irradiated hosts, HSCs home preferentially near the endosteum [51, 52]. However this view on homing is arguably challenged by the fact that irradiation induces damage to sinusoids, [55] leaving open questions for the significance of one niche over the other. Furthermore, MSC-derived heterotopic ossicles become invaded by host vasculature and enable HSC recruitment (P. S. Lienemann, unpublished data, EPFL these N° 6124) indicating that osteo-progenitors can promote the formation of a perivascular-like niche.

Consequently, multiple mesenchymal stem, progenitor and stromal cells with osteolineage potential and expressing a wide range of HSC maintenance factors, have been described in both regions of the endosteum and in the perivascular (Figure 1.5 and Table 1.1).

Region	Marker	HSC maintenance factors	Reference
Perivascular	<i>Cxcl12</i> -GFP	CXCL12	[56]
Endosteal/ Perivascular	<i>Nes</i> -GFP	CXCL12, SCF, Ang-1, IL-7, Vcam1, osteopontin	[7]
Endosteal	ALCAM	N-cadherin, M-cadherin, Coll, osteopontin, osteocalcin, JamB	[8]
Endosteal	<i>Sca-1</i>	CXCL12, SCF, Ang-1, Flt3l, Vcam1, TPO	[8]
Perivascular	<i>Lepr</i> -Cre	SCF, CXCL12, Vcam1, PDGFR α	[9]
Perivascular	<i>Mx-1</i> -Cre	osteocalcin, Nes, <i>Sca-1</i> , PDGFR α	[57]
Perivascular	<i>Prx-1</i> -Cre	CXCL12, <i>Sca-1</i> , PDGFR α	[58]
Perivascular	<i>Sp7</i> -Cre	CXCL12	[58]
Periarteriolar	<i>NG2</i> -Cre	CXCL12, SCF, Ang-1, Vcam1, osteopontin, Nes, <i>Sca-1</i>	[59]

Table 1. 1 Collection of to date suggested HSC niche cells. Summarized above are the proposed niche cells over the past decade according to *in vivo* location, marker expression, expression of HSC maintenance factors and overlapping niche cell markers.

Cre recombinase alleles have been used to conditionally delete some of these HSC maintenance factors, e.g. SCF and CXCL12, from various niche cell populations in order to study overlapping of the proposed markers, mainly in comparison to *Nes*-GFP⁺ MSCs [9, 58, 60]. SCF and CXCL12 expression in the bone marrow has been shown to strongly overlap. [60] As opposed to Nestin-expressing perivascular cells, SCF deletion from *Lepr*-Cre cells leads to a complete elimination of HSCs. And while CXCL12 deletion driven by *Lepr* was demonstrated to have mostly no impact on HSC pool size, its deletion under the *Prx-1* promoter leads to HSC depletion and mobilization from the bone marrow. Therefore HSC maintenance must partially arise from contributions of non-endothelial *Lepr*-negative cells, arguably *Nes*-GFP⁺ MSCs [61]. Due to their striking similarities to identified CXCL12-abundant reticular (CAR) cells, [62] and a strong overlap of *Nes*-GFP expression to that of *Lepr*-Cre, they may portray a CAR subpopulation or even possibly the upstream source for perivascular HSC supporting cells [4].

Taken together, the molecular and cellular composition of the bone marrow niche is slowly unraveling; yet the list of constituents that construct this specific niche remains presumably incomplete. Further, ambiguity about the overlapping of the various proposed niche cell populations remains unresolved.

Niche cell fate and microenvironmental implications

The bone marrow microenvironment can be globally categorized into two histologically distinct phenotypes according to skeletal location and physiological condition: (i) *medulla ossium rubra* (red or hematopoietically active marrow) and (ii) *medulla ossium flava* (yellow or hematopoietically inactive marrow). Mesenchymal stem and progenitor cells not only represent the source for hematopoietic-supportive osteo-progenitors and osteoblasts, but also serve as the source for adipocytes, the major residing cell type in the yellow marrow condition. It has been understood that the hematopoietic niche can dynamically change its function when exposed to environmental stress. Under homeostasis, most HSCs reside in a quiescent state while in contact to osteo-progenitors and osteoblasts in the endosteum. Irradiation or chemotherapy results in adipocyte infiltration of hematopoietic red marrow [63]. A high percentage of adipocytes present in the bone marrow is considered as the diagnostic phenotype of bone marrow failure [64]. Bone marrow reconversion, i.e. the transition from red to yellow marrow, is however also associated with aging. First during juvenile development, the diaphyseal marrow cavities of long bones progress towards highly adipocytic states [65] and generally with increasing age adipocyte numbers expand linearly to finally comprise more than half of the marrow cellularity [66]. Bone marrow adipocytes were long considered passive “space-fillers” until they were demonstrated to actively participate in hematopoietic maintenance and regulation [11]. HSCs reside in a highly quiescent state in adipocyte-rich marrow and the generation of short-term hematopoietic progenitors is actively inhibited. In a transplant setting, hematopoietic progenitor expansion and post-transplant recovery were enhanced in phenotypes where bone-marrow adipocytes were depleted either pharmacologically or genetically (Figure 1.6).

Adipocytes are therefore proposed as microenvironmental components of an opposing niche and a shift in balance between reciprocal lineages of bone marrow niche cells, i.e. osteogenesis versus adipogenesis, imposes regulatory influences on HSCs and hematopoietic progenitors under homeostasis and particularly stress. The molecular mechanisms governing the rapid differentiation processes of niche cells to enable this red to yellow marrow transition still remain unknown. The underlying

reason is, that dissecting and understanding these cellular and molecular interactions in the complex *in vivo* microenvironment is difficult due to the fact that the bone marrow is challenging to access and adipocytes are difficult to isolate and quantify and frequently lost in histological sections. Hence, tractable *in vitro* models of the bone marrow HSC niche cell interaction are needed.

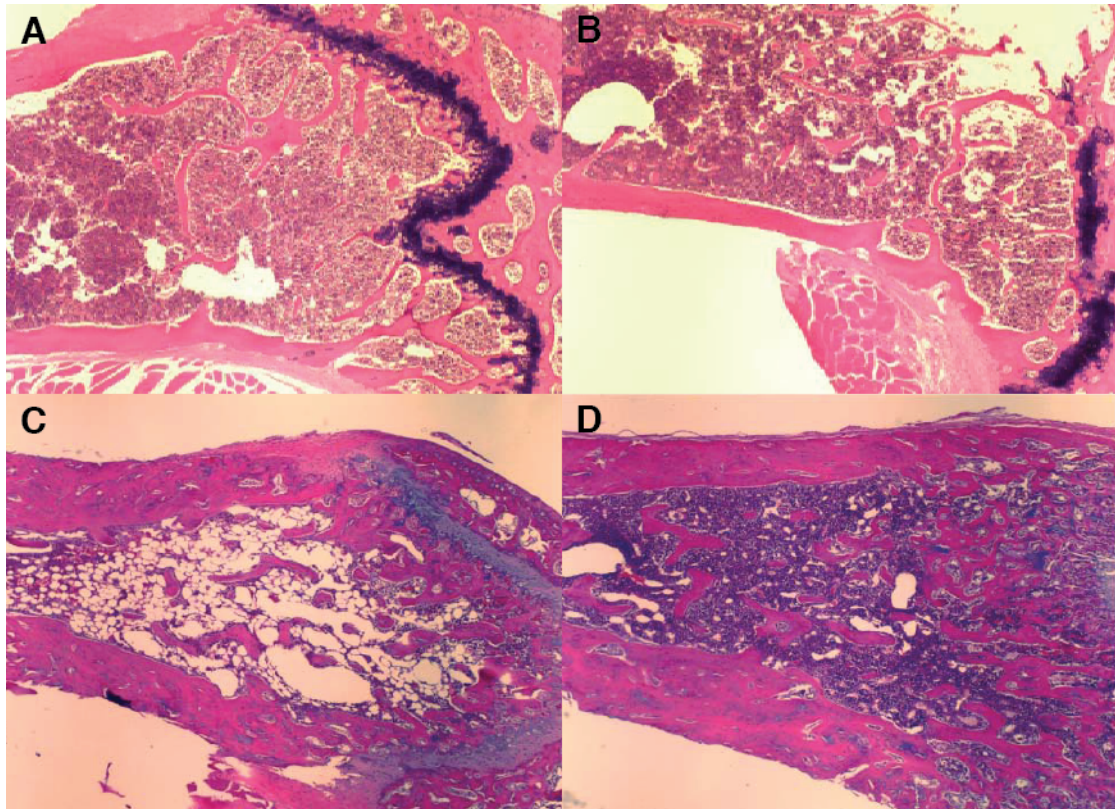


Figure 1. 6 Bone marrow phenotypes before and after irradiation. Hematoxylin and eosin (H&E) stains of 6 week-old femurs showing adipocyte-poor red bone marrow phenotype prior transplantation in (A) wild type and (B) genetically fatless (A-ZIP/F1) mice and showing yellow respectively red bone marrow post transplant in (C) wild type versus (D) fatless A-ZIP/F1 mice. Original magnification X40. Images compiled from [11].

Limiting factors for *ex vivo* hematopoietic niche assays

Mechanistic studies using mesenchymal niche cells are complicated by the fact that these cells, similar to primary HSCs, cannot be propagated *ex vivo*. Difficult isolation procedures, absence of markers for their prospective isolation and their relative low abundance additionally limit the feasibility of comprehensive *in vitro* studies.

The only functional *in vitro* culture condition for HSC niche cells is a non-adherent sphere-forming assay derived from neural crest and pericyte cultures (Figure 1.7). From the bone marrow of *Nestin-GFP* transgenic mice, CD45-negative GFP-positive cells give rise to clonal spheres *in vitro* with efficiencies around 7% (Figure 1.7 A-C) [7]. Sustained expression of HSC maintenance genes in such mesensphere cultures is however not preserved and similarly to adherent bulk cultures, the cells spontaneously differentiate towards mesenchymal lineages (Figure 1.7 D) [67].

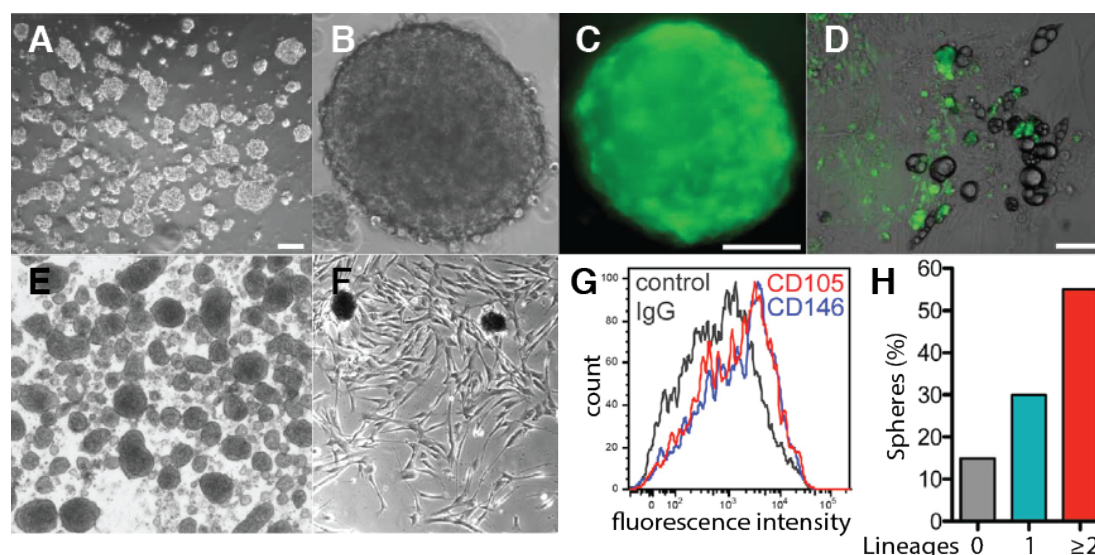


Figure 1. 7 Mesensphere culture of mouse and human HSC niche cells. (A-C) Mouse CD45- Nes-GFP⁺ BM cells form self-renewing mesenspheres, which maintain Nes-GFP expression over short term but (D) then spontaneously differentiate towards mesenchymal lineages, as seen by increased lipid vesicle accumulation and loss of GFP. (E) Human CD105⁺ BM cells similarly form mesenspheres, (G) which maintain expression of CD105 and CD146 over passages. (F) In the presence of serum, human mesenspheres attach to virtually any substrate. (H) After three passages, most human mesenspheres are not maintained. Images and graphs compiled from [7, 68].

Similarly to mouse bone marrow cells, mesosphere cultures have been adapted for the culture of human HSC niche cells (Figure 1.7 E) based on their expression of CD105, which partially overlaps with nestin-expression [68]. Only small numbers of primary mesospheres can be obtained from human bone marrow aspirates and after few passages more than half of the cells differentiate towards one or more mesenchymal lineages (Figure 1.7 H). However non-adherent culture of human MSCs maintained CD105 and nestin-expression (Figure 1.7 G) and HSC supportive characteristics longer and reduced the up-regulation of differentiation markers compared to standard adhesion culture using medium supplemented with serum (Figure 1.7 F). In accordance, suspension cultures have been suggested as a better alternative to preserve the differentiation potential of human mesenchymal progenitor cells [69].

Therapeutic potential of MSCs

Despite or rather additionally to their newly developing role in hematopoietic maintenance and regulation, mesenchymal stem and progenitor cells have been historically studied with respect to their therapeutic potential for virtually all cell types found within skeletal tissues [70] but also others [71-73]. One of the biggest issues in the regenerative field is the definition and characterization of a mesenchymal stem cell due to the lack of existence of distinct MSC markers. By definition a single skeletal stem cell should be able to regenerate an entire heterotopic bone or bone marrow organ (ossicle) *in vivo*. The attempt to set minimal criteria for defining multipotent mesenchymal stromal cells triggered the notion, that heterogeneous cultures of plastic-adherent cells with trilineage mesenchymal differentiation potential that express a limited range of unspecific surface markers *in vitro* represent “a culture of MSCs”. [74] These misconceptions lead to the belief that cellular characteristics observed *in vitro* could in turn be translated matchingly to any *in vivo* scenario, leading to dubious and nondescript “stem cell-based therapies” by intravenous administration of such cell populations (Figure 1.8).

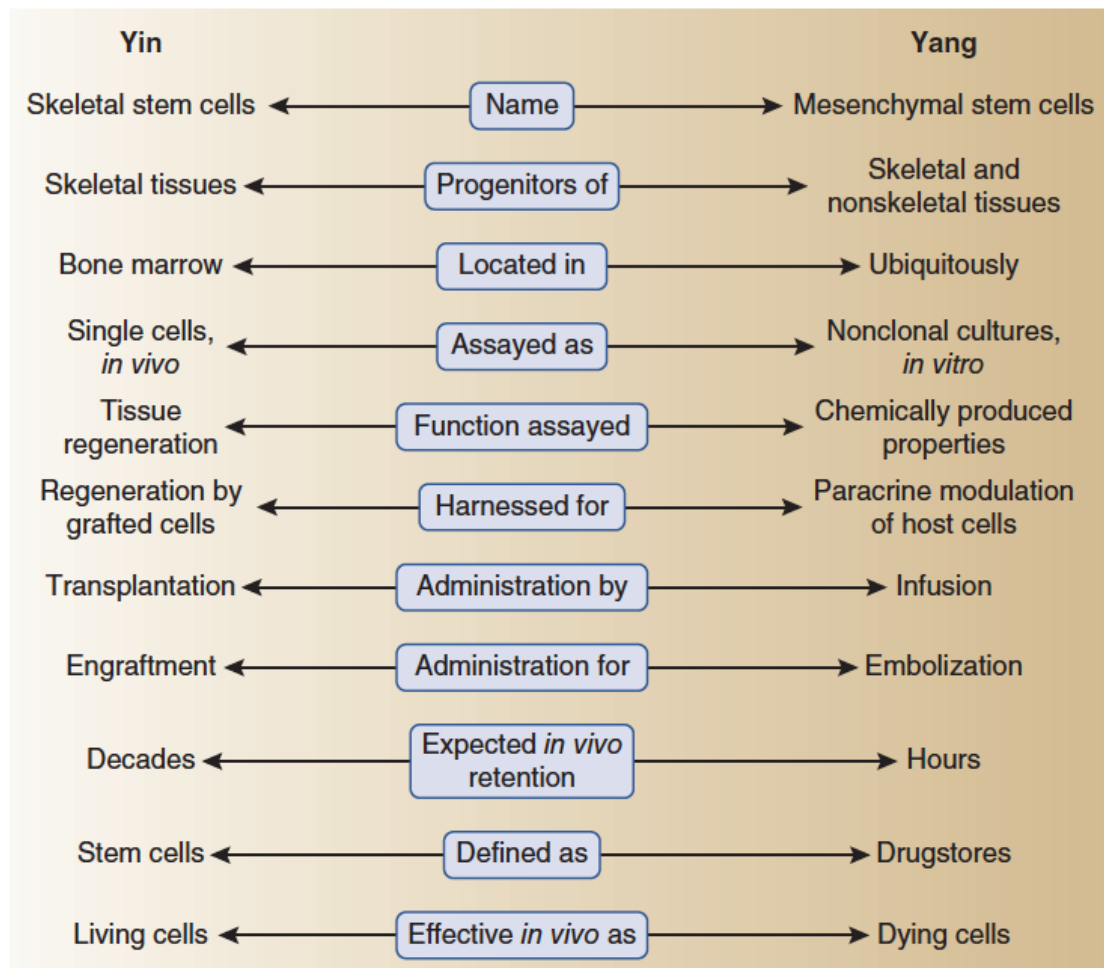


Figure 1. 8 The Yin and Yang of MSCs. A summary of scientific concepts and commercially exploitable translational aspects of cellular therapies. Adopted from [75].

The hype surrounding MSCs is not without reason, but should nonetheless be taken with a small grain of salt. Efficient *in vitro* lineage specification protocols that mimic more closely the naturally occurring processes within a tissue, as opposed to artificial chemically induced differentiation, are a prerequisite to effectively fertilize basic science and science for clinically relevant therapies. [75] To understand the mesenchymal involvement in forming microenvironments, organizing and regenerating tissues, tools need to be developed that open doors to the complexity and unique nature of these and other stem cell systems.

We therefore propose new technologies that will help to understand how contact-dependent niche signaling can be mimicked *in vitro* and how this system could be used to target a cell population of interest. Further we address how combinatorial niche signals can be on the one hand dissected using multifactorial cellular niche screening arrays and on the other hand architecturally reproduced using U-bottom microwell arrays for the generation of three-dimensional microtissues.

References

- [1] Cahn, J.Y., *Clinical bone marrow and blood stem cell transplantation*. Leukemia, 2004. **18**(10): p. 1743-1743.
- [2] Passweg, J.R., et al., *Hematopoietic SCT in Europe: data and trends in 2011*. Bone Marrow Transplant, 2013. **48**(9): p. 1161-7.
- [3] Ramalho-Santos, M. and H. Willenbring, *On the origin of the term "stem cell"*. Cell Stem Cell, 2007. **1**(1): p. 35-8.
- [4] Ehninger, A. and A. Trumpp, *The bone marrow stem cell niche grows up: mesenchymal stem cells and macrophages move in*. J Exp Med, 2011. **208**(3): p. 421-8.
- [5] Lutolf, M.P. and H.M. Blau, *Artificial stem cell niches*. Adv Mater, 2009. **21**(32-33): p. 3255-68.
- [6] Schoemans, H., et al., *Adult umbilical cord blood transplantation: a comprehensive review*. Bone Marrow Transplant, 2006. **38**(2): p. 83-93.
- [7] Mendez-Ferrer, S., et al., *Mesenchymal and haematopoietic stem cells form a unique bone marrow niche*. Nature, 2010. **466**(7308): p. 829-34.
- [8] Nakamura, Y., et al., *Isolation and characterization of endosteal niche cell populations that regulate hematopoietic stem cells*. Blood, 2010. **116**(9): p. 1422-32.
- [9] Ding, L., et al., *Endothelial and perivascular cells maintain haematopoietic stem cells*. Nature, 2012. **481**(7382): p. 457-62.
- [10] Calvi, L.M., et al., *Osteoblastic cells regulate the haematopoietic stem cell niche*. Nature, 2003. **425**(6960): p. 841-6.
- [11] Naveiras, O., et al., *Bone-marrow adipocytes as negative regulators of the haematopoietic microenvironment*. Nature, 2009. **460**(7252): p. 259-63.
- [12] Soen, Y., et al., *Exploring the regulation of human neural precursor cell differentiation using arrays of signaling microenvironments*. Mol Syst Biol, 2006. **2**: p. 37.
- [13] Engler, A.J., et al., *Matrix elasticity directs stem cell lineage specification*. Cell, 2006. **126**(4): p. 677-89.
- [14] Sabin, F.R., C.A. Doan, and C.E. Forkner, *The Production of Osteogenic Sarcomata and the Effects on Lymph Nodes and Bone Marrow of Intravenous Injections of Radium Chloride and Mesothorium in Rabbits*. J Exp Med, 1932. **56**(2): p. 267-89.
- [15] Sabin, F.R., et al., *Changes in the Bone Marrow and Blood Cells of Developing Rabbits*. J Exp Med, 1936. **64**(1): p. 97-120.
- [16] Till, J.E. and C.E. Mc, *A direct measurement of the radiation sensitivity of normal mouse bone marrow cells*. Radiat Res, 1961. **14**: p. 213-22.
- [17] Becker, A.J., C.E. Mc, and J.E. Till, *Cytological demonstration of the clonal nature of spleen colonies derived from transplanted mouse marrow cells*. Nature, 1963. **197**: p. 452-4.
- [18] Siminovitch, L., E.A. McCulloch, and J.E. Till, *Distribution of Colony-Forming Cells among Spleen Colonies*. Journal of Cellular and Comparative Physiology, 1963. **62**(3): p. 327-&.
- [19] Temple, S., *Division and differentiation of isolated CNS blast cells in microculture*. Nature, 1989. **340**(6233): p. 471-3.

- [20] Katz, B., *Terminations of Afferent Nerve Fibre in Muscle Spindle of Frog*. Philosophical Transactions of the Royal Society of London Series B-Biological Sciences, 1961. **243**(703): p. 221-&.
- [21] Mauro, A., *Satellite cell of skeletal muscle fibers*. J Biophys Biochem Cytol, 1961. **9**: p. 493-5.
- [22] Cheng, H. and C.P. Leblond, *Origin, differentiation and renewal of the four main epithelial cell types in the mouse small intestine. V. Unitarian Theory of the origin of the four epithelial cell types*. Am J Anat, 1974. **141**(4): p. 537-61.
- [23] Rheinwald, J.G. and H. Green, *Serial cultivation of strains of human epidermal keratinocytes: the formation of keratinizing colonies from single cells*. Cell, 1975. **6**(3): p. 331-43.
- [24] Kerkis, I., et al., *Isolation and characterization of a population of immature dental pulp stem cells expressing OCT-4 and other embryonic stem cell markers*. Cells Tissues Organs, 2006. **184**(3-4): p. 105-16.
- [25] Evans, M.J. and M.H. Kaufman, *Establishment in culture of pluripotential cells from mouse embryos*. Nature, 1981. **292**(5819): p. 154-156.
- [26] Martin, G.R., *Isolation of a pluripotent cell line from early mouse embryos cultured in medium conditioned by teratocarcinoma stem cells*. Proc Natl Acad Sci U S A, 1981. **78**(12): p. 7634-8.
- [27] Takahashi, K. and S. Yamanaka, *Induction of pluripotent stem cells from mouse embryonic and adult fibroblast cultures by defined factors*. Cell, 2006. **126**(4): p. 663-76.
- [28] Schofield, R., *The relationship between the spleen colony-forming cell and the haemopoietic stem cell*. Blood Cells, 1978. **4**(1-2): p. 7-25.
- [29] Flaim, C.J., S. Chien, and S.N. Bhatia, *An extracellular matrix microarray for probing cellular differentiation*. Nat Methods, 2005. **2**(2): p. 119-25.
- [30] LaBarge, M.A., et al., *Human mammary progenitor cell fate decisions are products of interactions with combinatorial microenvironments*. Integr Biol (Camb), 2009. **1**(1): p. 70-9.
- [31] Lutolf, M.P., et al., *Perturbation of single hematopoietic stem cell fates in artificial niches*. Integr Biol (Camb), 2009. **1**(1): p. 59-69.
- [32] Antonica, F., et al., *Generation of functional thyroid from embryonic stem cells*. Nature, 2012. **491**(7422): p. 66-71.
- [33] Eiraku, M., et al., *Self-organizing optic-cup morphogenesis in three-dimensional culture*. Nature, 2011. **472**(7341): p. 51-6.
- [34] Koehler, K.R., et al., *Generation of inner ear sensory epithelia from pluripotent stem cells in 3D culture*. Nature, 2013. **500**(7461): p. 217-21.
- [35] Lancaster, M.A., et al., *Cerebral organoids model human brain development and microcephaly*. Nature, 2013. **501**(7467): p. 373-9.
- [36] Suga, H., et al., *Self-formation of functional adenohypophysis in three-dimensional culture*. Nature, 2011. **480**(7375): p. 57-62.
- [37] Barker, N., et al., *Lgr5(+ve) stem cells drive self-renewal in the stomach and build long-lived gastric units in vitro*. Cell Stem Cell, 2010. **6**(1): p. 25-36.
- [38] Sato, T., et al., *Long-term expansion of epithelial organoids from human colon, adenoma, adenocarcinoma, and Barrett's epithelium*. Gastroenterology, 2011. **141**(5): p. 1762-72.

- [39] Sato, T., et al., *Single Lgr5 stem cells build crypt-villus structures in vitro without a mesenchymal niche*. Nature, 2009. **459**(7244): p. 262-5.
- [40] Dexter, T.M., T.D. Allen, and L.G. Lajtha, *Conditions controlling the proliferation of haemopoietic stem cells in vitro*. J Cell Physiol, 1977. **91**(3): p. 335-44.
- [41] Breems, D.A., et al., *Frequency analysis of human primitive haematopoietic stem cell subsets using a cobblestone area forming cell assay*. Leukemia, 1994. **8**(7): p. 1095-104.
- [42] Cumano, A., et al., *The influence of S17 stromal cells and interleukin 7 on B cell development*. Eur J Immunol, 1990. **20**(10): p. 2183-9.
- [43] Itoh, K., et al., *Reproducible establishment of hemopoietic supportive stromal cell lines from murine bone marrow*. Exp Hematol, 1989. **17**(2): p. 145-53.
- [44] Kodama, H., et al., *Involvement of the c-kit receptor in the adhesion of hematopoietic stem cells to stromal cells*. Exp Hematol, 1994. **22**(10): p. 979-84.
- [45] Moore, K.A., H. Ema, and I.R. Lemischka, *In vitro maintenance of highly purified, transplantable hematopoietic stem cells*. Blood, 1997. **89**(12): p. 4337-47.
- [46] van der Sluijs, J.P., et al., *Loss of long-term repopulating ability in long-term bone marrow culture*. Leukemia, 1993. **7**(5): p. 725-32.
- [47] Zhang, J., et al., *Identification of the haematopoietic stem cell niche and control of the niche size*. Nature, 2003. **425**(6960): p. 836-41.
- [48] Morrison, S.J. and D.T. Scadden, *The bone marrow niche for haematopoietic stem cells*. Nature, 2014. **505**(7483): p. 327-34.
- [49] Kiel, M.J., et al., *SLAM family receptors distinguish hematopoietic stem and progenitor cells and reveal endothelial niches for stem cells*. Cell, 2005. **121**(7): p. 1109-21.
- [50] Bourke, V.A., et al., *Spatial gradients of blood vessels and hematopoietic stem and progenitor cells within the marrow cavities of the human skeleton*. Blood, 2009. **114**(19): p. 4077-80.
- [51] Xie, Y., et al., *Detection of functional haematopoietic stem cell niche using real-time imaging*. Nature, 2009. **457**(7225): p. 97-101.
- [52] Lo Celso, C., et al., *Live-animal tracking of individual haematopoietic stem/progenitor cells in their niche*. Nature, 2009. **457**(7225): p. 92-6.
- [53] Wilson, A. and A. Trumpp, *Bone-marrow haematopoietic-stem-cell niches*. Nat Rev Immunol, 2006. **6**(2): p. 93-106.
- [54] Kiel, M.J. and S.J. Morrison, *Uncertainty in the niches that maintain haematopoietic stem cells*. Nature Reviews Immunology, 2008. **8**(4): p. 290-301.
- [55] Hooper, A.T., et al., *Engraftment and reconstitution of hematopoiesis is dependent on VEGFR2-mediated regeneration of sinusoidal endothelial cells*. Cell Stem Cell, 2009. **4**(3): p. 263-74.
- [56] Sugiyama, T., et al., *Maintenance of the hematopoietic stem cell pool by CXCL12-CXCR4 chemokine signaling in bone marrow stromal cell niches*. Immunity, 2006. **25**(6): p. 977-88.

- [57] Park, D., et al., *Endogenous bone marrow MSCs are dynamic, fate-restricted participants in bone maintenance and regeneration*. Cell Stem Cell, 2012. **10**(3): p. 259-72.
- [58] Greenbaum, A., et al., *CXCL12 in early mesenchymal progenitors is required for haematopoietic stem-cell maintenance*. Nature, 2013. **495**(7440): p. 227-30.
- [59] Kunisaki, Y., et al., *Arteriolar niches maintain haematopoietic stem cell quiescence*. Nature, 2013. **502**(7473): p. 637-43.
- [60] Ding, L. and S.J. Morrison, *Haematopoietic stem cells and early lymphoid progenitors occupy distinct bone marrow niches*. Nature, 2013. **495**(7440): p. 231-5.
- [61] Hanoun, M. and P.S. Frenette, *This niche is a maze; an amazing niche*. Cell Stem Cell, 2013. **12**(4): p. 391-2.
- [62] Omatsu, Y., et al., *The essential functions of adipo-osteogenic progenitors as the hematopoietic stem and progenitor cell niche*. Immunity, 2010. **33**(3): p. 387-99.
- [63] Caracappa, P.F., T.C.E. Chao, and X.G. Xu, *A Study of Predicted Bone Marrow Distribution on Calculated Marrow Dose from External Radiation Exposures Using Two Sets of Image Data for the Same Individual*. Health Physics, 2009. **96**(6): p. 661-674.
- [64] Bryon, P.A., O. Gentilhomme, and D. Fiere, *[Histomorphometric analysis of bone-marrow adipose density and heterogeneity in myeloid aplasia and dysplasia (author's transl)]*. Pathol Biol (Paris), 1979. **27**(4): p. 209-13.
- [65] Niu, J., et al., *Age-related marrow conversion and developing epiphysis in the proximal femur: evaluation with STIR MR imaging*. J Huazhong Univ Sci Technolog Med Sci, 2007. **27**(5): p. 617-21.
- [66] Justesen, J., et al., *Adipocyte tissue volume in bone marrow is increased with aging and in patients with osteoporosis*. Biogerontology, 2001. **2**(3): p. 165-171.
- [67] *Personal communication with P. S. Frenette*.
- [68] Isern, J., et al., *Self-renewing human bone marrow mesospheres promote hematopoietic stem cell expansion*. Cell Rep, 2013. **3**(5): p. 1714-24.
- [69] Baksh, D., J.E. Davies, and P.W. Zandstra, *Adult human bone marrow-derived mesenchymal progenitor cells are capable of adhesion-independent survival and expansion*. Exp Hematol, 2003. **31**(8): p. 723-32.
- [70] Pittenger, M.F., et al., *Multilineage potential of adult human mesenchymal stem cells*. Science, 1999. **284**(5411): p. 143-7.
- [71] Woodbury, D., et al., *Adult rat and human bone marrow stromal cells differentiate into neurons*. J Neurosci Res, 2000. **61**(4): p. 364-70.
- [72] Toma, C., et al., *Human mesenchymal stem cells differentiate to a cardiomyocyte phenotype in the adult murine heart*. Circulation, 2002. **105**(1): p. 93-8.
- [73] Caplan, A.I. and S.P. Bruder, *Mesenchymal stem cells: building blocks for molecular medicine in the 21st century*. Trends Mol Med, 2001. **7**(6): p. 259-64.

- [74] Dominici, M., et al., *Minimal criteria for defining multipotent mesenchymal stromal cells. The International Society for Cellular Therapy position statement*. *Cytotherapy*, 2006. **8**(4): p. 315-7.
- [75] Bianco, P., et al., *The meaning, the sense and the significance: translating the science of mesenchymal stem cells into medicine*. *Nat Med*, 2013. **19**(1): p. 35-42.

CHAPTER II

MICROENVIRONMENTAL REGULATORS OF STEM CELL DIFFERENTIATION

Substrate elasticity modulates the responsiveness of mesenchymal stem cells to commitment cues

Manuscript submitted to Integrative Biology
Received July 28, 2014

Hoehnel S^{1*}, Gobaa S^{1*}, Lutolf MP¹

¹ Laboratory of Stem Cell Bioengineering, Ecole Polytechnique Fédérale de Lausanne, CH
* The authors contributed equally to the presented work

Corresponding Author:

Prof. Matthias Lutolf
Laboratory of Stem Cell Bioengineering
Institute of Bioengineering
School of Life Sciences
Ecole Polytechnique Federale de Lausanne
CH-1015 Lausanne, Switzerland
Tel: +41216931876, Email: matthias.lutolf@epfl.ch

Abstract

Fate choices of stem cells are regulated in response to a complex array of biochemical and physical signals from their microenvironmental niche. Whereas the molecular composition and the role of mechanical niche cues have been extensively studied, relatively little is known about how both effectors act in concert to modulate stem cell fate. Here we utilized a recently developed artificial niche microarray platform to investigate whether the stiffness of a cell culture substrate influences how niche signaling factors exert their role on adipogenic differentiation of human bone marrow (BM) CD45^{neg} CD105^{pos} mesenchymal stem cells (hMSC). We found that substrate stiffness imposes a strictly non-overlapping range of differentiation, highlighting the dominance of biophysical over the biochemical factors. At a given stiffness, a significant protein-dependent effect on adipogenic differentiation was observed. Furthermore, we show that synergistic interactions between proteins can also be driven by the substrate stiffness. Our results thus highlight the importance of considering the mechanical properties of a target tissue when investigating biochemical niche signals *in vitro*.

Introduction

Cellular niches are composed of numerous biomolecules including growth factors, cell-cell interaction proteins and extracellular matrix (ECM) signals. Apart from these biochemical regulators, various stem cell types have been shown to alter their fate in response to biophysical properties of the niche including its elasticity [1] or topography [2, 3]. For instance, human MSCs actively sense the mechanical properties of their environment to differentially commit to osteogenic, myogenic or neuronal lineages depending on the elasticity of their substrates [4-6]. However, to what extent interactions between biophysical and biochemical niche cues modulate stem cell fate remains unclear [7].

Stem cell niches are complex entities whose effects on stem cell fate are difficult to elucidate directly *in vivo* where the loss of a biomolecule can be readily restored or compensated by other signals in the surrounding. [8] Traditional *in vitro* culture methods are often poorly suited to dissect the complex cocktail of biochemical cues that balance stem cell self-renewal and differentiation. To overcome this limitation, microenvironment arrays have been developed for the screening of extrinsic cell fate regulators via (high-throughput) robotic spotting of biomolecule combinations [9-12].

However, these platforms lack the ability to simultaneously explore biomechanical effectors, as they were produced on glass or acrylamide gels with fixed composition. In an effort to enrich the capabilities of such screening platforms by enabling the study of biochemical regulators in the context of variable substrate stiffness, we have developed artificial niche arrays consisting of poly(ethylene glycol) (PEG)-based hydrogel microwell arrays of variable substrate stiffness wherein each microwell can be functionalized independently with a desired combination of biomacromolecules [13].

In the present work our aim was to better understand the interplay of biochemical and biophysical factors that control adipogenic differentiation of human bone marrow MSCs.

Human bone-marrow nestin-positive cells were shown to have the capacity to form hematopoiesis-supportive mesenspheres [14], similarly to mouse nestin-GFP⁺ mesenchymal stem cells that have been identified as one of the various niche cell population for HSCs in the murine bone marrow [15]. Because nestin is an intermediate filament with intracellular cytoplasmic localization, it is a disadvantageous marker for the prospective isolation of stem cells, especially human cells. Candidate cell surface markers were identified to allow the isolation of human bone marrow nestin^{pos} cells. Human MSCs expressing the transforming growth factor b (TGF-b) receptor III endoglin/CD105, a marker also used for osteoprogenitor cells [16] and the melanoma cell adhesion molecule MCAM (CD146) were shown to harbor all the sphere forming capacity of CD45^{neg} bone marrow cells [14]. Mesenspheres derived from CD45^{neg} bone marrow show trilineage potential towards osteogenic, chondrogenic and adipogenic lineages and show strong *in vitro* HSC support demonstrated by higher engraftment potential of co-cultured CD34^{pos} cord blood cells [16]. Therefore, nestin^{pos} or CD105^{pos} CD146^{pos} MSCs are candidate HSC niche cells in the human bone marrow. One of the defining features of such a cell is to establish and organize the hematopoietic microenvironment *in vivo* [17]. Within this context a population of self-renewing CD45^{neg} CD146^{pos} perivascular cells with osteo-lineage potential were shown to generate bone and marrow when transplanted subcutaneously into immune-compromised mice [18]. On the contrary, bone marrow adipocytes, another bone marrow cell type arising from mesenchymal stem cells, were identified and proposed to form a “counter niche” for the hematopoietic microenvironment [19]. It was demonstrated that while HSCs are still residing in adipocyte-rich bone marrow, a phenotype linked to disease or age, they are highly quiescent and proliferation to committed progenitors is

actively inhibited. Further high adipocyte-count in the bone marrow lower engraftment time and efficiency post HSC transplantation [19].

Thus, while it is known that adipocyte content correlates inversely with hematopoietic activity, the mechanisms governing adipocytic transformation of the bone marrow are largely unknown. Therefore the understanding of the interplay of environmental cues responsible for inducing or inhibiting mesenchymal niche cell adipogenesis could contribute to the identification of novel drug targets to shorten the time of engraftment of transplanted HSCs and regulate the *in vivo* production of hematopoietic progeny to accelerate the post transplant recovery phase.

We therefore chose to simultaneously interrogate the effect of multiple protein combinations across variable substrate stiffness on the adipogenic differentiation of human BM CD45^{neg} CD105^{pos} CD146^{pos} MSCs. This approach allowed us to hierarchically classify the importance of each niche cue in inducing differentiation. We demonstrate that substrate stiffness always overrides the effect of biochemical signals. However, within stiffness categories, the action of proteins accounts for a large part of the adipogenic differentiation with protein effects that are either dominant or context-dependent. Our results stress the importance of considering physical microenvironmental parameters when testing the effect of particular biochemical signaling cues on stem cell fate.

Experimental methods

Measurements of substrate stiffness

Hydrogel discs of 1 mm thickness and 50 μl volume were cast between two SigmaCote (Sigma) treated glass slides. Shear moduli (G') of gels, left to swell for 24h prior to measurements, were obtained using a Bohlin Instruments C-VOR rheometer. Swollen hydrogel disks were placed centrally on the bottom plate. The gap size was lowered to 800 μm (compression: 0.2) to avoid gel movement. A linear frequency sweep was carried out from 0.1 to 10 Hz with 5% shear stress constantly applied to measure G' , G'' and the phase angle Θ . As G' values remained constant over the measured frequency range, the average G' was considered as the equilibrium shear modulus of the network.

Artificial niche array preparation

Hydrogel protein arrays were prepared as previously described [13]. In brief, thin PEG hydrogel films formed by two 10kDa PEG precursors with either thiol (TH) or vinylsulfone (VS) reactive groups (NOF corporation) were cast at the bottom of four-well plates (Nunc). Three distinct levels of stiffness were obtained by mixing the precursors at different mass to volume ratios. Excess TH-groups (1.2mM) as well as maleimide-functionalized Protein A (85 $\mu\text{g ml}^{-1}$) were introduced in the bulk PEG hydrogel to allow for covalent binding with maleimide-functionalized proteins or Fc-tagged proteins respectively. A topologically structured silicone stamp, custom-made by microfabrication, was used to emboss the partially cross-linked hydrogel film and to transfer desired proteins or protein combinations to the bottom of the imprinted microstructures, i.e. microwells. To achieve this, proteins and protein combinations were pre-mixed in a 384-microtiter master plate in a 10 μl volume prior to robotic printing using a QArray DNA spotter (Genetix Ltd.). A software interface (QSoft) was programmed to arrange protein combinations on the final array with two randomized designs. Subsequent to printing and embossing, arrays were de-molded, washed with PBS and UV-sterilized. Passivation of the arrays by overnight treatment with a 0.1% (w/v) Pluronic PE6800 (BASF) at 37°C was carried out to minimize non-specific cell attachment to the non-functionalized PEG surface.

Protein screen

Nine proteins were chosen among known MSC signaling cascades; i.e. Wnt-, BMP- and Notch-pathway. Two cell-cell interaction molecules as well as a

fibronectin fragment 9-10 (FN III(9-10)) were also included. A combinatorial screen was performed on the single proteins as well as their combinations of two. A full list of arrayed proteins and respective combinations, concentrations and suppliers are given in (Appendix A). All proteins were provided as recombinant and carrier-free. The bioactivity was guaranteed by the manufacturer. Lyophilized proteins were first reconstituted according to supplier instructions at concentrations between 250 to 1000 $\mu\text{g ml}^{-1}$. Protein candidates not harboring an Fc-tag were modified with a hetero-bifunctional NHS-PEG-maleimide linker (3.5 kDa, JenKem Technology) for covalent binding to excess thiols in the bulk PEG hydrogel. Proteins were prepared as printing solutions composed of the protein or proteins at a final concentration of 50 $\mu\text{g ml}^{-1}$ in PBS or borate buffer (0.1 M, pH8, Sigma-Aldrich), FN III(9-10) at a concentration of 800 $\mu\text{g ml}^{-1}$; all containing 30% (v/v) glycerol.

Cell culture

Human MSCs (hMSC patient 101001) were purchased from Biopredic. Cells were derived from the iliac crest of a 34 year old male donor and phenotypically characterized by FACS for the presence of the surface antigens CD13, CD90, CD73, CD29, CD166, CD105 and for the absence of CD45, CD31 and CD34. MSCs were obtained as passage 1 cells and expanded to passage 3 (p3) in expansion medium containing α -MEM (Gibco) supplemented with 10% fetal calf serum (FCS, Hyclone, batch AUA33984), 2 mM L-glutamine (Sigma), 100 U ml^{-1} penicillin/ streptomycin (Invitrogen) and 1ng ml^{-1} human FGF2 (Peprotech). Expanded hMSCs were stored as aliquots in FCS containing 10% DMSO (Sigma) in liquid nitrogen until use. The adipogenic potential of the p3 cells was verified by culturing hMSCs in adipogenic differentiation medium for 5 to 21 days consisting of low glucose DMEM (Gibco) supplemented with 20% FCS, 0.5 mM IBMX (Sigma), 60 μM indomethacin (Fluka) and 1 μM dexamethasone (Sigma) (data not shown). For array seeding, hMSCs p3 were unfrozen 24h prior to the experiment in expansion medium not containing FGF2. FGF2 was depleted from the expansion medium from this point onwards to avoid interactions of FGF2 with arrayed proteins. Cells were subsequently trypsinized using 0.05% trypsin/EDTA (Invitrogen) and cell density adjusted to 7.5E4 cells per 4 ml seeding volume per array. After 1h incubation, arrays were washed with PBS to remove non-adherent MSCs. Adipogenesis was induced by culturing the cells in the above mentioned differentiation medium for 11 days.

BM human MSCs p3 were seeded atop the arrays and captured within the microwells through gravitational sedimentation, where they attached in the presence of FNIII9-10. Unbound cells between microwells or in microwells harboring no cell-adhesive protein were washed off the array using PBS. Numbers of captured cells at day 0 (CellD0) were Poisson distributed across the whole array. We previously reported an optimal seeding density of $7.5E4$ cells per seeding volume for arrays probing adipogenic differentiation [13]. Resultantly, the majority of the microwells harbor two to four cells per microwell. Also, across the levels of stiffness, no difference in initial cell distributions could be observed.

Following cell capture, microwell arrays were cultured in adipogenic induction medium for a period of 11 days. To examine the effect of different proteins on adipogenic differentiation, proliferation and cell morphology, arrays were fixed at the end of the culture time and stained with Nile Red (lipid vesicles), DAPI (nuclei) or Phalloidin (cytoskeleton) respectively. Cell nuclei were identified using segmentation algorithms on the DAPI channel integrated in MetaMorph. Morphology was assessed by thresholding the Phalloidin signal per microwell. Differentiation was quantified by integrating the thresholded Nile Red signal per microwell. The measured parameters were extracted as indices averaged per total number of cells at day 11 (CellD11) in each respective microwell.

Immunohistochemistry

MSCs on arrays were fixed after 11 days in culture using 4% PFA (Fluka) for 15 min at RT. Adipogenic differentiation was detected by staining lipid content using Nile Red (Sigma, $1\mu\text{g ml}^{-1}$). Nuclei were stained with DAPI (Sigma, $1\mu\text{g ml}^{-1}$). After lipid vesicle imaging, cells on arrays were permeabilized for 5 min using 0.02% Triton-X prior to staining f-actin with Alexa488-phalloidin (Invitrogen, 2U ml^{-1}). Minimal staining volume for arrays is 1 ml to avoid drying-out.

Microscopy and data analysis

All images were acquired with a Zeiss Axio Observer Z1 Inverted Microscope. An incubation chamber controlling temperature and CO₂ levels allowed for live cell imaging. Image mosaics were acquired and reconstituted using MetaMorph software (MDS INC., USA). Full array scans in brightfield were taken at day 0 in order to determine initial cell numbers per well (CellD0). After 11 days of differentiation culture, arrays were stained with DAPI and the

relevant metabolic/ IHC protocol. Scanning was performed field-wise in order to adjust focus variations using an automated custom 'scanslide' script. A multivariate analysis using Generalized Linear Models (GLM) was performed on the entire dataset to explain differentiation and proliferation (R V2.15.1). Models were written to explain the variability of quantified traits by all controlled repressors (initial cell density, protein composition and substrate stiffness plus all possible interactions). The produced averages were obtained by the LSMeans function of SAS software V9.0.

Results and discussion

High-throughput screening of multifactorial microenvironments

Over the past decade a number of signaling pathways have been associated to the regulation of hMSC differentiation. Accordingly, Wnt and BMP signaling predominantly promote osteogenesis [20, 21] even though some reports challenged these findings by showing osteogenesis-inhibitory and pro-adipogenic effects [22, 23]. This suggests that protein actions could be highly context-dependent and possibly linked to other biochemical or biophysical signals. To better understand the multifactorial signaling system that controls hMSC differentiation, we interrogated the role of putative hMSC niche effectors by employing a previously developed artificial niche microarray technology [13]. We arrayed 67 combinations of 11 different proteins on hydrogel substrates with contrasted mechanical properties (Figure 2.1 A). Nine proteins were chosen as agonist or antagonist of Wnt-, BMP- and Notch-signaling pathways as well as two cell-cell or cell-ECM interaction molecules (N-Cadherin and Laminin). We also employed a cell-binding fibronectin fragment (fragment 9 and 10 of the fibronectin type III module, henceforth addressed as FNIII(9-10)) in all the microenvironments to promote cell adhesion.

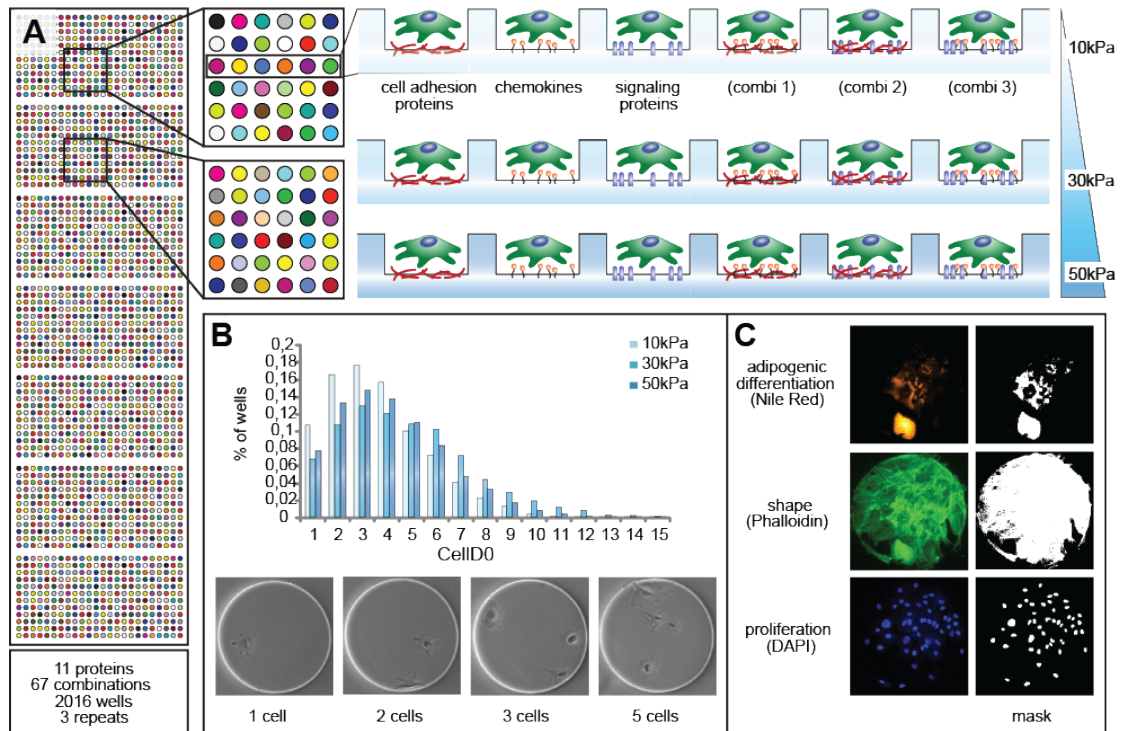


Figure 2. 1 Experimental design. (A) Schematic representation of the performed protein combinatorial assay on substrates of variable stiffness. (B) Seeded MSCs adhere in a similar fashion to all the microwell arrays regardless of the rigidity of the substrate. (C) Quantification of adipogenesis and cell surface area were performed by quantifying Nile Red and Phalloidin, respectively, in every microwell.

Each unique signaling microenvironment was printed 28 times per array. A fully randomized block design ensured that every microenvironment could be observed in at least eight distinct neighboring situations to avoid positional bias and local paracrine effects. The arrays were produced in triplicates allowing the collection of data in 84 microwells per protein combination and stiffness. Since the initial cell density per microwell can strongly influence adipogenic differentiation [13], all niche arrays were imaged within four hours after seeding and the initial cell densities were used as an explanatory variable in the constructed statistical Generalized Linear Model (GLM). Notably, no initial difference in average cell density on arrays of variable matrix stiffness was observed (Figure 2.1 B). After 11 days in adipogenic differentiation culture, cells were fixed and the extent of differentiation, measured by lipid accumulation stained by Nile Red, was quantified for every microwell (Figure 2.1 C). A multivariate statistical analysis was performed on the complete dataset in order to document the relative importance (hierarchy) of each artificial niche and to quantify the contribution of the interactions between niche effectors to adipogenic differentiation.

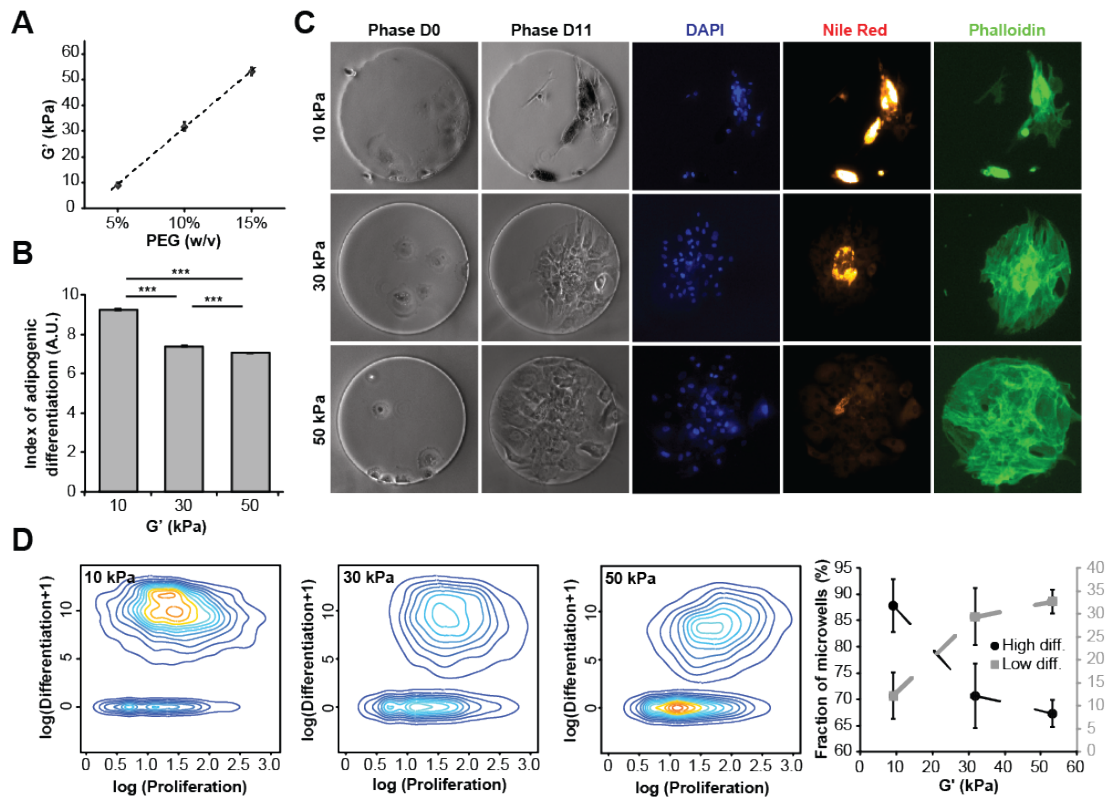


Figure 2. 2 hMSCs culture on artificial niche arrays on varying stiffness. (A) hMSCs were seeded on arrays of low (10kPa), intermediate (30 kPa) and high (50 kPa) elastic modulus, matching the mechanical properties of adipose tissue, muscle and cartilage. (B) Globally increasing stiffness of the substrate decreased adipogenic differentiation of hMSCs (C) as illustrated by Nile Red stainings. (D) Scattering all the observations as a function of proliferation and differentiation reveals the population dynamic behind adipogenic differentiation. A clear decrease in frequency of cells positive to Nile Red staining explains the lower differentiation on stiff substrates. Scale bar is 100 μ m.

We also quantified the hMSC surface area that was obtained by a cytoskeletal stain of fixed cells at the end of the experiment (Figure 2. 1C). The rationale for including this read-out was to be able correlate differentiation with modification of the cell surface area. Indeed, these two traits are strongly negatively correlated ($R = -0.89$) in all of the microenvironments we analyzed (Figure 2. 6C). Higher lipid accumulation always resulted in smaller and increasingly round cells. In order to understand if this smaller surface area on soft gels was the result or was the cause of higher adipogenic differentiation, we quantified cell surface area as early as six hours after cell seeding, before

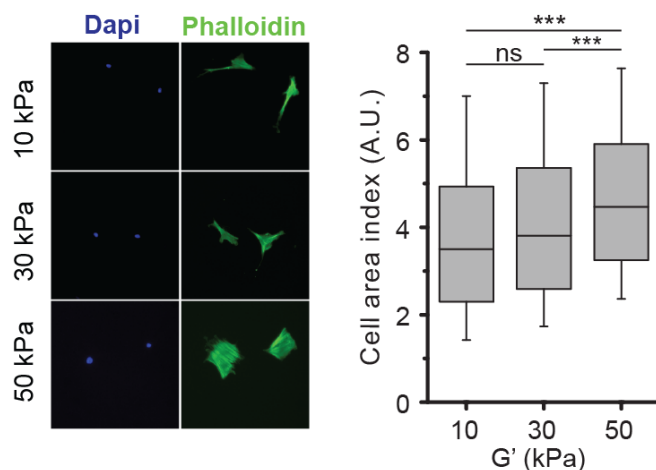


Figure 2. 3 Average effect of elastic modulus (G') on cell surface area within 6h after seeding.

the appearance of any lipid vesicle. We found that hMSC already acquired significantly lower ($p < 0.001$) cell surface areas on soft substrates (Figure 2. 3). This is in line with an extensive body of work demonstrating that stiffness-triggered cytoskeletal reorganization can drive stem cell differentiation [24].

Effect of substrate stiffness on adipogenic differentiation

In an attempt to recapitulate the range of mechanical properties to which hMSC can be exposed to *in vivo* [4], we produced arrays with shear moduli (G') ranging from 9 to 53kPa (corresponding to Young's moduli E of ca. 30-150kPa). This stiffness range was achieved by adapting the concentration of PEG precursors during the hydrogel formation process as previously reported [13] (Figure 2. 2A). As expected, the increase in matrix stiffness resulted in a decreased average adipogenic differentiation (Figure 2. 2B-C). Of note, when the observations made in every microwell were plotted as a function of differentiation and proliferation, hMSCs responses segregated into two distinct populations; one population characterized by quantifiable lipid accumulation and another where differentiation remained under or very close to the detection threshold. The relative importance of each population was significantly dependent on the rigidity of the culture substrate ($p < 0.001$) (Figure 2. 2D). Increasing stiffness clearly prevented a larger fraction of hMSCs to reach detectable lipid vesicle accumulation.

These data confirm that the lineage specification of stem cells can be determined by matrix elasticity [4, 25, 26]. Intriguingly, the observation of adipogenesis on artificial niches also revealed that lower stiffness allows a larger population of MSC to accumulate fat rather than a higher lipid content per differentiated cell. This challenges how the heterogeneous behavior of MSC is explained by imperfect isolation [27], as our data indicates that heterogeneity in hMSC fate can be at least partially driven by environmental cues (Figure 2. 2D).

Stiffness modulates the responsiveness to commitment cues

Our high-throughput artificial niche screening approach offers the unique ability to observe, in a single experiment, the combined effects of biophysical and biochemical cues. This sheds light on synergistic combinations highly instructive of stem cell fate. We first looked at the effect of the spotted protein across three levels of stiffness. We found that proteins could never counteract the effect of matrix elasticity on adipogenesis (Figure 2.4 A). Each stiffness imposed a strictly non-overlapping range of differentiation (Figure 2. 6C).

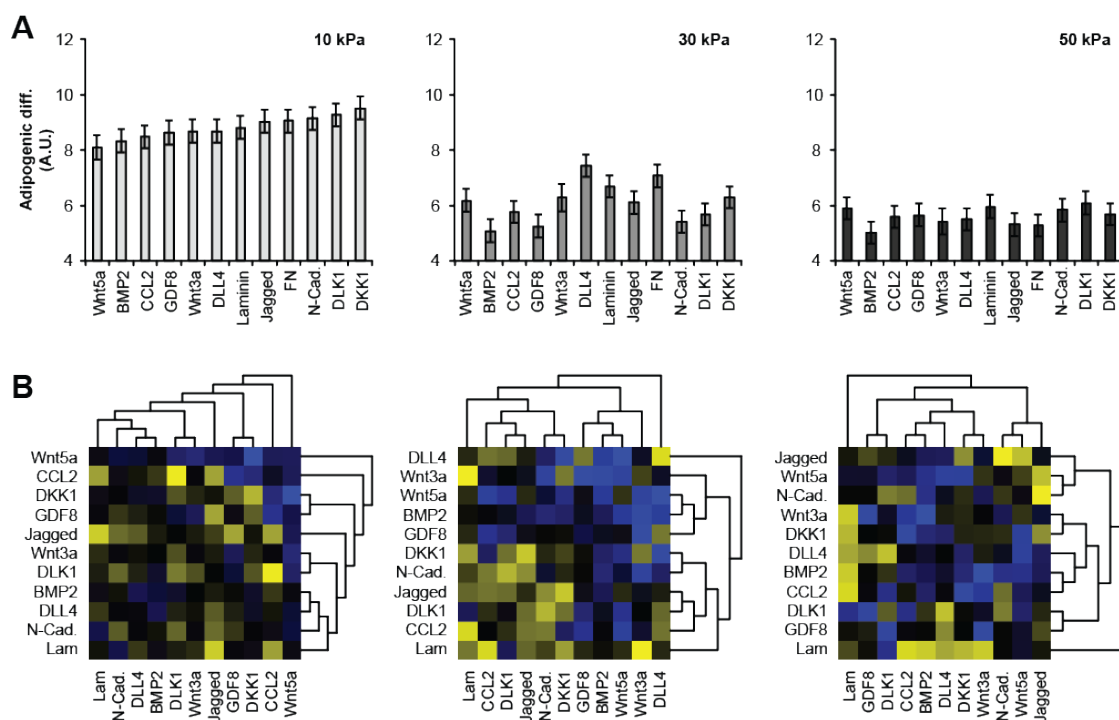


Figure 2. 4 Effects of spotted proteins on adipogenic differentiation of hMSC across soft, intermediate and hard substrates. (A) Considering single proteins alone, the effect of stiffness was clearly larger than the effect of any protein alone. However within each stiffness class, the biochemical microenvironment remained explicative of adipogenic differentiation. (B) Hierarchical clustering illustrating the interactions between proteins, across different stiffness, was performed to discriminate between context-dependent and dominant proteins. The 11 proteins could be classified into dominating or context-dependent effects. Yellow and blue colors correspond to respectively high and low levels of adipogenic differentiation. For every row, the proportion of blue versus yellow squares indicates the consistency of the effect of the corresponding protein.

However, for a given stiffness a significant protein-dependent effect on adipogenesis can be observed. These observations suggest that matrix stiffness is the key factor determining the range of achievable adipogenic differentiation. Within stiffness-imposed windows, biochemical cues seem to fine-tune adipogenic differentiation. Moreover, we observed the effect of proteins to be highly context-dependent. For instance Jagged1, CCL2 or Wnt5a clearly showed a smaller decrease in differentiation upon stiffness increase compared to the prediction of a linear model (Figure 2.5).

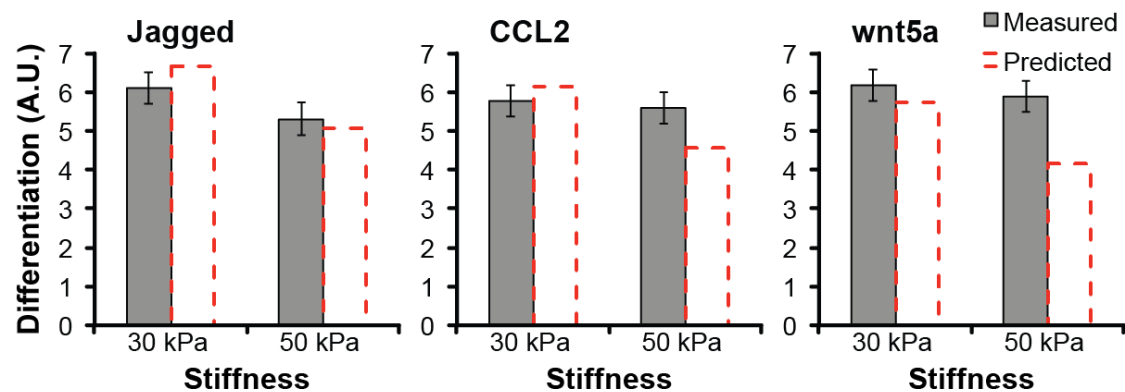


Figure 2. 5 Measured versus predicted effects of spotted proteins on hMSc adipogenic differentiation. This illustrates that the effects of Jagged1, CCL2 and Wnt5a better resist the increase of stiffness than the 8 other proteins used in this experiment.

This context-dependent effect results in a ranking of the proteins effects that is only poorly preserved across the three stiffness ranges, as shown by a Kendall's tau rank correlation coefficient varying between 0.2 and 0.5. Together, these results demonstrate that the interaction between mechanical and biochemical cues is dominated by the mechanical cue and that proteins largely differ in the ability to maintain a consistent effect across different stiffnesses.

Effect of tethered proteins on adipogenic differentiation

Although less dominant than substrate stiffness, some of the 67 tethered protein microenvironments were found to efficiently contribute to adipogenesis. Documenting the effect of each protein or protein combination confirmed the negative effect of BMP2 on adipogenic differentiation on all levels of stiffness (Figure 2.4 A). We also observed that Wnt signaling impaired adipogenic differentiation in our experimental setup. Conversely, the repression of the Wnt pathway by spotting an antagonist (DKK1) favored adipogenesis. Furthermore, triggering Notch signaling (Jagged, DLL4) or

antagonizing it (DLK1, also known as Pref-1) had effects that are dependent on the stiffness of the substrate. Cell-cell or cell-matrix interaction proteins, such as Laminin, Jagged or N-cadherin, and Notch signals showed additive pro-adipogenic effects. Whether these proteins are acting by imposing cytoskeleton remodeling [28, 29] or directly on the lipid metabolism needs to be further elucidated.

When all single proteins were combined, hierarchical clustering showed that every protein had either context-dependent or more dominant effects (Figure 2.4 B). On soft gels, Wnt5a had a dominant effect as it imposed lower adipogenic differentiation and larger cell area when spotted in combination with any of the other 10 proteins. Similarly, Laminin, Jagged1 and N-cadherin had a rather dominant effect, promoting higher differentiation and smaller cell areas. In contrast, proteins such as CCL2 or DLK1 were found in both pro- and anti-adipogenic microenvironments. We also observed that the classification as dominant or context-dependent effectors was strongly altered upon increase of the substrate stiffness. The level of organization in the three stiffness clusters is decreasing with increasing stiffness. Proteins such as BMP2, Wnt5a, Jagged or Laminin 1 are having less and less dominant effect on cell area and on differentiation when rigidity of the substrate increased.

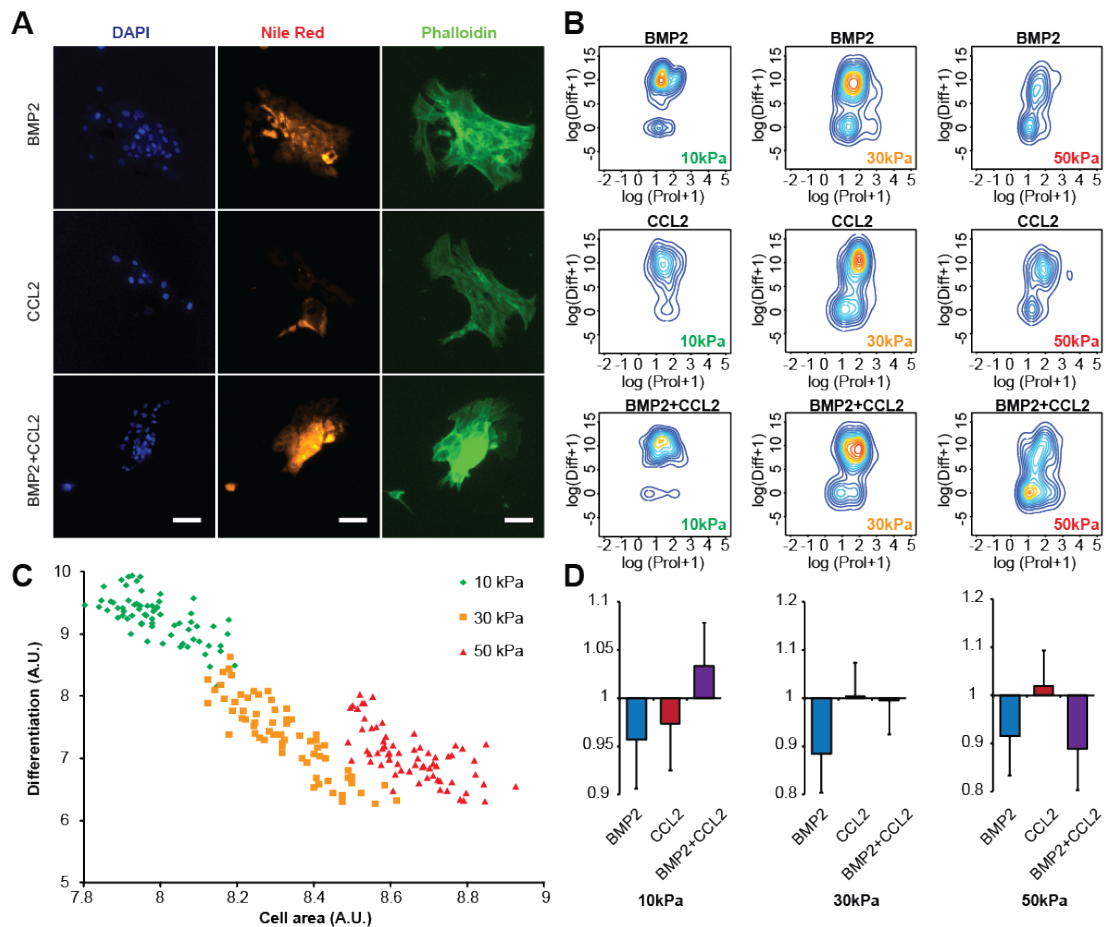


Figure 2. 6 Combination of BMP2 and CCL2 and its strong positive effect on adipogenic differentiation (A) When cultured in microwells containing either BMP2 or CCL2 hMSCs showed reduced levels of adipogenic differentiation, whereas the combination of the two proteins strongly increased lipid vesicle accumulation. (B) At the population level, the negative effect of CCL2 is explained by an average low but consistent accumulation of lipid vesicle. On the contrary, BMP2 was found to decrease the frequency of detectable lipid accumulation. The combination of the two proteins allowed higher quantity and a higher frequency of lipid accumulation. (D) This interaction was found to be occurring only for an elastic modulus approaching the elastic modulus of native adipose tissue (here $G' = 10\text{kPa}$). (C) Scatterplot representing the strong negative correlation between hMSC adipogenic differentiation and surface area. This correlation shows also that the effect of substrate stiffness overrides the spotted biochemical cues.

The effect of other proteins such as CCL2, DKK or DLK1 remained context-dependent across the investigated stiffness range. When all the combinations were taken into account, the negative correlation of substrate stiffness and adipogenesis was maintained for all protein combinations (Figure 2.4). We demonstrate how the mechanical stimulus can synergistically enhance or repress a given biochemical cue. We rule out that the immobilized proteins themselves can serve as mechanical triggers through differential anchoring on varying stiffness [30] as the adhesion on the PEG microwell arrays was mediated by a short fragment of fibronectin in all the conditions.

Furthermore, through our designed immobilization scheme of proteins via (i) Michael-type addition and (ii) incorporated Protein A, the amount of reaction sites was held constant and a possible conformation change of proteins consequently unlikely as additionally demonstrated previously by homogeneous immunofluorescence staining of immobilized proteins on varying stiffness [13].

Artificial niche screening reveals synergistic interactions

The artificial niche platform was finally used to investigate synergistic effects arising from 3-way combinations (two proteins across three stiffness domains). Here the platform offers the unique opportunity to contextualize the synergistic interaction and to classify them as stiffness-dependent or stiffness-independent. For instance, we observed that on average both BMP2 and CLL2 lowered adipogenesis when spotted alone on the softest substrates (Figure 2.6 A-B). It appeared that the negative effect of CCL2 was due to an average lower Nile red signal in all microwells containing only this protein, although the frequency of detectable differentiation was very high in the CCL2 microwells. BMP2 had the exact opposite effect, promoting high accumulation of lipid only at a low frequency. Interestingly, when these two proteins were spotted in combination, a microenvironment supporting strong adipogenesis was created. This microenvironment triggered higher lipid accumulation at higher frequency, demonstrating the synergy of the two modes of action. Noticeably, this interaction did not resist the increase of stiffness probably because the negative effect of BMP2 became dominant (Figure 2.6 B and D).

Conclusions

We demonstrate in this study that the elasticity of a given substrate can modulate the responsiveness of mesenchymal stem cells to differentiation signals. The high-throughput modulation of micro-environmental parameters in a single experiment allowed the establishment of a hierarchy of extrinsic cell fate effectors, where mechanical stimuli of adipogenic differentiation override the biochemical one. Moreover, dissecting the determinants of adipogenesis in a systematic fashion shed light on how this process is coordinated at the level of the cell population. We could demonstrate that two concurrent modes-of-action are at play. First, we found that the frequency of positive cells for lipid accumulation was mostly determined by substrate stiffness. But we also demonstrated that the extent of lipid accumulation was preferentially driven by the biochemical context. The intricate action of these two mechanisms was illustrated for example by the synergistic interaction between CCL2 and BMP2, yielding a highly potent microenvironment capable of increasing both frequency and intensity of adipogenesis specifically on low stiffness substrates. Taken together, the presented work emphasizes the need of performing experiments targeted to identify niche signals in a relevant biophysical context.

Acknowledgements

We thank Alessandra Griffa for her support with image analysis. The fibronectin fragment used in this study was generously provided by Mikaël Martino and Jeffrey Hubbell (EPFL, Switzerland). We thank Martin Ehrbar from the University of Zurich for providing recombinant BMP-2. This study was funded by the Swiss National Science Foundation grant CR23I3_143766 and the EU FP7 grant 'BIODESIGN' FP7-NMP-2010-LARGE-4.

References

- [1] Discher, D.E., D.J. Mooney, and P.W. Zandstra, *Growth factors, matrices, and forces combine and control stem cells*. *Science*, 2009. **324**(5935): p. 1673-7.
- [2] Unadkat, H.V., et al., *An algorithm-based topographical biomaterials library to instruct cell fate*. *Proc Natl Acad Sci U S A*, 2011. **108**(40): p. 16565-70.
- [3] Guilak, F., et al., *Control of stem cell fate by physical interactions with the extracellular matrix*. *Cell Stem Cell*, 2009. **5**(1): p. 17-26.
- [4] Engler, A.J., et al., *Matrix elasticity directs stem cell lineage specification*. *Cell*, 2006. **126**(4): p. 677-89.
- [5] Tse, J.R. and A.J. Engler, *Stiffness gradients mimicking in vivo tissue variation regulate mesenchymal stem cell fate*. *PLoS ONE*, 2011. **6**(1): p. e15978.
- [6] Gilbert, P.M., et al., *Substrate elasticity regulates skeletal muscle stem cell self-renewal in culture*. *Science*, 2010. **329**(5995): p. 1078-81.
- [7] MacQueen, L., Y. Sun, and C.A. Simmons, *Mesenchymal stem cell mechanobiology and emerging experimental platforms*. *J R Soc Interface*, 2013. **10**(84): p. 20130179.
- [8] Lutolf, M.P. and J.A. Hubbell, *Synthetic biomaterials as instructive extracellular microenvironments for morphogenesis in tissue engineering*. *Nature Biotechnology*, 2005. **23**(1): p. 47-55.
- [9] Flaim, C.J., et al., *Combinatorial signaling microenvironments for studying stem cell fate*. *Stem Cells Dev*, 2008. **17**(1): p. 29-39.
- [10] Soen, Y., et al., *Exploring the regulation of human neural precursor cell differentiation using arrays of signaling microenvironments*. *Mol Syst Biol*, 2006. **2**: p. 37.
- [11] Derda, R., et al., *Defined substrates for human embryonic stem cell growth identified from surface arrays*. *ACS Chem Biol*, 2007. **2**(5): p. 347-55.
- [12] LaBarge, M.A., et al., *Human mammary progenitor cell fate decisions are products of interactions with combinatorial microenvironments*. *Integr Biol (Camb)*, 2009. **1**(1): p. 70-9.
- [13] Gobaa, S., et al., *Artificial niche microarrays for probing single stem cell fate in high throughput*. *Nat Methods*, 2011. **8**(11): p. 949-55.
- [14] Isern, J., et al., *Self-renewing human bone marrow mesospheres promote hematopoietic stem cell expansion*. *Cell Rep*, 2013. **3**(5): p. 1714-24.
- [15] Mendez-Ferrer, S., et al., *Mesenchymal and haematopoietic stem cells form a unique bone marrow niche*. *Nature*, 2010. **466**(7308): p. 829-34.
- [16] Aslan, H., et al., *Osteogenic differentiation of noncultured immunisolated bone marrow-derived CD105+ cells*. *Stem Cells*, 2006. **24**(7): p. 1728-37.
- [17] Bianco, P., et al., *The meaning, the sense and the significance: translating the science of mesenchymal stem cells into medicine*. *Nat Med*, 2013. **19**(1): p. 35-42.
- [18] Sacchetti, B., et al., *Self-renewing osteoprogenitors in bone marrow sinusoids can organize a hematopoietic microenvironment (vol 131, pg 324, 2007)*. *Cell*, 2008. **133**(5): p. 928-928.
- [19] Naveiras, O., et al., *Bone-marrow adipocytes as negative regulators of the haematopoietic microenvironment*. *Nature*, 2009. **460**(7252): p. 259-63.

- [20] Gori, F., et al., *Differentiation of human marrow stromal precursor cells: bone morphogenetic protein-2 increases OSF2/CBFA1, enhances osteoblast commitment, and inhibits late adipocyte maturation*. J Bone Miner Res, 1999. **14**(9): p. 1522-35.
- [21] Day, T.F., et al., *Wnt/beta-catenin signaling in mesenchymal progenitors controls osteoblast and chondrocyte differentiation during vertebrate skeletogenesis*. Dev Cell, 2005. **8**(5): p. 739-50.
- [22] Boland, G.M., et al., *Wnt 3a promotes proliferation and suppresses osteogenic differentiation of adult human mesenchymal stem cells*. J Cell Biochem, 2004. **93**(6): p. 1210-30.
- [23] Huang, H., et al., *BMP signaling pathway is required for commitment of C3H10T1/2 pluripotent stem cells to the adipocyte lineage*. Proc Natl Acad Sci U S A, 2009. **106**(31): p. 12670-5.
- [24] Sun, Y., C.S. Chen, and J. Fu, *Forcing stem cells to behave: a biophysical perspective of the cellular microenvironment*. Annu Rev Biophys, 2012. **41**: p. 519-42.
- [25] Evans, N.D., et al., *Substrate stiffness affects early differentiation events in embryonic stem cells*. Eur Cell Mater, 2009. **18**: p. 1-13; discussion 13-4.
- [26] Watt, F.M., P.W. Jordan, and C.H. O'Neill, *Cell shape controls terminal differentiation of human epidermal keratinocytes*. Proc Natl Acad Sci U S A, 1988. **85**(15): p. 5576-80.
- [27] Alhadlaq, A. and J.J. Mao, *Mesenchymal stem cells: isolation and therapeutics*. Stem Cells Dev, 2004. **13**(4): p. 436-48.
- [28] D'Souza, B., A. Miyamoto, and G. Weinmaster, *The many facets of Notch ligands*. Oncogene, 2008. **27**(38): p. 5148-67.
- [29] Giniger, E., *Notch signaling and neural connectivity*. Current Opinion in Genetics & Development, 2012. **22**(4): p. 339-346.
- [30] Trappmann, B., et al., *Extracellular-matrix tethering regulates stem-cell fate*. Nat Mater, 2012. **11**(7): p. 642-9.

CHAPTER III

HIGH-THROUGHPUT GENERATION AND MANIPULATION OF CELL SPHEROIDS

U-bottom microwells for the high-throughput generation and long-term culture of cell aggregates

Patent pending

Hoehnel S^{1*}, Brandenburg N^{1*}, Lutolf MP¹

¹ Laboratory of Stem Cell Bioengineering, Ecole Polytechnique Fédérale de Lausanne, CH

* The authors contributed equally to the presented work

Corresponding Author:

Prof. Matthias Lutolf
Laboratory of Stem Cell Bioengineering
Institute of Bioengineering
School of Life Sciences
Ecole Polytechnique Federale de Lausanne
CH-1015 Lausanne, Switzerland
Tel: +41216931876, Email: matthias.lutolf@epfl.ch

Abstract

Historically prevalent two-dimensional (2D) cell culture assays are increasingly replaced by more physiologically relevant yet also more intricate three-dimensional (3D) cell aggregates cultures. The use of such cultures is complicated by considerably high time expenditure and throughput realization. Therefore, parallelization and miniaturization are key requirements for augmenting existing 3D cell culture systems for basic biological and pharmaceutical research. We here report a novel high-density array of U-bottom shaped microwells of desired size, aspect ratio, shape and density. The microwell plates can be generated from a multitude of cell-compatible substrates such as synthetic or naturally derived hydrogels. This technology for example enables the aggregation of a desired cell suspension through simple gravitational sedimentation and also supports the culture and manipulation of aggregates for extended periods of time. Controlled cell aggregate manipulation can be achieved either through bioconjugation of the microwell surface with desirable cell-signalling molecules, or through the delivery of bioactive factors via a microfluidic network underneath the microwell surface. The combination of these characteristics opens the door for high-resolution screenings of physico-chemical and spatio-temporal parameters for the optimization of *in vitro* organoid cultures.

Introduction

Tissues form through cellular self- and re-organization. They represent complex three-dimensional entities composed of specialized cells, adjacent support cells, extra-cellular matrix (ECM) components and other structural elements that continuously interact to ensure and maintain function [1]. Traditional 2D cell culture systems, in which cells are grown in complete isolation from their multifactorial 3D context can only poorly recapitulate tissue-level physiological phenomena such as maintenance, expansion or differentiation of cell types of interest [2]. Not surprisingly, over the past decade experimental designs in cell culture have strongly shifted towards the implementation of more relevant 3D models, such as the culture of cell aggregates [3-5] or the growth of cells in biomimetic 3D microenvironments [6, 7]. Perhaps most strikingly, recent work by Clevers [8-10] and Sasai [11, 12] and their co-workers as well as others [13-15] have shown that *in vitro* some stem cells have the inherent ability to self-organize into tissue- and organ-like structures, termed organoids, if cultured in the appropriate dimensional context. For example, aggregates of pluripotent stem cells have already been induced to self-organize to primitive organ-like structures such as the optic cup [11], the adenohypophysis [12]

or the cerebral cortex [13]. The implications of such 3D organoid culture systems are sensational as they can be used for better understanding developmental processes, for human disease-specific drug discovery and, in the far future, for generating clinically useful building blocks to augment tissue regeneration.

However, current protocols for organoid generation are tedious, highly inefficient and irreproducible [16]. For example, hanging drop systems have been established to reliably form cell clusters in a well-controlled manner [17]. In short, cells are suspended in drops of medium from the lid of a culture plate to induce cell aggregation by gravitational forces. This method is labor- and time-consuming and generally not scalable. While nutrient delivery is ensured to the complete surface of the generated spheroid, medium exchange to enable long-term culture of the aggregates in this format is impossible. Furthermore, only a certain range of sizes for cell clusters can be covered with this system [18].

Alternatively, conventional U-bottom polystyrene 96-well plates are the most widely used culture format for *in vitro* organogenesis assays [11-13, 19]. While this culture format permits a near-natural conformation, i.e. spherical ground cavity, for the production of cell clusters of a wide range of sizes, drawbacks include the difficulty of medium exchange without disturbance of the formed spheroid and lack of throughput.

In another instance, high-density arrays of pyramidal microwells, commercially available as AggreWell™ (Stem Cell Technologies), have been proposed to fill the gap of high-throughput spheroid formation platforms [20]. While the AggreWell™ platform allows the short-term formation of clusters of different sizes, the pyramidal cavity confines the cell clusters in non-natural conformations and shapes, a process, which has been demonstrated to induce aberrant differentiation [21]. Further, the PDMS substrate does not enable nutrient diffusion and the surface is prone to biomolecule adsorption over time [22].

To overcome these limitations, we here propose a novel cell aggregate concept that enables the high-throughput formation and long-term culture of cellular spheroids. Our 3D culture system is composed of an array of high-aspect ratio U-bottom shaped microwells with low pitch sizes and high side walls that can be reproduced various materials such as PDMS and plastics but, more importantly, various hydrogel substrates such as PEG, agarose, alginate or gelatin (Figure 3.3). To fabricate these U-shaped structures, we take advantage of surface tension forces induced by the solvent evaporation of a photo-curable resist. These structures are then moulded into substrate of interest. The advantages of using especially PEG-based hydrogels as substrate materials lie in the high permeability of nutrients,

optimal biocompatibility while ensuring otherwise biological inertness [6]. Furthermore PEG-based substrates permit the selective conjugation of desired biomolecules to the bottom of the microwells, allowing the study of also non-soluble factors on cellular behaviour and aggregate development. By playing on the architecture of the U-bottom microwells, especially the aspect ratio of well depth to diameter, spheroids can be embedded below the surface plane of the culture substrate to minimize disturbance through handling procedures such as movement or medium changes. Minimal pitch sizes in the range of few cell diameters between the wells are sufficient to inhibit single cells resting on these borders, a process that can disturb equal cell distribution in each well and that can exhibit uncontrolled signalling. Additionally, this platform can be applied to deliver biomolecules to the formed aggregates either statically through immobilization on the hydrogel surface or spatio-temporally through integration of microfluidics.

Experimental methods

U-bottom microwell fabrication

Using a Si Bosch process, holes of 400 μ m in diameter were etched 400 μ m deep into silicon substrate. After oxygen plasma treatment of the silicon substrate, UV curable photoresist GM1030 SU-8 (Gersteltec) was inkjet printed into the silicon wells. Using surface tension forces and hydrophilicity of the silicon substrate, the photoresist can wet the microwell wall and form then, upon solvent evaporation, U-shaped structures. Evaporated SU-8 was further cross-linked using UV exposure and processed to allow its adhesion into the wells. Post silanization using Trichloro(1h,1h,2h,2h-perfluorooctyl)-silane, this silicon substrate was used as a pattern for PDMS replica molding, which in return, after silanization, was then used as a molding pattern for the final substrate (e.g PEG hydrogel). This replica molding process allows the replication of the silicon substrate geometry into virtually any desired final substrate.

PEG hydrogel U-bottom microwell arrays were produced by polymerizing a solution of stoichiometrically balanced 10kDa PEG precursors with either thiol (TH) or vinylsulfone (VS) reactive groups (NOF corporation) between the silanized U-bottom microwell stamp in PDMS and a 3-mercaptopropyltrimethoxysilane (MPS)-treated coverslip. The U-bottom microstructured PEG hydrogel arrays bound on one side to the MPS-treated coverslips were then demolded in PBS and subsequently UV sterilized.

Cell culture and Flow Cytometry analysis

Murine Oct4::GFP embryonic stem cells (mESCs) provided by Austin Smith (University of Cambridge) were routinely expanded without feeders in Dulbecco's Modified Eagle Medium (DMEM) supplemented with leukemia inhibitory factor (LIF), 10% ESC screened fetal bovine serum (FBS, Gibco), sodium pyruvate (10mM) and β -mercaptoethanol (0.1 mM), hereafter referred as ES cell medium.

Human mesenchymal stem cells (hMSCs, PT-2501, Lonza) and OP9 murine stromal cells were routinely maintained in α -MEM supplemented with 10% FCS (Hyclone, batch AUA33984) and recombinant human fibroblast growth factor (FGF-2, Peprotech, 1ng/mL).

NIH3T3 fibroblasts, MDA-MB231 human breast cancer cells, C2C12 mouse myoblast cells, NMuMG E9 mouse breast cancer cells and human embryonic kidney (HEK) 293 cells were routinely maintained DMEM supplemented with 10% fetal bovine serum (FBS, Gibco), HEPES (10 mM) and sodium pyruvate (1 mM).

Aggregate formation

The cells were detached using 0.05% trypsin. A cell suspension with a density of interest was prepared (i.e. 3×10^5 cells/mL, 6×10^4 cells/mL, and 1000 cells/mL for achieving 500 cells/microwell, 100 cells/microwell and 1 cell/microwell, respectively) in the cell-type specific media. The U-bottom shaped microwell arrays were cast at the well bottom of 12-well plates and 2mL of the prepared cell solution was added in the well. Prior to increasing the volume of culture medium to 2mL, cells were left to settle down by gravitational sedimentation. The cells were subsequently cultured for 5 days and the respective media were changed every 2-3 days.

Statistical analysis

For two-group analysis, a nonparametric unpaired Kolmogorov-Smirnov test was used. For all cases, p-values less than 0.05 were considered statistically significant. GraphPad Prism 6.0 software was used for all statistical evaluations.

Results

Generation of U-bottom microwells composed of various substrates

U-bottom microwell arrays were fabricated by dispensing defined amounts of the epoxy-based negative photoresist SU-8 through multi-nozzle inkjet printing into pre-etched deep silicon wells (Figure 3.1). The specification of these pre-etched silicon wells underlie no geometrical restrictions. Interwell distances as well as diameter and depth are determined by the etching design and are not limited to restrictions, allowing the fabrication of arrays with user-defined geometries. By taking advantage of the solvent evaporation of the resist and subsequent surface tension forces through hydrophilic interactions with the silicon sidewalls, round structures can be generated at the bottom of the well, resulting in U-bottom microwells.

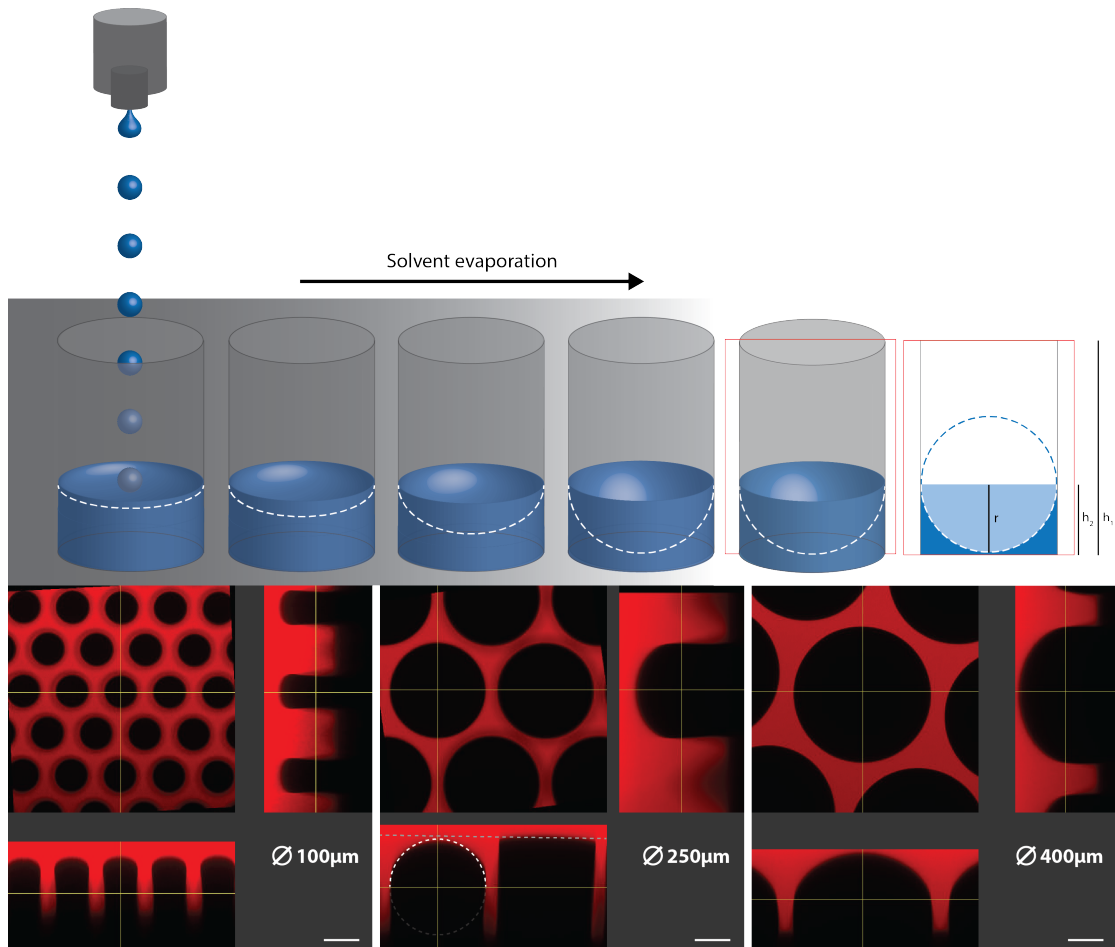


Figure 3. 1 U-bottom microwell fabrication process. U-bottom microwells in silicon are formed through inkjet printing dilute solutions of the epoxy-based photoresist SU-8. Post solvent evaporation, the SU-8 wets the side wall of the well and forms an inverted half spherical bottom shape at the bottom of the wells following surface tension forces. After exposure and processing, the silicon-SU-8 hybrid template can be used for replica moulding to fabricate microwell arrays. A perspective illustration of a single Si well with inverted SU-8 cap at the bottom of the well is shown including a cross-section along the center (in red). r depicts the radius of the inverted cap, that equals the radius of the pre-etched well. h_1 relates to the depth of the well equal to the depth pre-etched in Si. h_2 relates to the total height of printed SU-8 before solvent evaporation, approximating the radius of the pre-etched well. Geometries are determined by the initial etch design in silicon. U-bottom microwells can be produced with varying diameters, depths and inter-well distances (pitch sizes) as demonstrated by confocal images of three different geometries in maleimide-546 labeled PEG hydrogel (bottom panel).

These structures can be produced in any desired size (Figure 3.1 bottom panel) and replica molded into cell culture compatible hydrogel substrates such as PEG.

To test whether substrates of varying stiffness could be fabricated, the U-bottom microwell arrays were molded into PEG with polymer content (w/v) between 1.5% to 10% (Figure 3.2). The lowest PEG stiffness could be generated from 1.5% PEG precursors, corresponding to a stiffness determined by rheology of 150 Pa. At lower precursor content, the microwell structure started to deteriorate.

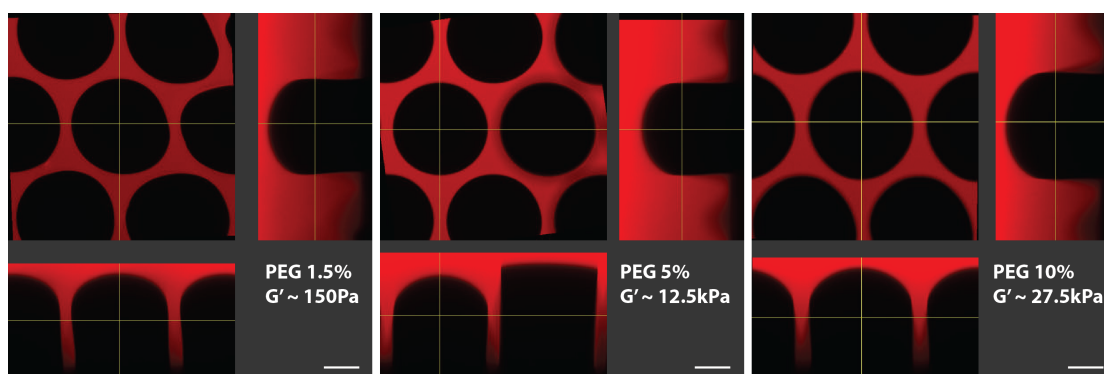


Figure 3. 2 Substrate stiffness. U-bottom microwells can be replica molded in PEG with varying polymer contents (w/v). Confocal images of maleimide-546 labeled PEG in 1.5% (corresponding to $G' \sim 150\text{Pa}$), 5% (corresponding to $G' \sim 12.5\text{kPa}$) and 10% (corresponding to $G' \sim 27.5\text{kPa}$) illustrate the conserved architecture of the microwell structures.

U-bottom microwell arrays can also be replica-molded into PDMS and various other cell-culture compatible substrates, such as agarose, alginate and gelatin (Figure 3.3). The application of U-bottom microwells is therefore not limited to a predetermined substrate, but can be adapted to given experimental restrictions and designs.

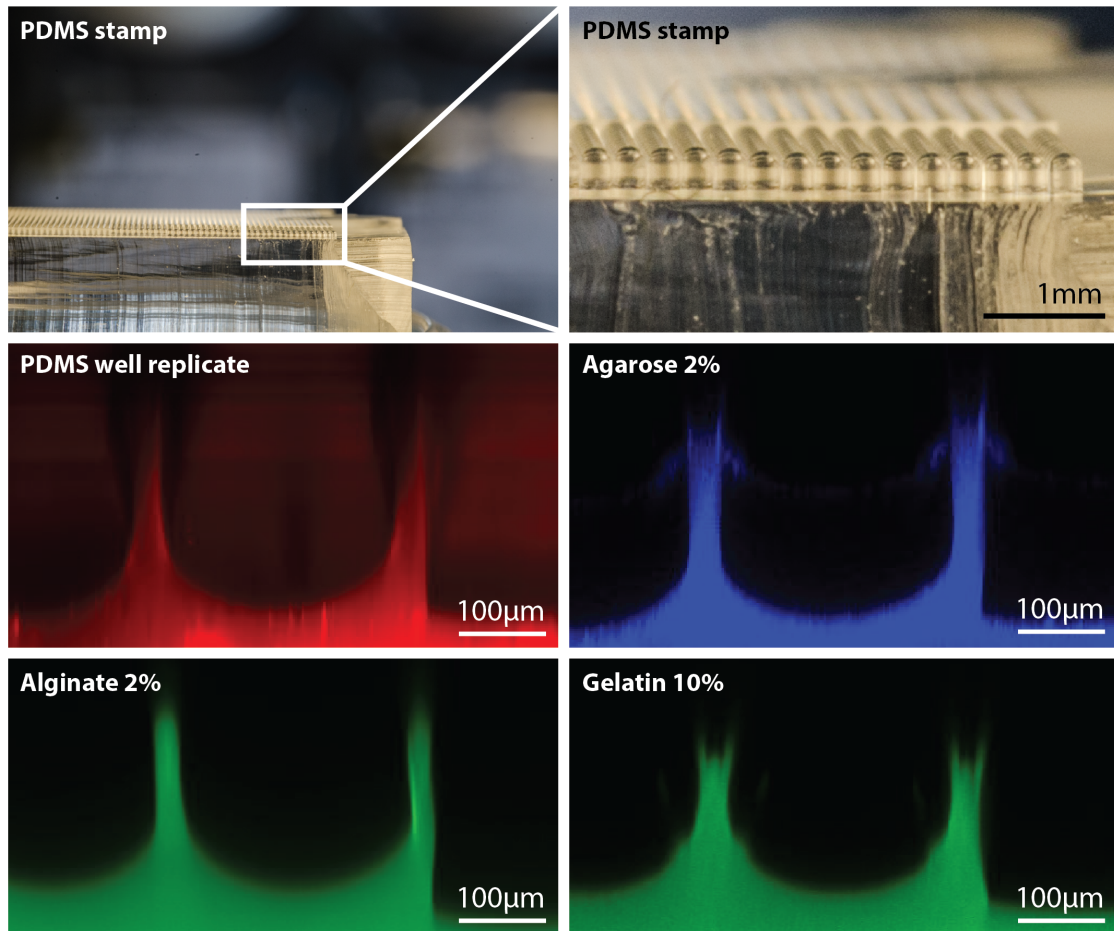


Figure 3. 3 Moldable materials. From the PDMS negative mold, U-bottom microwells can be replicated in a variety of cell culture compatible materials. Negative replica molding of the PDMS stamp to produce U-bottom microwells in PDMS is possible. More importantly, U-bottom microwells can also be reproduced in standard natural hydrogels, such as agarose, alginate and gelatin.

The possibility to generate U-bottom microwells in such hydrated substrates enables the long-term culture of spheroids because nutrient-diffusion is ensured throughout the complete substrate.

Generation of spheroids of different, homogenous sizes

U-bottom microwell arrays in 5% (w/v) PEG hydrogels were used to aggregate and culture transgenic Oct4::eGFP mouse embryonic stem (ES) cells. Aggregate sizes are controlled by modulating the initial cell-seeding density. Densities of 1000, 2000 and 3000 cells per embryoid body (EB) were targeted (Figure 3.4 A-F). Aggregate sizes 24h after seeding were compared between EBs generated in U-bottom microwells with diameters of 400 μ m (μ U400, Figure 3.4 A-C) versus state-of-the-art AggreWells™400 (Figure 3.4 D-F). We observed that as opposed to U-bottom microwells the pyramidal shape of the AggreWell™ cavity lead to the generation of deformed EBs caused by the aggregates adapting the shape of the well (Figure 3.4 A-C, black arrows).

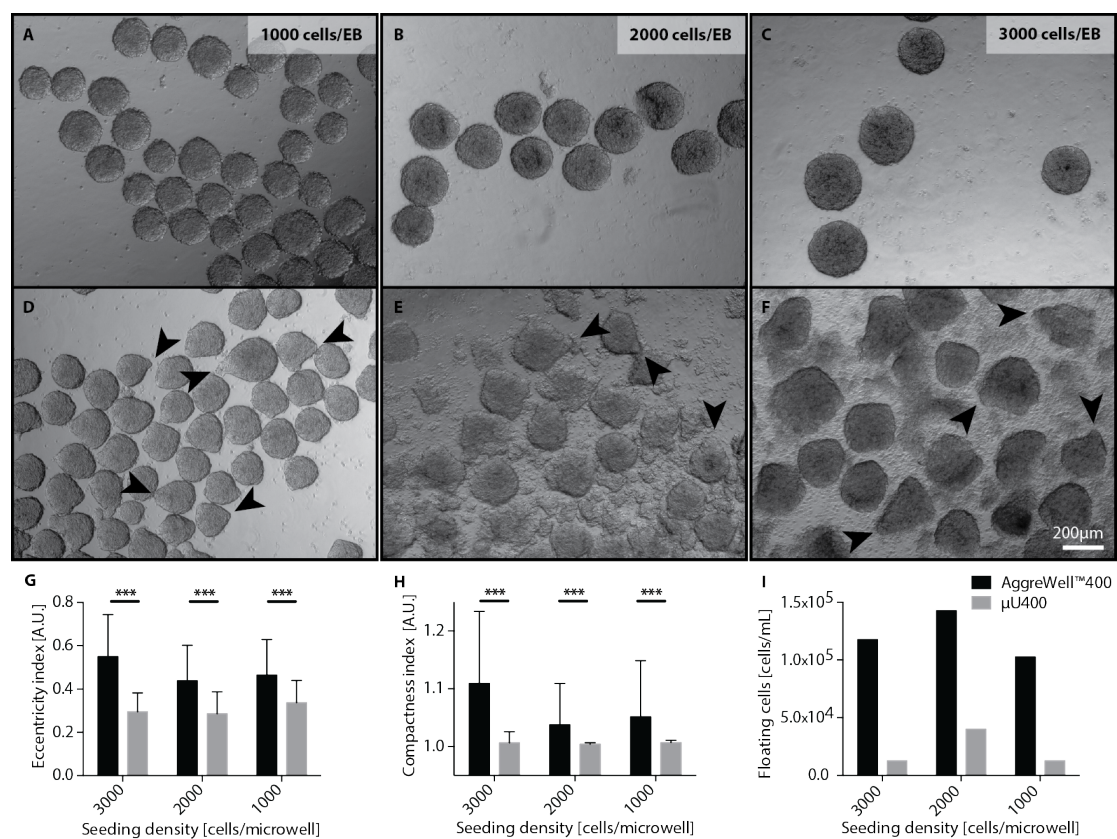


Figure 3. 4 Cell aggregation. Brightfield representations of embryoid bodies (EBs) formed in U-bottom microwells with a diameter of 400 μ m (μ U400, A-C) versus AggreWell™400 (D-F). Cells aggregating in pyramidal shaped microwells adopt a pyramidal shape (D-F, black arrows). This can be seen at different cell seeding densities, for example 500 cells per microwell, 1000 cells per microwells, and 2000 cells per microwells. Cell aggregates formed in U-bottom microwells generally demonstrate higher eccentricity (G) and compactness (H) indexes. At cell densities above 2000 cells/EB less cells contribute to the formed aggregate in AggreWell™400 compared to U-bottom microwells, as illustrated by higher counts of floating cells in the supernatant (I).

We also observed that at higher seeding densities (2000 and 3000 cells/EB) more robust spheroid formation was observed for U-bottom microwells compared to AggreWells™ (Figure 3.4 B-C versus E-F), as demonstrated by the

lower counts of floating cells in the supernatant (Figure 3.4 I). Generally, EBs formed in U-bottom microwells displayed higher indices of eccentricity (Figure 3.4 G) and compactness (Figure 3.4 H). These results indicate that spheroid formation is generally enhanced in U-bottom microwells.

Further we observed that ES cells aggregated and cultured in AggreWells™, frequently started to attach to the PDMS surface within less than 24h (Figure 3.5). The attached aggregates use the borders of sloped pyramidal microwells to crawl along the edges. This lead to the fusion of aggregates and the formation of more disperse spheroid populations.

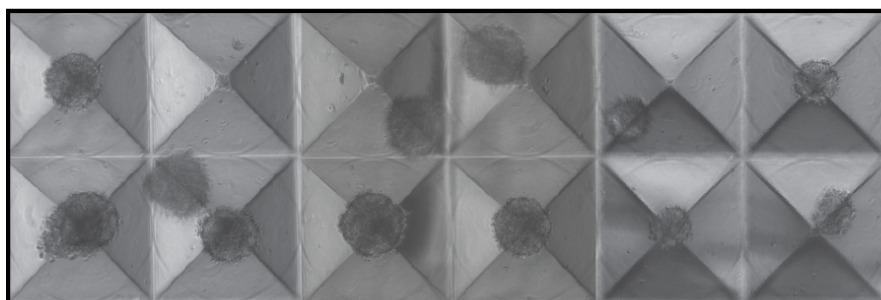


Figure 3. 5 Cell attachment in AggreWell™. Using time-lapse imaging cell aggregates seeded onto AggreWell™ surface (PDMS substrate) were observed to crawl along the microwells walls (bottom). Frequently these cells will move into adjacent wells to fuse with neighboring aggregates.

Aggregate growth, recovery and population dispersity

Spheroid growth was observed over the time course of five days from Oct4::eGFP ES cell aggregates of a starting density of 500 cells between U-bottom microwells with a diameter of 400 μ m in PEG (μ U400) and AggreWell™400 (Figure 3.6). The culture over this time period leads to larger and more monodisperse aggregate populations on U-bottom microwells in PEG (Figure 3.6 C) compared to AggreWell™400 in PDMS (Figure 3.6 B). Medium was exchanged on both array types every 24h for each of the five consecutive days by aspirating the complete volume of old medium and exchanging with the same amount through gentle pipetting at the side wall of the culture plate. Aggregate loss for both AggreWell™400 and U-bottom microwells is comparable and below 10% (data not shown). Aggregates can be recovered by pipetting up and down in the center of the well three times with complete liquid exchange each pipetting round, and subsequently transferring the supernatant to a new culture plate. Complete aggregate recovery can be achieved for both AggreWell™400 and U-bottom microwells (data not shown). Recovered aggregates can be used for other biological analyses. We

determined the expression of Oct4 by cells dissociated cells from cultured EBs on U-bottom microwells by flow cytometry. After five days of culture, 99% of the cells retained their Oct4 expression (Figure 3.6 D).

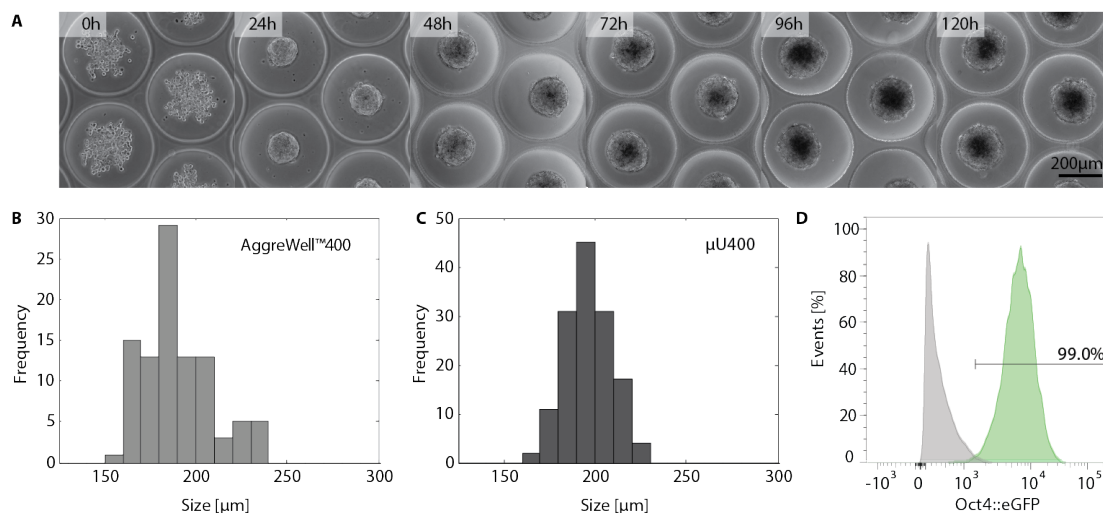


Figure 3. 6 Aggregate growth of murine Oct4::GFP ESCs. The growth of murine Oct4::GFP transgenic embryonic stem cells was assessed during a 5 day time-lapse in U-bottom microwells (A) in comparison to AggreWell™. The size distribution of the aggregates was assessed at day 5. U-bottom microwells show higher monodispersity of the aggregate size compared to the AggreWell™ (B and C). The maintenance of the embryonic pluripotency marker Oct4 was analysed by FACS everyday (data not shown). At day 5 (D), 99.0% of the cells retain Oct4 expression, which is comparable to standard two-dimensional cultures.

Aggregation of various cell types

Aggregates of various cell types were formed within U-bottom microwell arrays at a given starting density (Figure 3.7). C2C12, HEK293T, NIH 3T3 fibroblasts, NMuMG clone E9, MCF-7, OP9 and human mesenchymal stem cells could efficiently form clusters on U-bottom microwells within 24 hours. Importantly, U-bottom microwells can also be used to analyze cells that are unable to aggregate with conventional cell culture methods, as demonstrated by the non-spheroid forming cancer cell line MDA MB231. Within 24 hours the cells formed loosely packed clusters, which compacted further over the subsequent days in culture. These clusters remain stable and can be efficiently harvested after culture, as demonstrated for human MSCs (Figure 3.7 hMSC PT-2501 harvested).

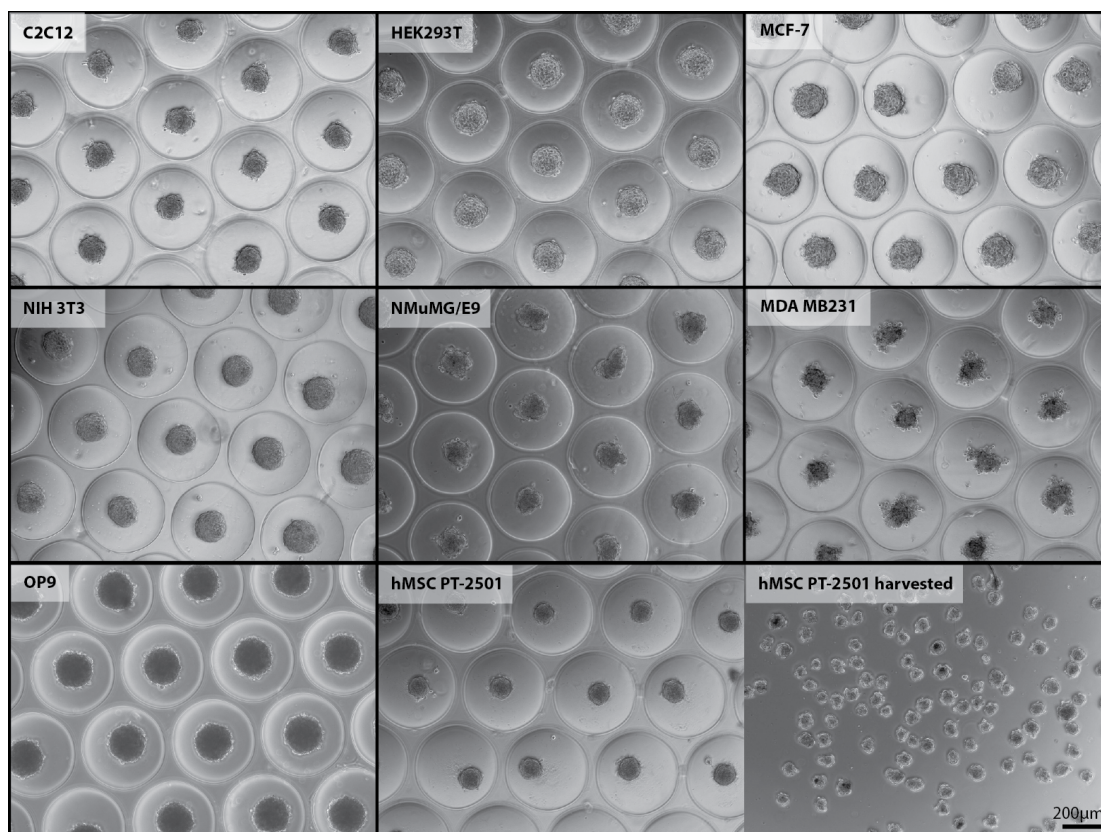


Figure 3. 7 Aggregation of various cell types. Different cell types were seeded onto U-bottom microwell arrays. Brightfield representations of C2C12, HEK293T, MCF-7, NIH3T3 fibroblasts, NMuMG/E9, MDA MB231, OP9 and human MSCs (PT-2501) are shown. The different cell types successfully formed aggregates and could be maintained for 5 days. Also aggregates can be successfully harvested and remain aggregated during this harvesting process (data shown for hMSCs PT-2501 only, as a representative example).

Microwell functionalization and microfluidic biomolecule delivery

In order to study the effect of a given biomolecule on the formation and growth of cellular spheroids, U-bottom microwells can be functionalized with different proteins according to previously described methods [23]. In brief, thin films of protein are formed on an acrylamide gel-coated glass slide on which a PDMS stamp is placed to allow adsorption of the protein onto the PDMS surface. During the subsequent molding step of PEG, the protein is transferred to the hydrogel surface where can be incorporated into the hydrogel network through covalent bonds. As proof of principle we used Alexa-647 labeled BSA to functionalize 5% (w/v) PEG-Alexa488 hydrogels (Figure 3.8 A).

To allow local and temporal biochemical manipulation of cell spheroids after formation without the need of transfer to a new culture plate, microfluidic channels can be generated just below the surface (<500µm distance) to ensure diffusion of the desired molecules within 24h (Figure 3.8 B-

G). As proof of principle FITC-labeled high molecular weight (2000kDa) dextran was perfused through channels beneath U-bottom microwell arrays. The dextran cannot perfuse through the hydrogel network, therefore efficiently and selectively labeling only the inside of the microfluidic channel (Figure 3.8 D-G).

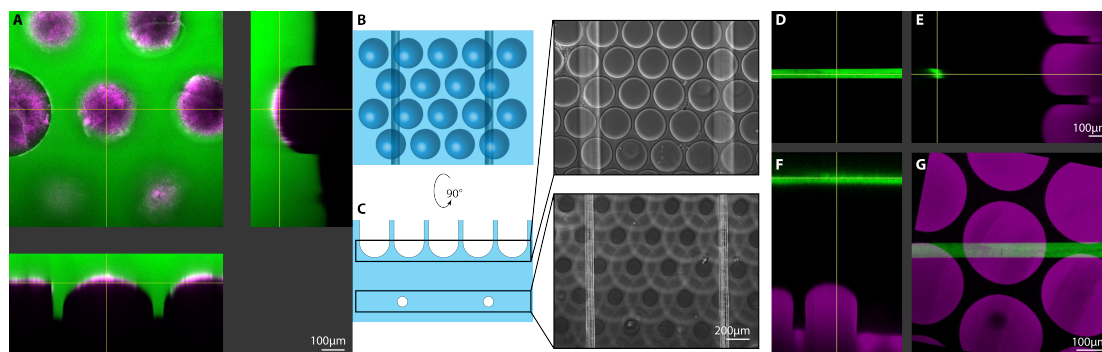


Figure 3. 8 Biomolecule delivery in U-bottom microwells. Confocal representation of a U-bottom shaped microwell (270µm in diameter, 400µm in height, 40µm pitch, fluorescently labeled in green). The bottom of the microwell is functionalized with fluorescently labeled BSA (magenta) (A). Microfluidic channels can be integrated through micro-molding beneath the microwell plane (B-G). Brightfield representations demonstrate the implementation of this concept (B and C). Both the microwell array focal plane (top) and the microfluidic network focal plane (bottom) are shown. Confocal images show the planar (C), and orthogonal views (E and F) of a microfluidic channel perfused with high molecular weight Dextran-FITC. The collapsed stack (G) demonstrates that alignment of the wells and the microfluidic network can be achieved.

Discussion

In the present work, we describe a novel culture platform composed of high-density micrometer-scale U-bottom shaped microwells for the reproducible formation and long-term culture of cellular aggregates. State-of-the-art technologies for cell aggregation [20, 24-27] are poorly suited for reproducible *in vitro* organoid cultures, because they either display insufficient aggregation efficiencies or lack the required throughput for the numbers of aggregates needed for statistically relevant screenings. The most widely used platforms to date with the best compromise of reproducibility and throughput are 96-well U-bottom plates. Nonetheless they remain unsatisfactory to producing multiple thousands of the needed aggregates. Therefore, culture surfaces with miniature well structures that imitate 96-well U-bottom architectures and aspect ratios are required.

However, spherical micrometer-scale pattern fabrication is a main bottleneck in microtechnologies, as most of the standard processes form structures with edges, to which cells preferably attach. By taking advantage of solvent evaporation with resulting surface tension forces at the interface of

viscous liquids on rigid surfaces, we succeed in forming spherical microstructures with high geometrical reproducibility. The main strength of our approach is the decoupling of the microwell diameter, height and the inter-well distance that grants complete freedom in array geometry. The ability to vary these three parameters independently for the first time will be instrumental to move aggregate-based cell cultures to the next level.

Also, we chose to fabricate these U-bottom-shaped microwell arrays with soft and highly hydrated substrates such as hydrogels rather than elastomers, such as PDMS, to mimic more closely the physiological environment of cells and to enable their long-term culture. All tested cell types formed tightly packed aggregates within five days. The aggregation of pluripotent stem cells illustrates the potential of U-bottom microwells for the high-throughput generation of *in vitro* miniature organoids. Cellular spheroids can be efficiently and reproducibly formed by varying initial seeding densities to target a specific cell number per microwell. The fact that nearly all seeded cells participate in aggregate formation, especially at higher cell densities, is of high importance for *in vitro* organogenesis assays, where a defined number of cells initiate organ formation and budding.

Finally, producing these U-bottom microwell arrays in PEG-based substrates potentiates the *in situ* manipulation of the formed aggregates through the immobilization of biofunctional molecules onto the microwell surface [23]. This enables the assessment of the influence of tethered cues on the cultured aggregates. The use of hydrated substrates allows the integration of microfluidic networks underneath the microwell plane to enable the investigation of spatio-temporal biomolecule delivery on the formed organotypic spheroids. Our technology will help to improve existing protocols of organoid cultures and enable the generation of 3D cultures of other clinically relevant tissues.

Acknowledgements

We thank the members of the Center of MicroNanoTechnology (CMi) at EPFL, especially Cyrille Hibert and Joffrey Pernollet, for their valuable help and constant support during all microfabrication processes. We also thank Jürgen Brugger and Mattia Marelli for their open ears and valuable discussions. Our gratitude also goes out to the Bioimaging and Optics platform for their help with microscopy and image analysis.

References

- [1] Li, L. and T. Xie, *Stem cell niche: structure and function*. Annu Rev Cell Dev Biol, 2005. **21**: p. 605-31.
- [2] Griffith, L.G. and M.A. Swartz, *Capturing complex 3D tissue physiology in vitro*. Nat Rev Mol Cell Biol, 2006. **7**(3): p. 211-24.
- [3] Zhang, S., *Beyond the Petri dish*. Nat Biotechnol, 2004. **22**(2): p. 151-2.
- [4] Abbott, A., *Cell culture: biology's new dimension*. Nature, 2003. **424**(6951): p. 870-2.
- [5] Pampaloni, F., E.G. Reynaud, and E.H.K. Stelzer, *The third dimension bridges the gap between cell culture and live tissue*. Nature Reviews Molecular Cell Biology, 2007. **8**(10): p. 839-845.
- [6] Lutolf, M.P. and J.A. Hubbell, *Synthetic biomaterials as instructive extracellular microenvironments for morphogenesis in tissue engineering*. Nature Biotechnology, 2005. **23**(1): p. 47-55.
- [7] Tibbitt, M.W. and K.S. Anseth, *Hydrogels as Extracellular Matrix Mimics for 3D Cell Culture*. Biotechnology and Bioengineering, 2009. **103**(4): p. 655-663.
- [8] Barker, N., et al., *Lgr5(+ve) stem cells drive self-renewal in the stomach and build long-lived gastric units in vitro*. Cell Stem Cell, 2010. **6**(1): p. 25-36.
- [9] Sato, T., et al., *Long-term expansion of epithelial organoids from human colon, adenoma, adenocarcinoma, and Barrett's epithelium*. Gastroenterology, 2011. **141**(5): p. 1762-72.
- [10] Sato, T., et al., *Single Lgr5 stem cells build crypt-villus structures in vitro without a mesenchymal niche*. Nature, 2009. **459**(7244): p. 262-5.
- [11] Eiraku, M., et al., *Self-organizing optic-cup morphogenesis in three-dimensional culture*. Nature, 2011. **472**(7341): p. 51-6.
- [12] Suga, H., et al., *Self-formation of functional adenohypophysis in three-dimensional culture*. Nature, 2011. **480**(7375): p. 57-62.
- [13] Lancaster, M.A., et al., *Cerebral organoids model human brain development and microcephaly*. Nature, 2013. **501**(7467): p. 373-9.
- [14] Koehler, K.R., et al., *Generation of inner ear sensory epithelia from pluripotent stem cells in 3D culture*. Nature, 2013. **500**(7461): p. 217-21.
- [15] Greggio, C., et al., *Artificial three-dimensional niches deconstruct pancreas development in vitro*. Development, 2013. **140**(21): p. 4452-62.
- [16] Sasai, Y., M. Eiraku, and H. Suga, *In vitro organogenesis in three dimensions: self-organising stem cells*. Development, 2012. **139**(22): p. 4111-21.
- [17] Keller, G.M., *In-Vitro Differentiation of Embryonic Stem-Cells*. Current Opinion in Cell Biology, 1995. **7**(6): p. 862-869.
- [18] Lin, R.Z. and H.Y. Chang, *Recent advances in three-dimensional multicellular spheroid culture for biomedical research*. Biotechnol J, 2008. **3**(9-10): p. 1172-84.
- [19] Nasu, M., et al., *Robust formation and maintenance of continuous stratified cortical neuroepithelium by laminin-containing matrix in mouse ES cell culture*. PLoS One, 2012. **7**(12): p. e53024.
- [20] Ungrin, M.D., et al., *Reproducible, ultra high-throughput formation of multicellular organization from single cell suspension-derived human embryonic stem cell aggregates*. PLoS One, 2008. **3**(2): p. e1565.
- [21] Shiku, H., et al., *Noninvasive measurement of respiratory activity of mouse embryoid bodies and its correlation with mRNA levels of*

- undifferentiation/differentiation markers*. Mol Biosyst, 2013. **9**(11): p. 2701-11.
- [22] Toepke, M.W. and D.J. Beebe, *PDMS absorption of small molecules and consequences in microfluidic applications*. Lab Chip, 2006. **6**(12): p. 1484-6.
- [23] Kobel, S.A. and M.P. Lutolf, *Fabrication of PEG hydrogel microwell arrays for high-throughput single stem cell culture and analysis*. Methods Mol Biol, 2012. **811**: p. 101-12.
- [24] Giselsbrecht, S., et al., *3D tissue culture substrates produced by microthermoforming of pre-processed polymer films*. Biomed Microdevices, 2006. **8**(3): p. 191-9.
- [25] Chen, C.S., et al., *Shrinky-dink hanging drops: a simple way to form and culture embryoid bodies*. J Vis Exp, 2008(13).
- [26] Choi, Y.Y., et al., *Controlled-size embryoid body formation in concave microwell arrays*. Biomaterials, 2010. **31**(15): p. 4296-303.
- [27] Liu, T., M. Winter, and B. Thierry, *Quasi-spherical microwells on superhydrophobic substrates for long term culture of multicellular spheroids and high throughput assays*. Biomaterials, 2014.

CHAPTER IV

THREE-DIMENSIONAL IN VITRO BONE MARROW MODELS

Generation of 3D *in vitro* bone marrow models

Manuscript in preparation

Hoehnel S¹, Brandenburg N¹, Naveiras O², Lutolf MP¹

¹ Laboratory of Stem Cell Bioengineering, Ecole Polytechnique Fédérale de Lausanne, CH

² Laboratory of Regenerative Hematopoiesis, Ecole Polytechnique Fédérale de Lausanne, CH

Corresponding Author:

Prof. Matthias Lutolf

Laboratory of Stem Cell Bioengineering

Institute of Bioengineering

School of Life Sciences

Ecole Polytechnique Fédérale de Lausanne

CH-1015 Lausanne, Switzerland

Tel: +41216931876, Email: matthias.lutolf@epfl.ch

Abstract

Hematopoietic stem cell (HSC) transplantations are well-established curative therapies for various hematological malignancies. However, achieving adequate HSC numbers from donor tissues is the limiting factor towards transplant efficacy and outcome. The theory that this limitation can be overcome by expanding the HSC population prior to transplantation is the driving force to develop efficient *ex vivo* expansion protocols. The stromal compartment of the bone marrow was early hypothesized to critically influence HSC pool sizes *in vivo* and their expansion *in vitro*. Within this stromal compartment, mesenchymal stem cells (MSCs) expressing nestin were recently identified to constitute the niche for HSCs in the mouse. These MSCs can however only be propagated in three-dimensional (3D) aggregate cultures, termed mesenspheres. Mesensphere protocols rely on single cell deposition in ultra-low adhesion culture vessels. Co-culture methods with HSCs are generally associated with the attachment of these mesenspheres together with a loss of their hematopoietic-supportive abilities. Enabling a three-dimensional bone marrow-like co-culture that better recapitulates the niche environment is suggested to provide means for enhanced HSC expansion. To achieve this goal, we used U-bottom microwell arrays to generate multicellular spheroids of hematopoietic cells together with HSC-supportive OP9 stromal cells. The spheroid maintenance culture of OP9 lead to the induction of adipogenic differentiation similar to the differentiation observed in chemically cued adipogenesis. The 3D co-culture of HSCs together with OP9 significantly inhibited this differentiation process. Compared to 2D co-cultures, 3D bone marrow-mimicking spheroids supported nearly two-fold higher expansion of hematopoietic progenitors. In a next step and to enhance *in vitro* hematopoietic expansion, the paradigm needed to be adapted to the culture of primitive niche cells, as given by the example of CD146^{pos} CD105^{pos} human mesenchymal stem cells. Thus, we demonstrate the ability to generate mesenspheres derived from single cells and in high-throughput using U-bottom microwells. We propose these miniature bone marrow-like spheroids as a promising first step towards the generation of high-throughput 3D bone marrow models that may enable more physiological HSC niche recapitulation and enhanced HSC self-renewal *in vitro*.

Introduction

The necessity for niche cell types to support *ex vivo* hematopoietic cultures has been demonstrated since the early days of *Dexter cultures* [1]. HSCs coexist in the bone marrow with multiple cell types of which MSCs have recently been proposed to constitute the true HSC niche cell *in vivo* [2-4]. However, these MSCs still remain as an ill-defined population of cells with the characteristic capability of trilineage differentiation towards osteoblasts, adipocytes and chondrocytes [5]. These properties may explain early reports wherein osteoblasts and endothelial cells themselves have been implicated as responsible for regulating HSC pool sizes [6-8]. The MSC-HSC niche hypothesis is equally supported by the fact that MSC-like cell lines such as OP9 cells, a stromal cell line derived from the calvaria of neonatal M-CSF deficient mice, efficiently retain HSC activity *in vitro* [9, 10].

Classical hematopoiesis-supportive co-cultures rely on 2D confluent layers of stromal cells on which hematopoietic cells are seeded. Adapting these co-culture systems to recently identified niche MSCs is complicated by the observation that plastic-adherence cultures drastically alter MSC phenotype resulting in a significant drop in their ability to express factors responsible for hematopoietic maintenance [4].

As a result, alternative culture methods for MSCs have been investigated. 3D spheroid cultures for MSCs, also referred to as mesenspheres, have been shown to enable maintenance of multipotency and to critically enhance their differentiation capacity during *ex vivo* culture [11, 12]. Recently, mesenspheres have been shown to also serve as an applicable culture format to maintain hematopoiesis-supportive mesenchymal niche cells expressing nestin both in mouse and in human [3, 4]. Comparative studies between the co-cultures of hematopoietic cells together with MSCs demonstrated that maintenance of the mesensphere phenotype during co-culture was associated with higher nestin expression, reduced spontaneous differentiation of these cells and maintenance of their hematopoietic-supportive characteristics.

Therefore, the generation of 3D models between niche cells and hematopoietic cells to better recapitulate architectural organisation and phenotypic states found in the *in vivo* bone marrow is of high relevance. Indeed it has been recently demonstrated that cartilage pellets formed by human bone marrow MSCs *ex vivo* can generate marrow-like ossicles harbouring bone, CD146^{pos} stroma and hematopoietic cells upon transplantation *in vivo* [13]. Being able to fully generate similar structures *in vitro* is a milestone that has thus far not been achieved.

An underlying reason is that direct co-cultures of hematopoietic cells and hematopoiesis-supportive MSCs lead to phenotypic changes in the niche cell population associated with a decrease in their ability to secrete HSC-supportive factors, largely due to lack of appropriate culture platforms. Enabling a direct 3D co-culture between HSCs and MSCs in mesosphere format is therefore the first step towards implementing a relevant *in vitro* bone marrow-mimicking organoid culture. Such organoid cultures are instrumental to recapitulate the architectural organization of a native bone marrow to enable relevant screening paradigms and eventually to establish functional *in vitro* expansion protocols for HSCs.

Using our novel U-bottom microwell arrays described in Chapter 3, we assessed the generation of adult micro-tissues of the model mesenchymal-like cell line OP9 together with hematopoietic cells. Further, to assess the feasibility of a more relevant co-culture system with primitive cell types, we tested the high-throughput generation of human CD146^{pos} CD105^{pos} mesospheres on this platform as means to provide the basis for generating primitive *in vitro* bone marrow organoids. We were able to show that, using our platform, mesospheres could be derived clonally and in high-throughput. Furthermore, as opposed to plastic cultures, these mesosphere cultures are morphologically resistant to perturbations of medium composition, enabling direct co-cultures of primary bone marrow cells using either mesosphere or hematopoietic medium.

These direct spheroid co-cultures will provide novel insights into the local relationship between stem cells and their niche with respect to the 3D arrangement of the cells and architecture of their environment.

Experimental methods

Cell culture and marker expression analysis by Flow Cytometry

Human MSCs were purchased from Biopredic, Lonza and received from the University Hospital Zurich. MSCs were obtained as passage 1 cells and expanded up to passage 3 (p3) on plastic in maintenance medium containing α -MEM (Gibco) supplemented with 10% fetal calf serum (FCS, Hyclone, batch AUA33984), 2 mM L-glutamine (Sigma), 100 U ml⁻¹ penicillin/ streptomycin (Invitrogen) and 1ng ml⁻¹ human FGF2 (Peprotech). Expanded hMSCs were stored as aliquots in FCS containing 10% DMSO (Sigma) in liquid nitrogen until use. Passaged hMSCs were verified for maintenance of marker expression by flow cytometry by staining with mouse anti-human CD45-Pacific Blue (Lifetechnologies), mouse anti-human CD34-PE-Cy5.5 (Lifetechnologies), mouse anti-human CD105-APC (Lifetechnologies) and mouse anti-human CD146-APC (R&D). An isotype control was used as negative control for positive markers. All antibodies were used at a concentration of 1:50.

OP9 cells were cultured in maintenance medium containing α -MEM (Gibco) supplemented with 10% fetal bovine serum (FBS, Gibco, lot 41F3240K), 2 mM L-glutamine (Sigma), 100 U ml⁻¹ penicillin/ streptomycin (Invitrogen).

Adipogenic controls were induced in adipogenic differentiation medium containing low glucose DMEM (Gibco) supplemented with 20% FCS, 0.5 mM IBMX (Sigma), 60 μ M indomethacin (Fluka) and 1 μ M dexamethasone (Sigma).

Mesosphere culture

For mesosphere culture of human MSCs, cells were plated at low density into Lipidure (NOF Corporation) coated 10cm petri dishes. The mesosphere medium contained 0.1 mM β -mercaptoethanol; 1% nonessential amino acids (Sigma); 1% N2 and 2% B27 supplements (Invitrogen); recombinant human fibroblast growth factor (FGF-2, 20 ng/ml), recombinant human epidermal growth factor (EGF, 20 ng/ml), recombinant human platelet-derived growth factor (PDGF-AB, 20 ng/ml), recombinanthuman oncostatin M (227 aa OSM, 20 ng/ml) and recombinant human IGF-1 (40 ng/ml; Peprotech) in Dulbecco's modified Eagle's medium (DMEM)/F12 (1:1) / human endothelial (1:2) serum-free medium (Invitrogen) and supplemented with 15% chicken embryo extract (CEE).

The cultures were kept at 37°C in a water-jacketed incubator and left untouched for 1 week to prevent cell aggregation.

For passage, spheres were enzymatically dissociated in a solution containing 0.25%

type I collagenase (Gibco) and 20% FBS in PBS for 30 min at 37°C, with mechanical dispersion every 10 min. Cells were washed with PBS once and replated with mesosphere medium on 5% (w/v) PEG U-bottom microwell arrays either as aggregates of cells or single cells and cultured for five days.

CD34^{pos} cord blood culture

Thawed CD34^{pos} cells were cultured in hematopoietic culture medium: StemSpan medium (Stem Cell Technologies) supplemented with TPO (20ng/mL; PeproTech), SCF (100ng/mL; PeproTech), Interleukin-6 (20ng/mL; Gibco), and Flt3-ligand (100ng/mL; PeproTech).

Mice

C57BL/6 mice were purchased from Charles River Laboratories International. Tg(ACTB-DsRed*MST)1Nagy/J mice were bred hemizygous in house. Mice were maintained at the Center for Studying Living Systems (CAV) at the EPFL in microisolator cages. Mice were provided continuously with sterile food, water and bedding.

Isolation and purification of LKS and LKS CD48^{neg}/CD150^{pos} cells FACS

Hematopoietic cells were isolated from the flushed bone marrow of 8–12 week-old donor wildtype and DsRed mice. Cell suspensions were filtered through 40µm cell strainers (BD Biosciences). Prior to lineage depletion using MACS, erythrocytes were eliminated using red blood cell (RBC) lysis buffer (eBiosciences). Cells were stained with 1 µg/ml rat anti-mouse c-kit-PE/Cy7 (BioLegend), 2µg/ml rat anti-mouse Sca-1-APC (BioLegend), 5 µg/ml hamster anti-mouse CD48-Pacific Blue (Biolegend), 0.7 µg/ml rat anti-mouse CD150-PE/Cy5 (Biolegend) Streptavidin-TexasRed (Molecular Probe, Invitrogen) for lineage-positive selection and propidium iodide (PI) to label dead cells. PI^{neg} Lin^{neg} c-Kit^{pos} Sca-1^{pos} (LKS-DsRed) (CD48^{neg} CD150^{pos}) were sorted by FACS on a FACS Aria II instrument (BD Biosciences).

Aggregate formation and co-culture

Stromal cells were detached using 0.05% trypsin. A cell suspension with a cell density of 3 Mio cells/mL was prepared, of which 200 μ L . The U-bottom shaped microwell arrays were casted at the well bottom of 12-well plates and the prepared cell solution was added on top of the microwell array. Prior to increasing the volume of culture medium to 2mL, cells were left to settle down by gravitational sedimentation. The cells were cultured for 5 days and up to 2 weeks and the respective media was changed every 2-3 days.

Histology

Spheroids were harvested by pipetting the complete medium up and down several times and transferring the suspension to a new tube. An equal volume of 4% PFA was added and the spheroids were fixed for 1h at RT. Fixed spheroids were subsequently embedded in 15% sucrose/ 7.5% gelatin solution in 0.12M phosphate buffer prior to flash freezing in isopentane at -70°C. Gelatin blocks were later cut at 10 μ m thickness on a cryostat. Following cryosectioning, samples were stained with hematoxylin and eosin (H&E) and OilRedO. Hematopoietic cells were counter-stained with rat anti-mouse CD45 clone 30-F11. Human MSCs were stained with mouse anti-human CD105 clone SN6.

Real-time quantitative RT-PCR

RNA extraction was performed using TRIzol Reagent (ambion, life technologies) according to the manufacturer's instruction. RNA was co-precipitated using 7.5 μ g RNase-free glycogen (glycoblue, life technologies). cDNA was synthesized using 1 μ g RNA using iScript Select cDNA Synthesis Kit (Bio-Rad) and real-time PCR was carried out with the primer sets, listed in Table 3.1, designed for both human and mouse samples using Power SYBR Green PCR Master Mix (Applied Biosystems) with the Applied Biosystems 7900HT System. The expression of genes of interest was normalized to that of YWHAZ in all samples.

TBP	Forward 5'-3'	ACAGGAGCCAAGAGTGAAGAAC
	Reverse 5'-3'	ACATCACAGCTCCCCACCAT
YWHAZ	Forward 5'-3'	CAAAGACAGCACGCTAATAATGC
	Reverse 5'-3'	GTGGGACAGCATGGATGACA
GAPDH	Forward 5'-3'	GGAGCCAAAAGGGTCATCATCT
	Reverse 5'-3'	GCTAAGCAGTTGGTGGTGCG
18S	Forward 5'-3'	GTAACCCGTTGAACCCATT
	Reverse 5'-3'	GCCTCACTAAACCATCCAATCG
PPARγ	Forward 5'-3'	CCTGCATCTCCACCTTATTATTCT
	Reverse 5'-3'	AAACCCTTGCATCCTTCACA
AdipoQ	Forward 5'-3'	AGCCTCTCAAGAAGGACAAGG
	Reverse 5'-3'	TACACCTGGAGCCAGACTTGG
LPL	Forward 5'-3'	GGCCGCCCTGTACAAGAGA
	Reverse 5'-3'	AACTCCTCCTCCATCCAGTTGA
C/EBPα	Forward 5'-3'	GGTGGACAAGAAGCAACGA
	Reverse 5'-3'	GCGGTCATTGTCACTGGTCA
Pref-1	Forward 5'-3'	CTGAAGGTGTCCATGAAAGAGC
	Reverse 5'-3'	ATGTGGTTGTAGCGCAGGTT
PDGFRα	Forward 5'-3'	GCGCTGACAGTGGCTACATC
	Reverse 5'-3'	TGGTCTCGTCCTCTCTTTGA

Table 4. 1 List of primers. Primers were optimized for use in gene expression analysis in both human and mouse samples.

Statistical analysis

For two-group analysis, a nonparametric unpaired Kolmogorov-Smirnov test was used. For all cases, p-values less than 0.05 were considered statistically significant. GraphPad Prism 6.0 software was used for all statistical evaluations.

Results

3D aggregate culture of OP9 and human MSCs

Aggregates of the murine stromal cell line OP9 and human mesenchymal stem cells were formed by targeting between 1000 and 2000 cells per microwell. Cells were cultured in classic serum-containing medium (α -MEM supplemented with 10% FCS) for five days (in the case of OP9, Figure 4.1 A-C) or for up to two weeks (in the case of human MSCs, Figure 4.1 D-F). Spheroids could be efficiently harvested for further analyses (Figure 4.1 C). During the culture of OP9 in U-bottom microwells, we observed morphological changes of the cell spheroids associated with the accumulation of large quantities of vesicles (Figure 4.1 C zoom).

Human MSCs expressed the surface markers CD105 (endoglin) and CD146 (MCAM) (Figure 4.1 G). MSC clusters efficiently formed in the first days of culture, however over long culture periods, cell cluster size decreased (Figure 4.1 F), indicating low cell survival presumably because the maintenance medium used for the 2D expansion of MSCs is insufficient to support their 3D expansion.

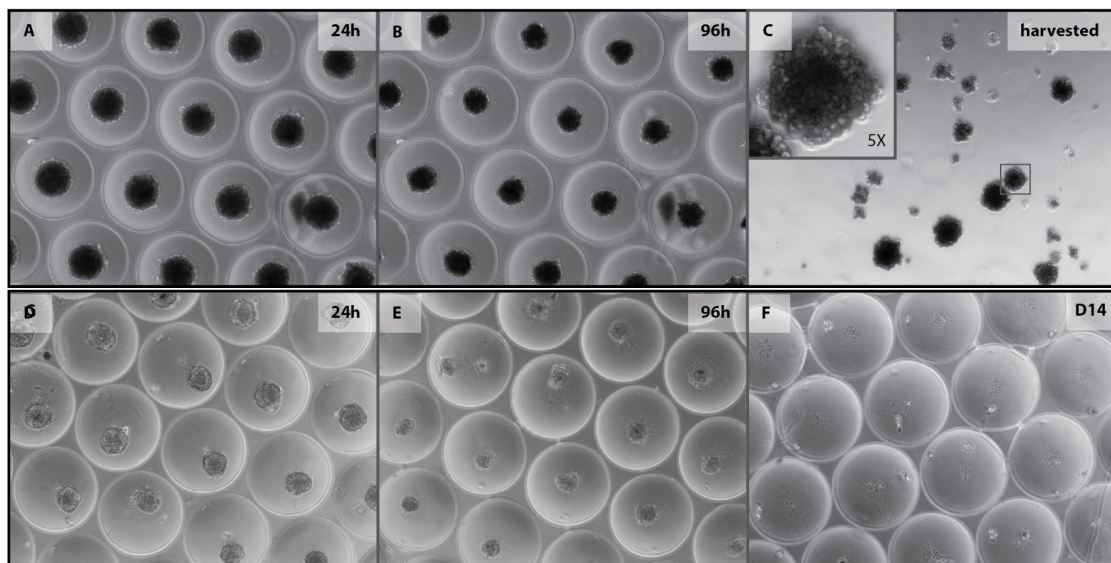
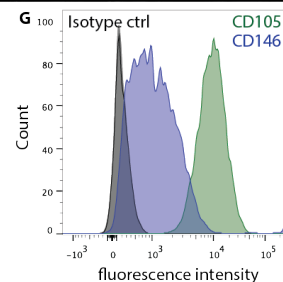


Figure 4. 1 Aggregation of HSC-supportive cells. OP9 cells (A-C) and human mesenchymal stem cells (B-F) expressing CD105 and CD146 (G) were seeded into U-bottom microwells. Within 24h both cell types formed stable cell spheroids (A and D), which were kept in culture for up to two weeks. Within 5 days OP9 clusters exhibited a strong accumulation of lipid vesicles (C). Human MSCs showed low survival in spheroid cultures maintained for two weeks (F).



OP9 lipospheres

To investigate and characterize the accumulation of lipid vesicles in the 3D culture of OP9 cells in U-bottom microwells (Figure 4.1 C zoom), OP9 spheroids were harvested each day for five consecutive days for subsequent qPCR analyses (Figure 4.2 A) and histological stainings (Figure 4.2 B-K). The spheroid culture in maintenance medium was compared to 2D culture of confluent OP9 layers on standard tissue culture plastic either in maintenance or adipogenesis-induction medium. For all culture conditions, using quantitative PCR analyses, we observed the up-regulation of adipogenic genes such as adiponectin (AdipoQ), lipoprotein lipase (LPL) and CCAAT/enhancer-binding protein alpha (CEBP α). The adipogenic differentiation of OP9 cells is also associated with the down-regulation of maintenance genes such as pre-adipocyte factor-1 (Pref-1, also called Dlk1 (Delta-like protein 1)) and platelet-derived growth factor receptor alpha (PDGFR α). This down-regulation of maintenance genes was not observed in the case of 2D spontaneous differentiation of OP9 in maintenance medium as opposed to the induced adipogenic differentiation in 2D and the 3D liposphere culture (Figure 4.2 A red box). The accumulation of lipid vesicles throughout the spheroids can be followed by histological cuts and staining with Oil Red O (Figure 4.2 B-F). The lipospheres are viable for five day in culture and do not exhibit necrotic cores, illustrated by H&E staining (Figure 4.2 G-K). These results confirm existing studies demonstrating that morphological confinement itself can induce cellular differentiation [14]. Within the spheroid culture, OP9 cells are constrained to adopt a small and non-spreading phenotype, which promote their adipogenic differentiation. This spontaneous adipogenesis in a 3D environment in standard maintenance medium presents genetic fingerprints similar to those of the chemical cued adipogenic differentiation of OP9 cells in 2D.

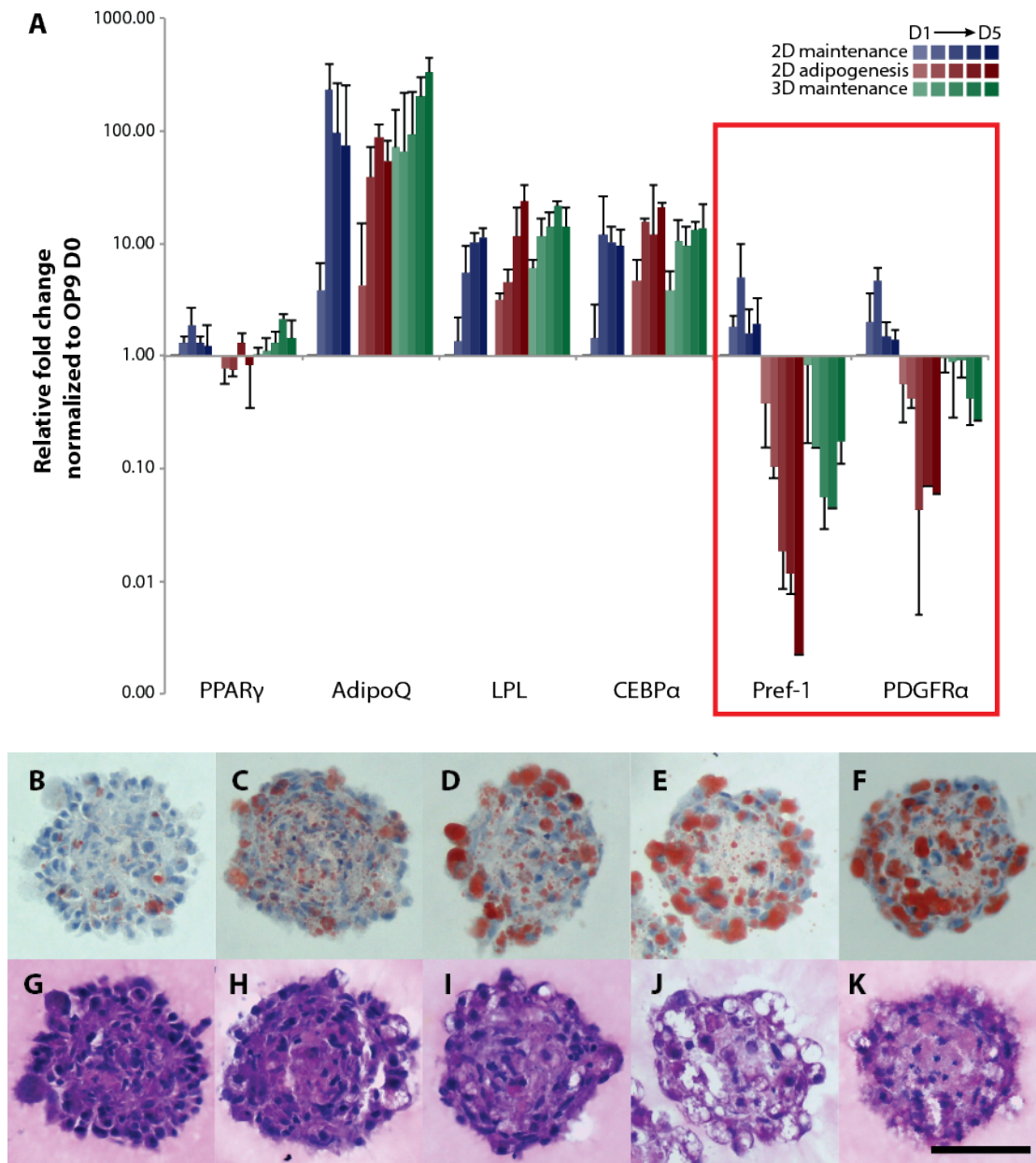


Figure 4. 2 OP9 lipospheres. OP9 cells cultured as spheroids in maintenance medium differentiated towards mature adipocytes, named lipospheres. Time-course quantitative PCR analyses over five days revealed the up-regulation of key adipogenic genes and down-regulation of maintenance genes (red box) in 3D maintenance cultures comparable to levels achieved in 2D differentiation cultures. Histological sections revealed the increasing presence of adipocytes stained by OilRedO over five days (B-F) where B illustrates a cluster at day 1 and F a cluster at day 5. Hematoxylin and eosin (H&E) stainings are shown to illustrate the preserved compactness of the lipospheres. Scale bar is 100 μ m.

Bone marrow-like spheroid co-culture

Using U-bottom microwells, we next investigated the possibility to form 3D *in vitro* bone marrow-like co-culture systems using hematopoietic cells and hematopoiesis-supportive cells, here OP9. OP9 cells were pre-aggregated six hours before addition of hematopoietic cells from the mouse bone marrow (LKS or LKS CD48^{neg} CD150^{pos}; Figure 4.3 A) to ensure compacting of the

supportive cells and allow self-organization observations. To evaluate the number of initial hematopoietic cells per cluster, hematopoietic cells were seeded in U-bottom microwells (Figure 4.3 B) and whole arrays imaged and cell counts performed. Less than 6% of all wells did not harbor any hematopoietic cell (Figure 4.3 F). Hematopoietic cells quickly attached to pre-clustered OP9 cells, as illustrated by overlay images of brightfield OP9 spheroids with LKS-DsRed cells (in red, Figure 4.3 C). Comparative cultures of hematopoietic cells in OP9-conditioned medium (Figure 4.3 D) versus 3D OP9 co-culture (Figure 4.3 E) and 2D OP9 co-culture (Figure 4.3 I), revealed higher numbers of hematopoietic progenitors accumulating in the 3D spheroid co-culture condition. This can also be illustrated by the higher cell counts of hematopoietic cells in the harvested supernatant of the 3D versus 2D co-culture (Figure 4.3 G).

OP9 co-culture spheroids were dissociated and analyzed by flow cytometry to reveal the presence of hematopoietic cells in the spheroid core. Indeed, a population of CD45^{pos} cells was abundant. (Figure 4.3 H, red population).

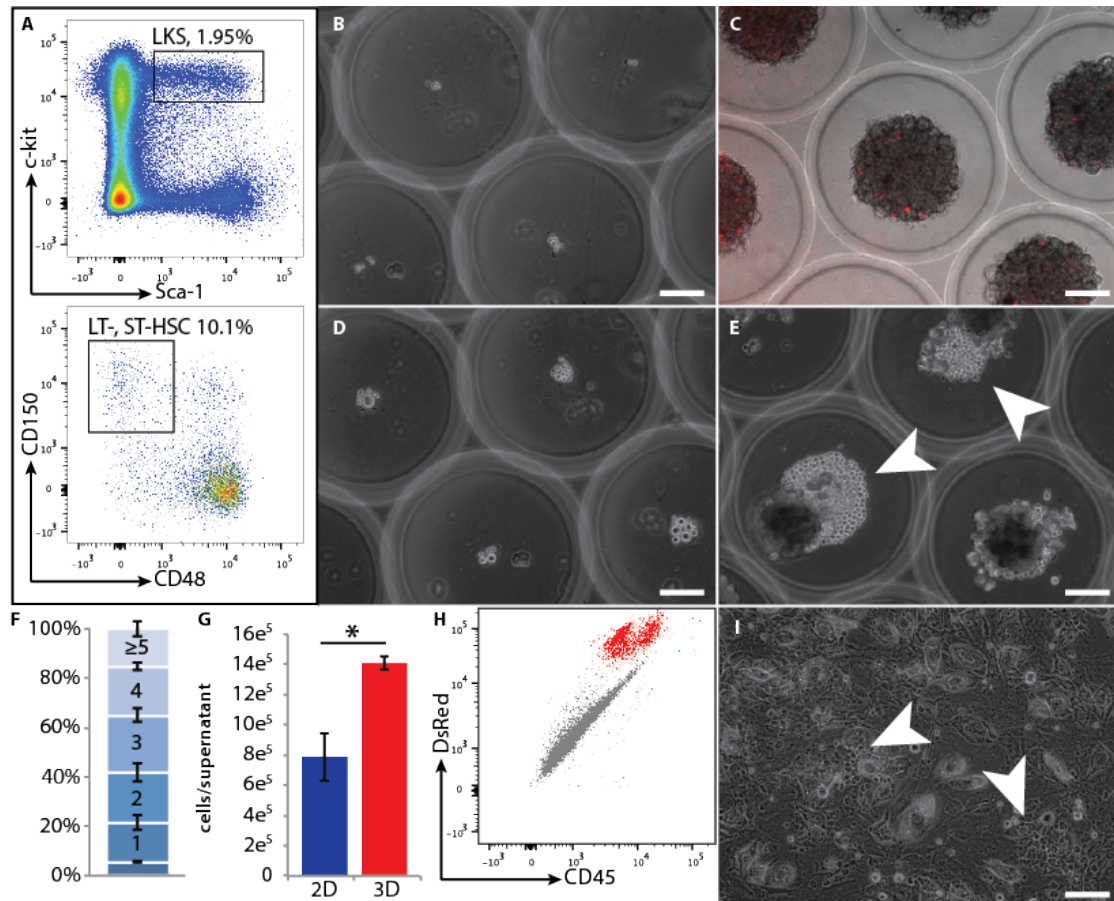


Figure 4. 3 3D *in vitro* bone marrow co-cultures. LKS CD48^{neg} CD150^{pos} bone marrow cells were sorted (A) and seeded in U-bottom microwells (B). The initial distribution of hematopoietic cells was quantified and less than 6% of the microwells remained without any cell (F). OP9 cells were clustered in U-bottom microwells 6 hours prior to HSC seeding on top. To illustrate the co-culture Ds-Red HSCs were also utilized (C). The expansion of HSCs was observed after a five day culture in OP9 conditioned medium (D), OP9 3D co-cultures (E) and OP9 2D co-cultures (I). A significant higher accumulation of hematopoietic cells was observed in the 3D co-culture condition (E, arrows). In 2D co-cultures the HSCs migrated beneath the stromal layer to form cobble stones. (I, arrows). A two-fold higher count of hematopoietic cells was observed in the supernatant of the 3D co-culture. The presence of CD45 positive cells was verified by dissociating OP9 spheroids after the five day co-culture (H, red population). Scale bar is 100 μm.

Further histological sections and stainings after the five-day co-culture demonstrated decreased accumulation of lipid vesicles throughout the spheroid and especially within the core (Figure 4.4 C) compared to lipospheres cultured without the presence of hematopoietic cells (Figure 4.4 A). These results strongly suggest the occurrence of molecular and cellular interactions between hematopoietic cells and OP9 stromal cells to induce progenitor expansion and to inhibit anti-hematopoietic processes such as adipogenesis.

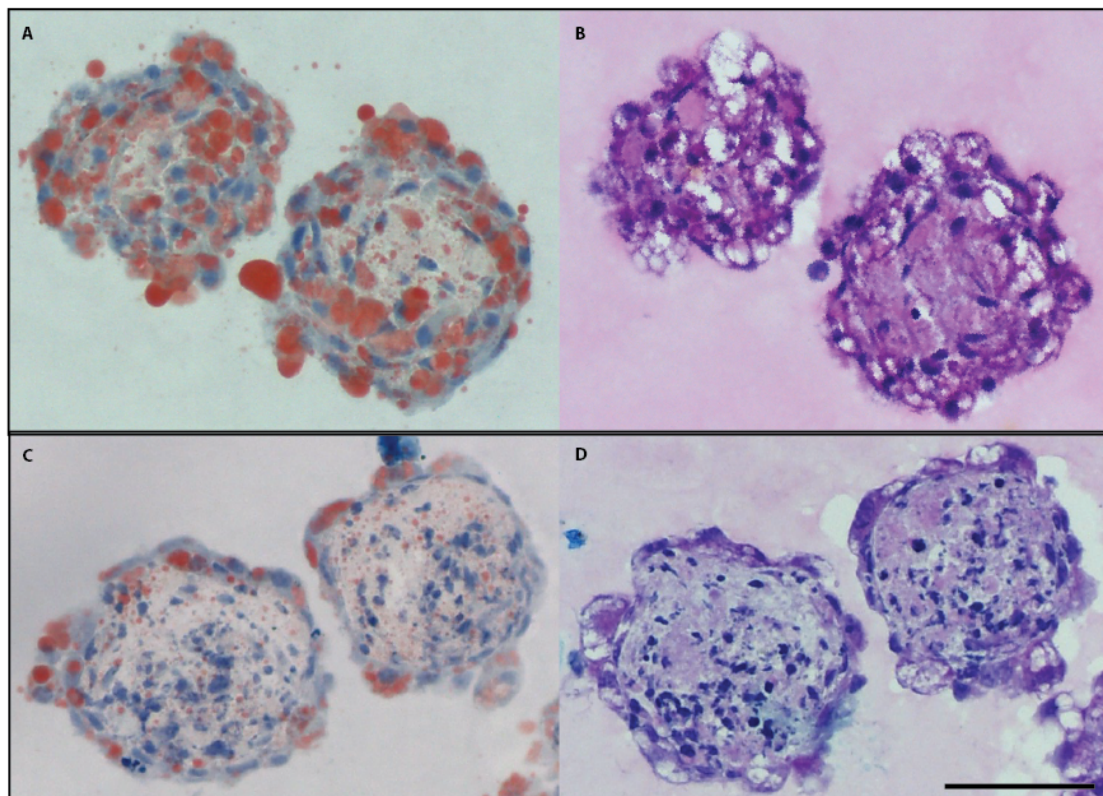


Figure 4. 4 Histology of lipospheres and co-culture spheroids. (A) OP9 cells cultured for 5 days in aggregates accumulate large amounts of lipid vesicles as stained by OilRedO. (B) The co-culture of OP9 together with HSCs decreases the amount of lipid vesicles observed at day 5 especially in the center of the aggregate (C). Corresponding H&E stainings are shown in B and D. Scale bar is 100 μ m.

However, OP9 stromal cells may not pose as the ideal model cell type to maintain hematopoiesis in a 3D bone marrow model *in vitro*. Indeed these cells undergo spontaneous adipogenic differentiation, a process known to negatively influence hematopoiesis *in vivo* [15]. We therefore investigated how such 3D bone marrow models could be formed using primitive HSC-niche cells, i.e. human CD146^{pos} CD105^{pos} mesenchymal stem cells.

High-throughput generation of human mesenspheres

Classic mesenchymal culture media do not permit the long-term survival of human MSCs in aggregate cultures (Figure 4.1). We therefore investigated the maintenance and growth of CD105^{pos} CD146^{pos} human mesenchymal stem cells in hematopoiesis-supportive mesensphere cultures [4].

Mesensphere cultures on flat polystyrene surfaces frequently lead to the fusion of multiple mesenspheres, resulting in disperse spheroid populations (Figure 4.5 A). To generate mono-disperse mesensphere populations, human mesenspheres can be derived through either aggregate culture of multiple MSCs or clonally from targeting single cells within U-bottom microwells (Figure 4.5 C and D). The cells display continuous survival and linear growth over a period of five days as opposed to the quiescence and cell death observed when culturing in serum-containing 2D maintenance medium (Figure 4.5 B).

The spheroid formation efficiency from single cells derived from a passaged 2D mesensphere culture was determined at $62.5 \pm 2.4\%$. Clonal mesenspheres reached an average size of $36.2 \pm 3.3 \mu\text{m}$. Flow cytometry analysis of CD105 and CD146 revealed marker retention throughout mesensphere expansion cultures (Figure 4.5 F) as well as percentage of live cells within spheroids at around 85%.

Deriving clonal mesenspheres in high-throughput and without the fear of fusion as observed on flat plastic cultures poses the first step to the generation of primitive 3D direct bone-marrow co-cultures. In order to maintain these co-cultures *in vitro* we tested whether the mesensphere phenotype could be preserved through medium changes to hematopoiesis-supportive medium. We seeded CD34^{pos} cord blood cells on top of five day expanded mesenspheres in PEG U-bottom microwells and observed no change in mesensphere culture, i.e. the cells remained compact spheroids and did not start attaching.

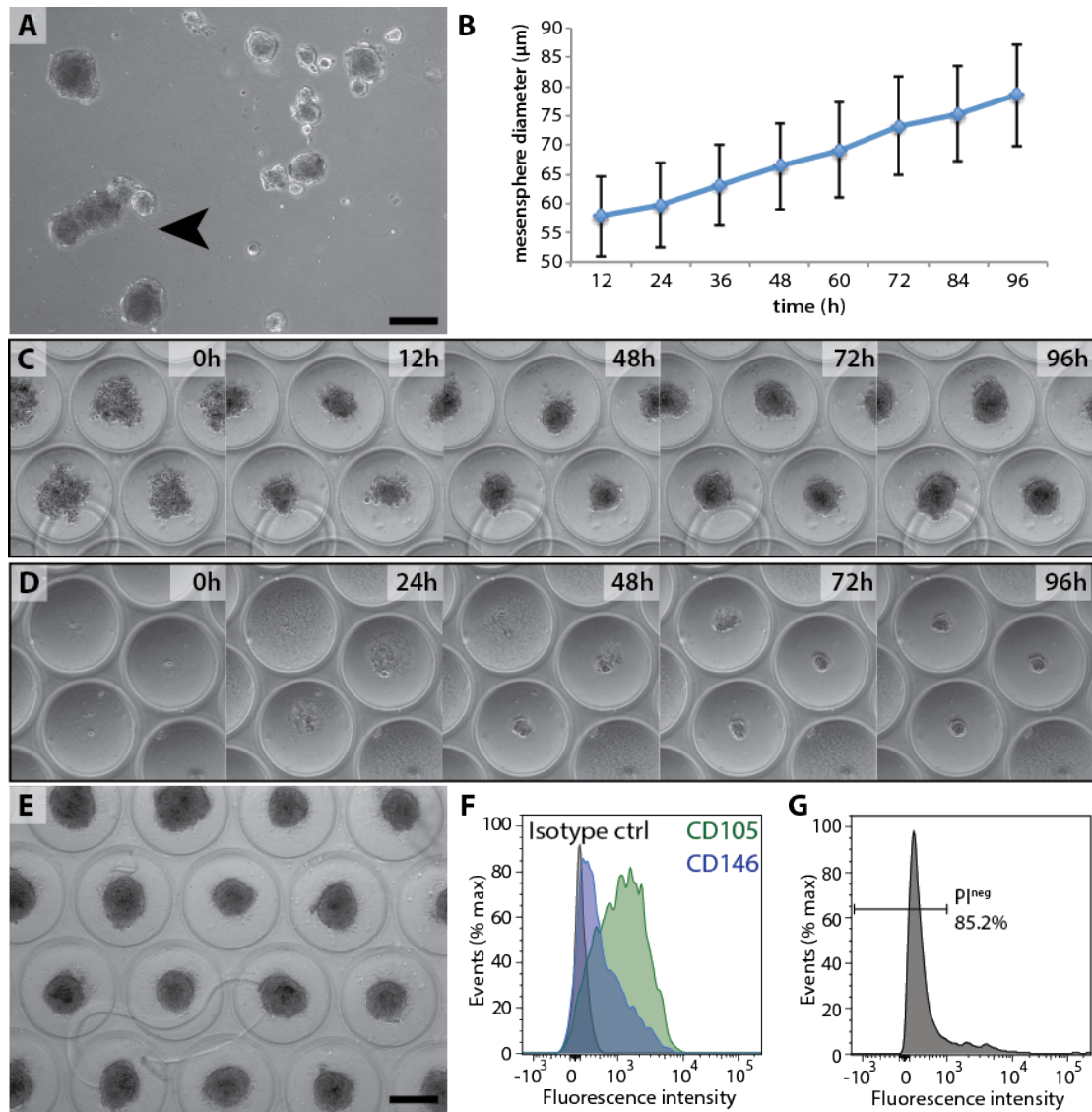


Figure 4. 5 High-throughput mesensphere cultures. (A) Mesensphere cultures on plastic frequently result in fusion of spheroids. (B) Human MSCs grown in mesensphere medium on PEG U-bottom microwell arrays display constant linear growth curves as determined by average diameters. Mesenspheres can be derived through (C) aggregate culture or (D) clonally from single cells. (E) Medium change to non-mesensphere medium does not lead to cell attachment. (F-G) Mesenspheres on U-bottom microwells retain expression of CD146 (blue) and CD105 (green) and within mesenspheres 85% of the cells are alive as marked by PI staining. Scale bar is 200µm.

Discussion

The aim of this study was to demonstrate that 3D bone marrow organoids can be formed using U-bottom microwell arrays and to evaluate their physiological and functional relevance for clinical applications. 3D cultures of bone marrow MSC niche cells have been shown to better preserve their self-renewal capacities and their ability to support functional HSCs [3, 4]. However, direct co-culture methods of hematopoietic cells together with MSCs currently are not sufficient to maintain their phenotype as MSCs tend to attach and lose their hematopoiesis-supportive characteristics. To overcome these limitations, we demonstrate here how sphere cultures of hematopoiesis-supportive OP9 stromal cells can be initiated and how the 3D co-culture together with murine hematopoietic cells from the bone marrow enable the study of the direct cellular interactions between these two cell types.

Applying the U-bottom microwell platform described in Chapter 3, we report here that aggregates of OP9 stromal cells as well as human MSCs can be formed within few hours. While MSCs show reduced viability and survival over time in a classic 2D maintenance medium, OP9 stromal cells acquired a somewhat surprising phenotype. Within these spheroids, we observed an increased adipogenic differentiation as illustrated by the vast accumulation of lipid vesicles and the up-regulation of adipogenic genes such as adiponectin, LPL and CEBP α and down-regulation of maintenance genes such as Pref-1 and PDGFR α . Importantly, we demonstrated that this adipogenic differentiation does not result from the chemical cueing of the cells through adipogenic inductive factors such as IBMX, Indomethacin or Insulin but is the result of the confinement of the cells in a closely packed spheroid format.

Co-cultures are possible by either initially seeding multiple cell types simultaneously or through the addition of additional cell types to an ongoing spheroid culture. We decided to initiate co-culture by addition of LKS CD48^{neg} CD150^{pos} hematopoietic cells to an already aggregated OP9 culture to avoid biased observations of HSCs in the core of the spheroid from the start of the experiment. We observed that this co-culture format inhibits the strong adipogenic differentiation observed in an OP9 culture alone and instead leads to an increased production of hematopoietic cells in comparison to conditioned medium cultures or 2D co-cultures. The co-culture spheroids exhibited a significant loss of lipid vesicles especially within the core of the aggregate, indicating the presence of anti-adipogenic signaling. Dissociation of these OP9-HSC spheres revealed the presence of CD45 positive cells within

these structures. In order to validate the maintenance of primitive hematopoietic cells, further assays are needed to characterize these CD45 positive cells within the spheroids. Such functional analyses include the evaluation of colony forming units of these dissociated CD45 cells as well ectopic transplantation of co-culture spheroids underneath the renal capsule [16] or subcutaneously [13] to assess whether spheroids can similarly form functional bone-marrow ossicles *in vivo* and whether incorporated CD45 marked cells can contribute to the formation of marrow within these structures. In a final step to evaluate the hematopoietic expansion potential of these 3D co-culture systems, HSC transplantations will be needed to evaluate the potential of *in vitro* expanded hematopoietic cells to contribute to the long-term reconstitution the blood system.

Considering our proposed model system, OP9 stromal cells do not pose as the ideal cell type to mimic 3D hematopoietic niches *in vitro*, especially given the fact that these cells undergo spontaneous adipogenic differentiation, a process known to counter-balance the hematopoietic activity of the bone marrow *in vivo* [15]. We therefore assessed the possibility to initiate 3D bone marrow co-cultures using human MSCs. As these cells exhibited decreased survival when aggregates were formed in standard culture media, we assessed the potential of applying U-bottom microwell arrays to maintain the mesensphere phenotype of CD105^{pos} CD146^{pos} human mesenchymal stem cells using a medium adapted from neural crest and pericyte cultures [17, 18].

As detailed in the introduction, this culture format permits the self-renewal of hematopoietic niche-forming MSCs while maintaining their capacity to support cord blood HSCs [3, 4]. Notably, through lack of culture methods allowing reliable 3D co-culture, beneficial effects of direct cell-cell contact of these mesensphere-cultured niche cells together with HSCs could to date not be shown. We show how U-bottom microwells can be used to grow human mesenspheres from aggregates of CD146^{pos} CD105^{pos} MSCs or clonally from single cells. Enabling this high-throughput single mesensphere culture while eliminating drawbacks of current culture methods such as fusion or attachment of spheres, this approach represents the first step towards the *in vitro* generation of primitive 3D bone marrow-like co-cultures. Medium exchange of these human MSC aggregate cultures from mesensphere medium to HSC medium did not lead to the attachment of the spheroids to the PEG surface. Using U-bottom microwells we are therefore able to eliminate the negative influence of plastic culture surfaces.

We think that the potential to exploit these sphere-based co-cultures are substantial. On the one hand, these 3D co-cultures can be used as “miniature bioreactors”, wherein progenitors around the formed spheroids can be regularly harvested while allowing the continuing culture of the multicellular spheroids. On the other hand, these spheroid cultures permit the study of cellular organization within a 3D architecture. Using U-bottom microwells larger cell spheroids can also be generated, offering the potential to study the formation of oxygen gradients within these structures and their effect on cellular behavior and migration patterns, as quiescent HSCs, for example, are known to preferentially reside in hypoxic regions of the bone marrow *in vivo*.

Conclusions

We propose multicellular bone marrow spheroids as a promising three-dimensional culture model to better recapitulate the physiological organization of the native bone marrow niche *in vitro*. Generating relevant bone marrow models *ex vivo* are critical to successfully adopting functional medical screening paradigms and to establish efficient stem cell expansion methods for clinical settings.

Acknowledgements

We thank Jessica Sordet-Dessimoz and Gianni Mancini from the histology core facility (HCF) at EPFL, especially for their precious help and guidance, for sample preparation and processing. A special thank you is also addressed to the Flow Cytometry Core Facility (FCCF) at EPFL for their precious time, good spirits and valuable help during cell sorting. Also, we would like to thank the laboratoire de dynamique des cellules souches (LDCS) under Yann Barrandon for donating DsRed mice. Also our sincere gratitude goes to Simón Méndez-Ferrer from the CNIC Madrid for his valuable help in setting up human mesensphere cultures and generously providing chicken embryo extract.

References

- [1] Dexter, T.M., T.D. Allen, and L.G. Lajtha, *Conditions controlling the proliferation of haemopoietic stem cells in vitro*. J Cell Physiol, 1977. **91**(3): p. 335-44.
- [2] Nakamura, Y., et al., *Isolation and characterization of endosteal niche cell populations that regulate hematopoietic stem cells*. Blood, 2010. **116**(9): p. 1422-32.
- [3] Mendez-Ferrer, S., et al., *Mesenchymal and haematopoietic stem cells form a unique bone marrow niche*. Nature, 2010. **466**(7308): p. 829-34.
- [4] Isern, J., et al., *Self-renewing human bone marrow mesospheres promote hematopoietic stem cell expansion*. Cell Rep, 2013. **3**(5): p. 1714-24.
- [5] Bianco, P., et al., *The meaning, the sense and the significance: translating the science of mesenchymal stem cells into medicine*. Nat Med, 2013. **19**(1): p. 35-42.
- [6] Calvi, L.M., et al., *Osteoblastic cells regulate the haematopoietic stem cell niche*. Nature, 2003. **425**(6960): p. 841-6.
- [7] Zhang, J., et al., *Identification of the haematopoietic stem cell niche and control of the niche size*. Nature, 2003. **425**(6960): p. 836-41.
- [8] Sugiyama, T., et al., *Maintenance of the hematopoietic stem cell pool by CXCL12-CXCR4 chemokine signaling in bone marrow stromal cell niches*. Immunity, 2006. **25**(6): p. 977-88.
- [9] Gao, J.A., et al., *Characterization of OP9 as authentic mesenchymal stem cell line*. Journal of Genetics and Genomics, 2010. **37**(7): p. 475-482.
- [10] Takakura, N., et al., *Preferential proliferation of murine colony-forming units in culture in a chemically defined condition with a macrophage colony-stimulating factor-negative stromal cell clone*. J Exp Med, 1996. **184**(6): p. 2301-9.
- [11] Baraniak, P.R. and T.C. McDevitt, *Scaffold-free culture of mesenchymal stem cell spheroids in suspension preserves multilineage potential*. Cell Tissue Res, 2012. **347**(3): p. 701-11.
- [12] Wang, W.J., et al., *3D spheroid culture system on micropatterned substrates for improved differentiation efficiency of multipotent mesenchymal stem cells*. Biomaterials, 2009. **30**(14): p. 2705-2715.
- [13] Serafini, M., et al., *Establishment of bone marrow and hematopoietic niches in vivo by reversion of chondrocyte differentiation of human bone marrow stromal cells*. Stem Cell Res, 2014. **12**(3): p. 659-72.
- [14] Engler, A.J., et al., *Matrix elasticity directs stem cell lineage specification*. Cell, 2006. **126**(4): p. 677-89.
- [15] Naveiras, O., et al., *Bone-marrow adipocytes as negative regulators of the haematopoietic microenvironment*. Nature, 2009. **460**(7252): p. 259-63.
- [16] Friedens.Aj, et al., *Heterotopic Transplants of Bone Marrow - Analysis of Precursor Cells for Osteogenic and Hematopoietic Tissues*. Transplantation, 1968. **6**(2): p. 230-&.
- [17] Pardal, R., et al., *Glia-like stem cells sustain physiologic neurogenesis in the adult mammalian carotid body*. Cell, 2007. **131**(2): p. 364-77.

- [18] Crisan, M., et al., *Purification and culture of human blood vessel-associated progenitor cells*. *Curr Protoc Stem Cell Biol*, 2008. **Chapter 2**: p. Unit 2B 2 1-2B 2 13

CHAPTER V

MANIPULATING CELL-CELL INTERACTIONS IN THE NICHE

SNAP-tag technology for the manipulation of cell-cell interactions

Manuscript in preparation.

Hoehnel S¹, Lutolf MP¹

¹ Laboratory of Stem Cell Bioengineering, Ecole Polytechnique Fédérale de Lausanne, CH

Corresponding Author:

Prof. Matthias Lutolf
Laboratory of Stem Cell Bioengineering
Institute of Bioengineering
School of Life Sciences
Ecole Polytechnique Federale de Lausanne
CH-1015 Lausanne, Switzerland
Tel: +41216931876, Email: matthias.lutolf@epfl.ch

Abstract

Juxtacrine or contact-dependent signaling is a major form of cell communication in multicellular organisms. The involved cell-cell and cell-extracellular matrix (ECM) interactions are of utmost importance for the organization and maintenance of tissue architecture and function. However, since cell-cell contacts are rather weak, it is not possible to isolate neighboring cells in their native state, for example to study how specific cell types interact with others (e.g. stem cells with niche cells) and where they locate within tissues to execute specific tasks. In order to overcome this bottleneck, we propose artificial *in situ* cell-to-cell linking systems based on SNAP-tag and CLIP-tag, engineered mutants of the human O⁶-alkylguanine-DNA alkyltransferase (hAGT). Here we demonstrate that SNAP-tag can be utilized for the efficient covalent tethering of cells to poly(ethylene glycol) (PEG)-based hydrogel substrates that were functionalized with its substrate benzylguanine (BG). Furthermore, using PEG-based spherical microgels to mimic geometrical features of cells, we are able to maximize concentrations of SNAP and BG to demonstrate artificially induced clustering, reminiscent of cell-cell pairing. However, further optimization of SNAP-tag expression levels as well as improved functionalization of cell membranes with BG are necessary to enable future applications in direct cell-cell pairing for marker-free cell isolation.

Introduction

Within complex three-dimensional (3D) tissues, cells are physically constrained by adjacent neighboring and support cells as well as the architecture of the ECM. Arising from these microenvironmental contacts, cell-cell and cell-to-ECM interactions are important regulators of numerous biological functions such as development, homeostasis, tissue regeneration and repair [1-5]. To probe the organization of cells within tissues, the only reliable current technique in place is histotechnology, which involves fixation, sectioning, staining and imaging of desired tissue samples [6]. In addition to being time-consuming and expensive, histology cannot be applied to capture live cell interactions in a dynamic tissue environment. Therefore we propose in this work a fast and efficient *in situ* system to target and eventually isolate close-interacting neighboring cells of a given cell-type using SNAP-tag technology.

SNAP-tag is a self-labeling protein tag mutated from the human suicide protein O⁶-alkylguanine-DNA alkyltransferase (hAGT), which was engineered by the Johnsson lab at EPFL to specifically and covalently bind O⁶-benzylguanine (BG) derivatives [7].

Subsequently, a second mutant, CLIP-tag, was generated by the same group that reacts irreversibly and rapidly with O²-benzylcytosine (BC) derivatives [8], forming an orthogonally applicable system to the SNAP-tag technology useful for simultaneous labeling with different probes [9].

SNAP-tag has been developed for the efficient labeling of fusion proteins in living cells [7, 10, 11] and has been validated for live fluorescent pulse-chase imaging *in vitro* [12]. Importantly, interference of SNAP-tag with protein function has been ruled out for various fusion proteins [7, 13-17]. The SNAP-tag substrate BG was historically developed as a potent anti-cancer drug for tumors showing augmented activity of human AGT [18, 19]. Pharmacologic studies on BG treatment could not link major side effects to its administration in mice, rats or humans [20-22]. To our knowledge, there are no studies addressing the potential side effects of the CLIP-tag substrate BC. However, BG and BC are structurally very similar, differing only in their respective leaving group, i.e. guanine versus cytosine, which display similar pK_A's [23]. Arguably one can assume that therefore also BC should not show any major pharmacologic adverse effects. Given these properties, SNAP-tag technology was proposed as an attractive system to not only sense and image protein-protein interactions inside living cells but also complete living organisms. Indeed SNAP-tag has been employed for pulse-chase experiments to determine protein half-life in living mice [16].

In this study, we demonstrate the ability of extending the use of the SNAP-tag system from the molecular level to the cellular level. Within the context of the bone-marrow niche, futile efforts have been made to identify a functionalized 2D substrate that would allow the propagation of non-adherent niche cells, such as mouse nestin-GFP^{pos} cells [24, 25]. We use SNAP-tag expressed globally and fused to a GPI-anchor to attach cells to artificial substrates. SNAP-technology can therefore open the possibility to create a universal substrate for cells whose adhesion ligands are unknown. Furthermore we sought to apply the system to form covalent bonds between cells in order to permit custom cell-cell pairing. As proof-of-principle, we utilized spherical PEG microgels (microbeads) functionalized on the one hand with SNAP-protein and on the other with the SNAP-tag substrate BG to form covalent bonds between beads. This method should offer the possibility to isolate close-interacting cells, such as stem cells together with their respective niche cells, in a completely unbiased fashion. That is, the advantage of this system lies in the opportunity to marker-free isolate a cell population of interest with unknown phenotype through another better characterized cell type.

Experimental methods

Plasmid constructs

The plasmid containing pFUT.CLIP-GPI was generated by insertion of the CLIP sequence from pEGFP-F.CLIP-GPI [26] into pFut.SNAP-GPI [16] using the restriction sites AgeI and BspEI. The plasmid containing pET51b.CLIP-mCherry was generated by excising the CLIP sequence from the CLIPf vector (NEB) using the restriction sites BsrGI and XhoI and cloning the generated CLIP insert into the pET51b.SNAP-mCherry vector [27] by replacing the SNAP-encoding sequence using the restriction sites Acc65I and XhoI. DNA sequences were verified using Sanger sequencing (Microsynth).

Virus production

Lentiviral particles for pFut.SNAP-GPI and pFut.CLIP-GPI were produced by transfecting HEK293T cells using Xtreme Gene HP transfection reagent. Supernatants were collected at hours post transfection, filtered through 0.22 μ m filters and concentrated 1000X using ultracentrifugation.

Cell culture and cell lines

HEK293T were cultured in Dulbecco's Modified Eagle Medium (DMEM; Gibco) supplemented with 2mM Glutamax, 10% (v/v) fetal bovine serum (FBS, Gibco), 1 mM sodium pyruvate (Gibco), 5 mM HEPES (Gibco) and 100 U ml⁻¹ penicillin/streptomycin (Invitrogen). The cells were stable transfected using pFut.SNAP-GPI and pFut.CLIP-GPI concentrated virus titers. Transfected cells were FACS sorted using rabbit polyclonal anti-SNAP-tag antibody (NEB, recognizing both SNAP- and CLIP-tag) at 1:200 and secondary Alexa-647 labeled goat anti-rabbit (Invitrogen) at 1:1000. In a second round of FACS sorting, cells were labeled with BG-488 or BC-488 additionally to anti-SNAP-tag antibody labeling and single cells of the high 5% positive stained population were sorted into 96 well plates to generate monoclonal cell lines for each SNAP- and CLIP-tag. Monoclonal SNAP- and CLIP-tag cell lines were chosen according to proliferation rate and tag-expression based on labeling with BG-488 and BC-488.

Protein expression and purification

To express SNAP-mCherry, the construct were transformed into Rosetta-gami (DE3) competent cells. Bacterial cultures harboring the expression construct were grown in LB broth containing 100 μ g/mL ampicillin (AppliChem) at 37°C overnight under constant shaking. Overnight cultures of bacterial cells were diluted 100-fold into 2L LB broth supplemented with ampicillin, cultured as above until an OD₆₀₀ of 0.4-0.6

was reached. The culture was subsequently cooled to 16°C, induced by adding isopropyl-D-galactopyranoside (IPTG) to a final concentration of 1 mM and additionally grown over night at 16°C under constant shaking. After harvesting by centrifugation at 4,000g for 10 min at 4°C, bacterial pellets were resuspended in IMAC lysis buffer supplemented with 1mg/mL Lysozyme and sonicated 3 times for 30s on ice. After centrifugation at 12,000g for 10min to remove insoluble materials, the supernatant was purified by Ni-NTA agarose chromatography according to manufacturer's instructions (Qiagen).

Purified proteins were dialysed against binding buffer (150 mM NaCl, 25 mM sodium phosphate, pH 8.0) and concentrated to working concentrations using Ultra-4 10K centrifugal filters (Amicon).

Microgel Generation

Computer-controlled syringe pumps (neMESYS from Cetoni, Germany) were used to control flow rates. Syringes were filled with PEG solutions and hexadecane with 2% (w/v) ABIL EM surfactant used as oil phase. Tygon tubings were used to connect the syringes to the microfluidic chip inlets. Microgels were generated by loading two microfluidic channels with PEG precursors with concentrations depending on a specified molar excess of functional groups: for a 20% thiol-excess we chose 8.33% (w/v) PEG-VS and 20% (w/v) PEG-TH precursors. Microgels had a diameter of 120µm. The oil phase was removed by filtering microgels with 70µm cell strainers (BD Biosciences, USA) and extensive washing with PBS. Microgels were then swollen in PBS overnight.

Immobilization of SNAP-mCherry

To immobilize SNAP-mCherry protein on artificial substrates, the protein was conjugated with a three-fold molar excess of a 3.5kDa NHS-PEG-maleimide linker (PEGylation) or a three-fold molar excess of a 341.38Da Biotin-NHS linker (biotinylation) for 60min at RT. PEGylated SNAP-mCherry could be immobilized by covalent interaction of the maleimide group with free thiols on PEG substrates. Biotinylated SNAP-mCherry was immobilized through interaction with incorporated maleimide-functionalized Neutraavidin or Streptavidin.

Statistical analysis

For two-group analysis, an unpaired nonparametric Kolmogorov-Smirnov test was used. For all cases, p-values less than 0.05 were considered statistically significant. GraphPad Prism 6.0 software was used for all statistical evaluations.

Results

Exclusive in vitro expression of SNAP-tag and CLIP-tag

We tested the efficiency and exclusivity of SNAP-tag or CLIP-tag expression and labeling on HEK293T cells. We generated stable cell lines using lentiviral vectors expressing either SNAP-tag or CLIP-tag fused to the glycosylphosphatidylinositol (GPI) signal sequence of human CD59 (pFUT.SNAP-GPI or pFUT.CLIP-GPI, respectively) from the ubiquitin C promoter [16]. The CLIP-GPI construct [28] was inserted into the lentiviral pFUT vector using the AgeI and BspEI restriction sites. Using an anti-SNAP-tag antibody, recognizing both SNAP-tag and CLIP-tag, we generated monoclonal cell lines from sorted single cells of the high 5% population to select for the highest expression of the transgene. To verify correct expression of SNAP-GPI and CLIP-GPI we labeled cells in culture with either BG-546 (SNAP substrate) or BC-488 (CLIP substrate). A cell surface specific signal for BG-546 was detected in cells harboring the SNAP-GPI transgene but neither on the wild-type controls nor the cell lines harboring the CLIP-GPI transgene. Respectively cell surface specific BC-488 labeling was detected in the CLIP-GPI cell lines, but not on wild-type cells or SNAP-GPI cell lines (Figure 5.1).

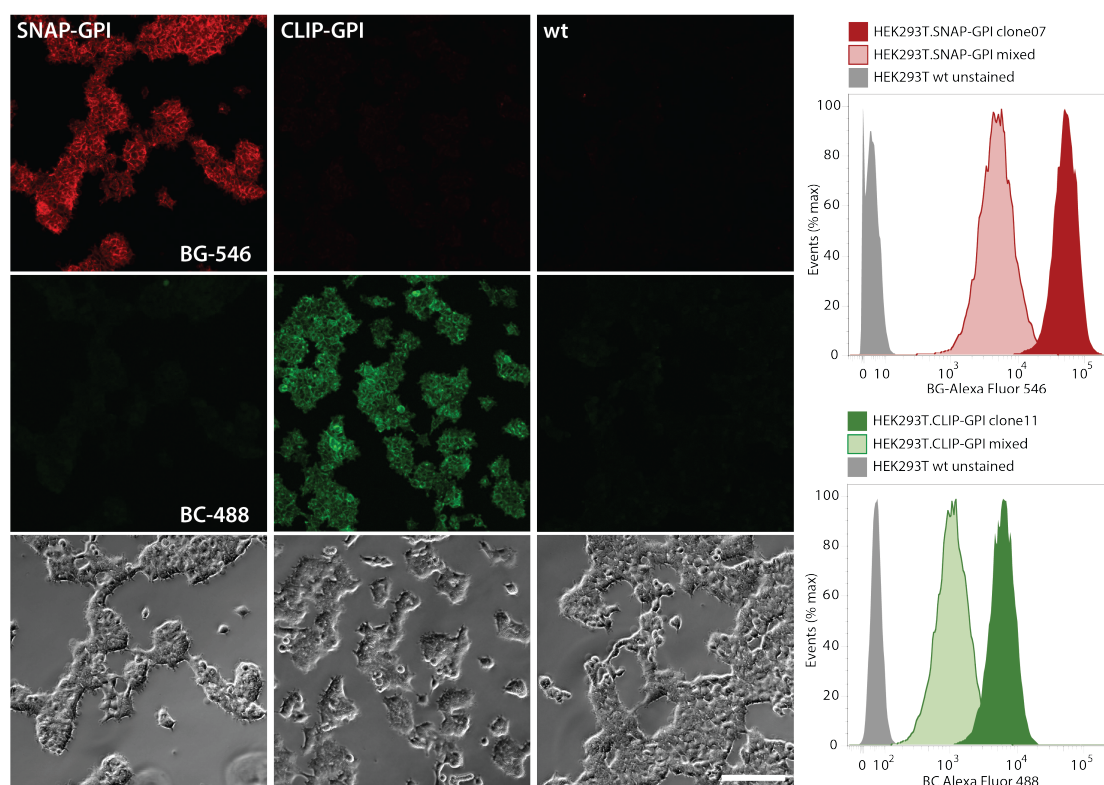


Figure 5. 1 Expression of SNAP-tag and CLIP-tag on cell lines HEK293T. Left : Immunofluorescence staining of SNAP-tag with BG-546 (red) and CLIP-tag with BC-488 (green). Right : FACS analysis of selected high expressing clones for SNAP-tag (red) and CLIP-tag (green) on HEK293T. Scale bar is 100 μ m.

Characterization of SNAP-GPI and CLIP-GPI

To evaluate the optimal labeling concentration for SNAP-GPI or CLIP-GPI, respectively, we stained the generated cell lines with varying concentrations of BG-546 or BC-488 respectively for 30min according to manufacturer's instructions (Figure 5.2 A-D). Fitted to Gaussian bell curves, the optimal staining concentration with the best signal to noise (background staining on wildtype cells) ratio was determined at 0.4 μ M BG-546 and 9.2-9.4 μ M BC-488. Above this concentration only the background from unbound probe was predominantly increasing.

Next we investigated the optimal staining time for BG-546 and BC-488 at the determined concentrations by staining at different time points within a range of 1-60min (Figure 5.3 E-H). SNAP-tag can be efficiently labeled within 10-15min. CLIP-GPI on HEK293T cells requires a staining time of 30min. By co-staining with BG-546 and BC-488 we assessed the specificity of the substrates to the respective tag (Figure 5.2 F and H). Except for minimal background noise of BC-488 on HEK293T.SNAP-GPI we observed no significant unspecific staining on the respective orthogonal tag.

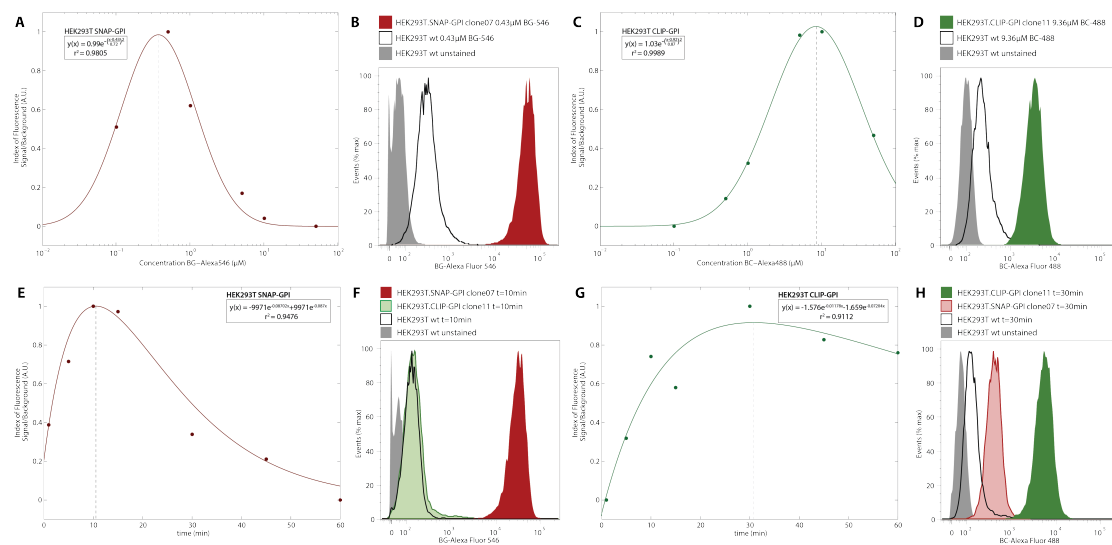


Figure 5. 2 Optimal staining concentration and time for SNAP-tag and CLIP-tag. (A-D) A range of concentration between 0.1-100 μ M was tested to determine the optimal label concentration of the two substrates for labeling SNAP-tag and CLIP-tag present on the cell surface. (B and D) FACS analysis showed specific signal for SNAP-BG labeling (red) and CLIP-BC labeling (green) over background labeling of substrate attaching non-specifically to wild-type cells (black outline). (E-H) Time points in a time frame between 1min to 1h were tested to determine the optimal time needed to label SNAP-tag and CLIP-tag present on the cell surface with their respective substrate BG and BC. (F) FACS analysis showed specific labeling of BG to surface-expressed SNAP-GPI (dark red) over unspecific binding to wild-type or CLIP-GPI-expressing cells (black outline and light green). (H) Similarly BC labeled specifically surface-expressed CLIP-GPI (dark green) over unspecific binding to wildtype or SNAP-GPI-expressing cells (black outline and light red).

BG cell surface functionalization and cell-cell pairing

In order to establish the basis of forming covalent cell-cell bonds using SNAP-tag technology (Figure 5.3 A), cell surfaces must be functionalized with the SNAP-tag substrate BG. Naturally abundant free surface thiols pose an ideal target for binding thiol-reactive compounds, such as maleimide-activated molecules [29]. Indeed, by exploiting the presence of such reduced thiols on cellular surfaces, drug-loaded nanoparticles have been efficiently conjugated to donor cells to increase their therapeutic impact [30]. We confirmed the abundance of reduced surface thiols by functionalizing wild-type HEK293T with a varying concentration of maleimide-activated alexa-fluor dyes (Figure 5.3 B) and maleimide-activated BG (Figure 5.3C). Maleimide-Alexafluor546 was titrated at concentrations between 0.1 μ M and 1mM. Within this range we observed a constant increase of signal through flow cytometry, indicating that saturation of free surface thiols was not reached. BG was labeled to the cell surface similarly through maleimide-thiol coupling. The maximal concentration of BG in the labeling solution was 0.5mM, limited by the solubility of BG in DMSO at 10mM. A labeling solution of 0.5mM corresponds to a final DMSO concentration of 5%, which is already 50-fold above standard cytotoxic limits. The presence and activity of BG after conjugation to the cell surface was verified by staining with SNAP-mCherry (Figure 5.3 C). BG-labeled HEK293T-GFP cells were incubated together with stable SNAP-tag expressing HEK293T cells that were labeled in red (Figure 5.3 D) to investigate the formation of covalent bonds between these two cell types (Figure 5.3 F). As a control SNAP-tag expressing cells were incubated with HEK293T-GFP that were not functionalized with BG-maleimide (Figure 5.3 E). We generally did not observe a marked increase in doublet or multiplet formation. However within the non-singlet cell population, we observed a two-fold increase of covalent SNAP-BG bonds, reflected by the cell population that is fluorescent both in the green and red channel (Figure 5.3 E and F).

These results indicate that SNAP-tag and its substrate BG each present on different cells cannot form sufficiently strong covalent bonds to induce and retain covalent cell-cell contact. We hypothesize that this is the result from either insufficient concentrations of either SNAP-tag or BG on the cells or from steric hindrance from other molecules present on the surface of cells.

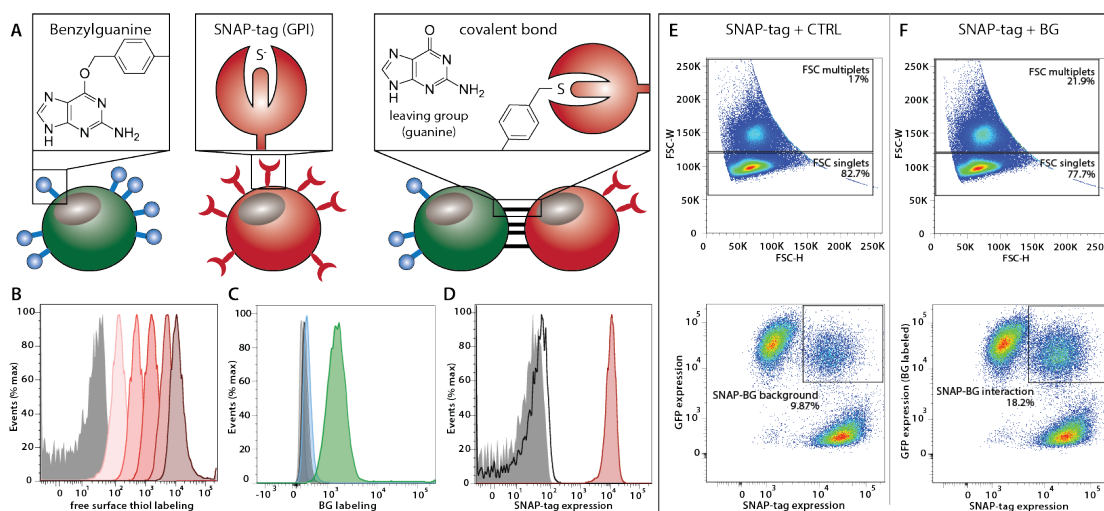


Figure 5.3 Cell-cell pairing part I. (A) In theory, cell-cell pairs can be formed through covalent bonds of SNAP-tag (red) with its substrate benzylguanine (BG, blue). To immobilize BG on the surface of cells (in green). (B) Free surface thiols are present on the surface of HEK293T cells as demonstrated by functionalization with Alexa546-maleimide at varying concentrations (grey: non-labeled cells, red gradient histograms from left to right: 0.1 μM, 1 μM, 10 μM, 100 μM, 1 mM). (C) These free-surface thiols can be targeted with maleimide-activated BG, the presence of which is validated by staining with SNAP-mCherry protein (green). The blue histogram shows wild-type HEK293T cells labeled with SNAP-mCherry. BG-labeled cells together with SNAP-tag expressing HEK293T cells (D) were incubated to form covalent cell bonds (E-F). (E) Shows singlet/multiplet FACS plots for control samples where SNAP-tag expressing cells incubated with non-BG labeled cells. (F) Shows singlet/multiplet FACS plots for samples where SNAP-tag expressing cells were incubated with BG-labeled cells.

Immobilized BG substrates could be withdrawn from cellular membranes through endocytic processes. We therefore investigated a different approach to forming artificial cell-cell bonds by utilizing a double functional linker harboring on one end the SNAP-tag substrate BG and on the other end the CLIP-tag substrate BC (Figure 5.4 A). This double functional linker was available at a concentration of 100 μM, limited by the initial stock concentration. The linker harbors a Cy5 fluorescent dye in the center, to allow fluorescent tracking by flow cytometry.

Covalent cell-cell bonds should be formed by mixing a population of CLIP-tag expressing cells (Figure 5.4 B) and a population of SNAP-tag expressing cells (Figure 5.4 C). As a control we incubated either SNAP-tag expressing cells or CLIP-tag expressing cells alone (Figure 5.4 D). When incubating SNAP-tag and CLIP-tag expressing cells together (Figure 5.4 E), we observed a slight increase (+ 5%) in the non-singlet cell population. However, within this population we could not observe any change in population morphology that would indicate the formation of covalent bonds between SNAP-tag and CLIP-tag expressing cells. In theory when these cells would form covalent bonds, the two populations observed in their single state (Figure 5.4 D, bottom, red and purple) should merge into one general population.

Again, we propose two reasons as the cause for the inability to form and observe the formation of covalent cell-cell bonds. Either the tags are available at insufficient amounts on the membrane of the cell or the concentration of the double functional linker is too low to form sufficient cell-cell bonds to keep doublets or multiplets of cells bound together during manipulation.

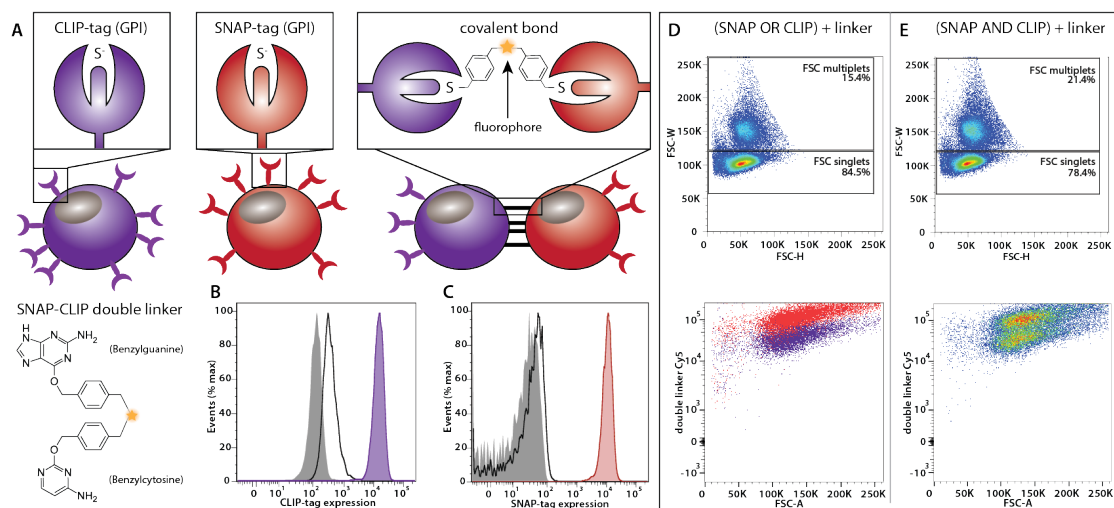


Figure 5. 4 Cell-cell pairing part II. (A) Cell-cell pairs between CLIP-tag and SNAP-tag expressing cells can be formed using a double functional linker molecule. The benzylcytosine active site can react with the CLIP-tag expressed on a GPI anchor on HEK293T cells (B) to release cytosine and the benzylguanine active site can react with SNAP-tag also expressed on a GPI anchor on HEK293T cells (C). As a control either SNAP-tag cells or CLIP-tag cells were incubated alone with a Cy5-harboring double linker (D). (E) SNAP-tag and CLIP-tag cells were mixed together in one tube to observe the formation of covalent bonds through FACS using the Cy5-double linker molecule.

SNAP-tag as a universal cell attachment substrate

To investigate the concentration of BG needed to form a covalent attachment of cells to a given surface, we used PEG hydrogels [31, 32] functionalized with different concentrations of benzylguanine ranging from 500 μ M to 10mM as a substrate for SNAP-tag expressing cells (Figure 5.5). At concentrations above 10mM, BG precipitated on the PEG hydrogel (data not shown).

We found that from a concentration above 5mM efficient cell attachment of SNAP-tag expressing HEK293T cells to the PEG hydrogel was guaranteed (Figure 5.5 B and C). Proliferation of SNAP-tag expressing cells on BG surfaces was not inhibited (Figure 5.5 B). Wild-type HEK293T cells could not form attachment sites to immobilized BG (Figure 5.5 A). To demonstrate that this attachment is indeed due to covalent bonds formed between the SNAP-tag expressed on cells and the BG immobilized on the PEG hydrogel, we trypsinized SNAP-tag expressing cells on BG-substrates (Figure 5.5 D) and on substrates that have been functionalized with

5mM RGD (Figure 5.5 E), which results in similar cell attachment. In the SNAP-BG condition the cells reduced their spreading and became more round, however remained attached to the PEG surface, even after multiple washing steps (Figure 5.5 F). In the SNAP-RGD condition, the cells completely detached from the hydrogel surface and could be washed away (Figure 5.5 G).

Indeed these results indicate the reason as to why covalent cell-cell pairing could not be observed previously. With high probability the amount of SNAP-tag (or CLIP-tag) substrate, immobilized on the cell surface or provided as a double-functional linker, was too low to induce the formation of cell-cell bonds.

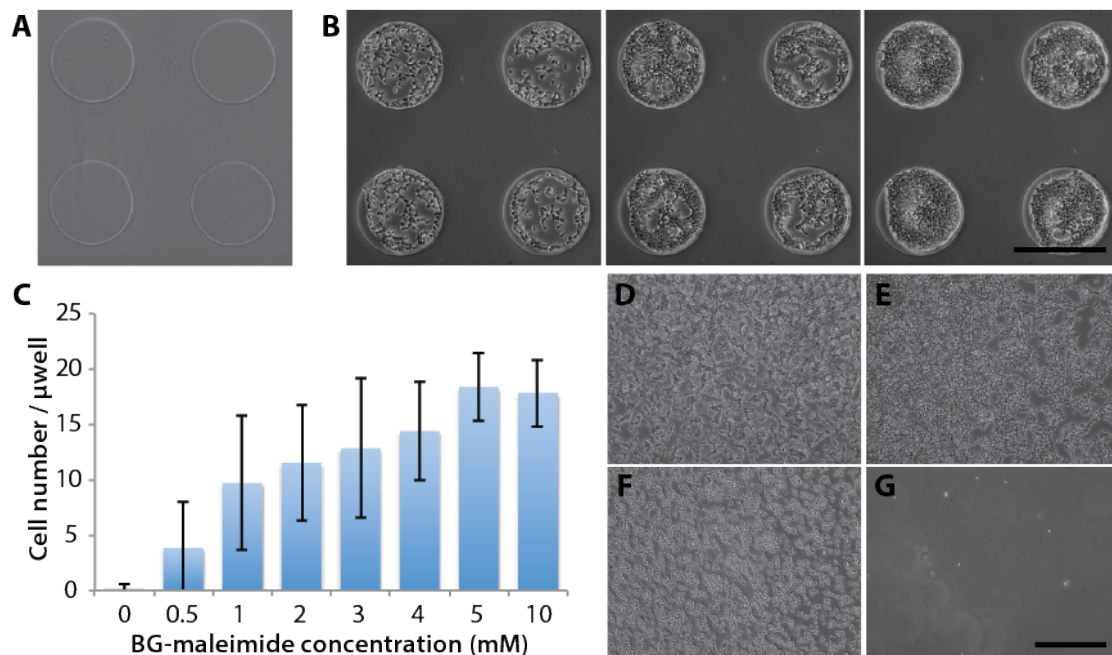


Figure 5. 5 BG as a universal substrate for SNAP-tag cells. (A) HEK293T wildtype cells and (B) HEK293T SNAP-tag expressing cells were seeded on top PEG hydrogel arrays functionalized with different amounts of BG (C). To validate the formation of covalent cell-cell bonds between SNAP-tag cells and the BG-PEG surface, SNAP-tag cells seeded on 5mM BG (D) and SNAP-tag cells seeded on 5mM RGD (E) were trypsinized for 15min. The SNAP-tag cells on BG remained attached (F), whereas the SNAP-tag cells on RGD detached and were removed during a subsequent washing step (G). Scale bar is 500 μ m.

Imitating cell-cell contact

Since we could not observe the formation of covalent bonds between cells harboring SNAP-tag and BG or SNAP-tag and CLIP-tag, probably due to concentration limitations on the surface of cells, we wanted to prove the principle of forming covalent bonds between non-flat surfaces using spherical PEG microgels (microbeads) [33]. In order to immobilize SNAP-mCherry protein on PEG surfaces, we investigated different functionalization methods. The activity of modified SNAP-mCherry protein was assessed by staining BG-functionalized cells and analyzing fluorescent signals through flow cytometry (Figure 5.6 A-D) in comparison to native SNAP-mCherry protein (Figure 5.6 A). PEGylation of SNAP-mCherry protein with an NHS-PEG-mal linker lead to complete loss of activity (Figure 5.6 B), probably due to the loss of the Cysteine in the active site of the protein by the maleimide unit. In a next step, we therefore utilized a Biotin-NHS linker to transfer biotin sites to the SNAP-mCherry molecules. We observed no loss in protein activity (Figure 5.6 C) and verified the presence of biotin molecules on the protein through staining with fluorescent-Streptavidin (Figure 5.6 D).

By first immobilizing Neutravidin-maleimide (NA-mal) on PEG microbeads through thiol conjugation, we were able to functionalize these NA-surfaces with increasing amounts of SNAP-mCherry-biotin (Figure 5.6 E and G-K). The amount of SNAP-mCherry that we were able to immobilize remained much lower than the 5mM BG units (Figure 5.6 L). The activity of immobilized SNAP-mCherry protein was verified by staining with fluorescently-labeled BG-Alexa488 (Figure 5.6 F and M-N). In a next step, we incubated BG-labeled PEG microbeads together with SNAP-mCherry-functionalized PEG microbeads. A short centrifugation step was necessary to obtain the formation of dense bead clusters (Figure 5.6 O). These microbead clusters displayed covalent binding of SNAP-tag to BG, as illustrated through mixed clusters of red and green microgels, and were resistant to breakage through physical pipetting.

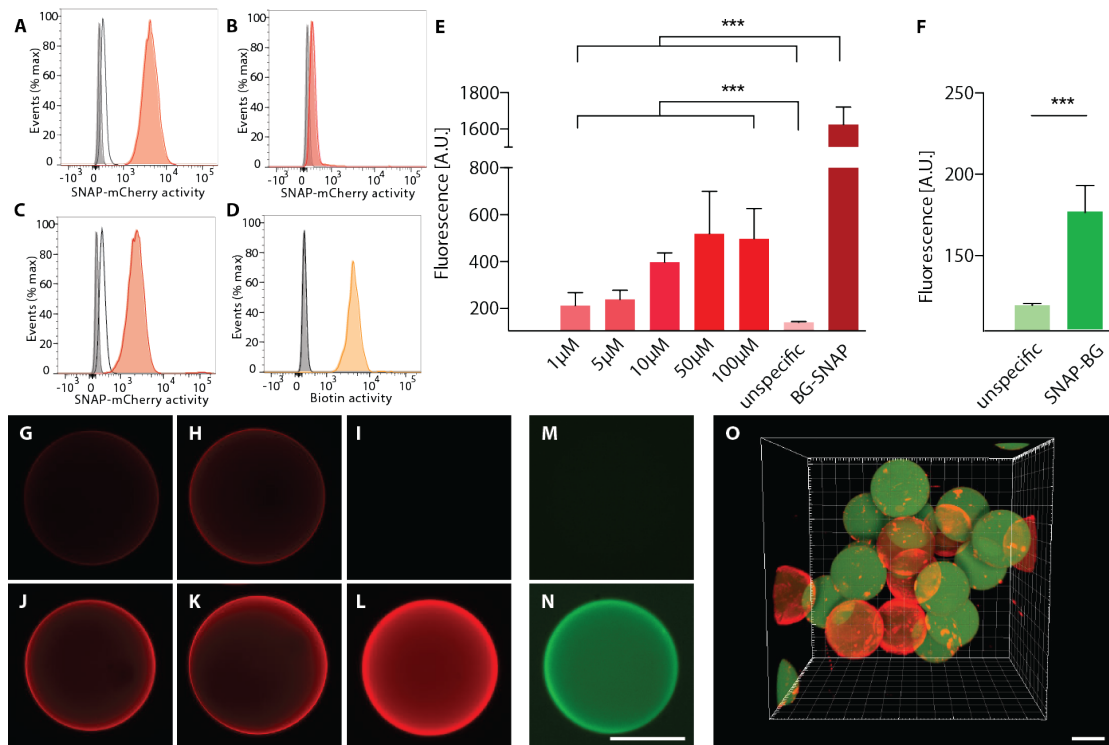


Figure 5.6 Microbead clusters. To imitate cell-cell clusters we utilized PEG-based microbeads, on which concentrations of BG and SNAP-protein can be maximized. (A-D) Shows the functionalization of SNAP-mCherry protein for subsequent immobilization on PEG surfaces. BG-functionalized cells were stained with (A) wildtype SNAP-mCherry, (B) PEGylated SNAP-mCherry and (C) Biotinylated SNAP-mCherry. (C) Shows staining of Biotin-sites on SNAP-mCherry with Streptavidin-Pacific Orange. (E) Varying concentrations of Biotin-SNAP-mCherry were immobilized on Neutravin-PEG microbeads. Unspecific staining shows the fluorescence signal from Biotin-SNAP-mCherry on PEG surfaces without Neutravidin. BG-SNAP shows the staining of SNAP-mCherry on BG-functionalized cells. (F) Activity of immobilized SNAP-mCherry was verified by staining with BG-Alexa488. Unspecific staining shows the background signal from BG-Alexa488 on Neutravidin-PEG without SNAP-mCherry. (G-N) shows representative imaged of PEG microbeads with (G) 1 μ M, (H) 5 μ M, (J) 10 μ M, (K) 50 μ M, (I) unspecific staining of SNAP-mCherry, (L) BG-SNAP-mCherry, (M) unspecific staining of BG-Alexa488 and (N) SNAP-BG-Alexa488. (O) SNAP-microbeads (red) and BG-microbeads (green) form stable clusters through the formation of covalent bonds. Scale bar is 100 μ m.

Discussion

Within their native microenvironment stem cells interact in close proximity with neighboring cells, which express factors that influence their maintenance and fate. However identifying markers for such rare cell populations is difficult and frequently results in the identification of multiple markers that might or might not overlap. A prominent example and initial motivation for this work is the characterization of multiple mesenchymal-like niche cells with different surface marker properties that interact with hematopoietic stem cells in the bone marrow of mice. Current knowledge suggests the existence of distinct locations of this niche: (i) the endosteal niche for quiescent HSCs and (ii) the perivascular niche for activated HSCs. Within these locally defined spaces niche cells with various phenotypes have been suggested, including markers such as CXCL12, nestin, Sca-1, ALCAM, leptin-receptor and others [24, 34-36]. The overlap of these populations is unresolved which ultimately leads to confusion whether one or multiple cell types are responsible for HSC maintenance. This in return is directly linked to difficulties in trying to reconstruct a bone marrow niche *in vitro*, given one needs to choose a relevant niche cell population to work with. Due to these limitations, we investigated the potential to develop a technology that would ultimately enable marker-free and thus unbiased cell isolation based on physiological cell-cell contacts.

Using SNAP-tag technology, we globally expressed SNAP and CLIP attached to a GPI anchor protein on HEK293T model cells. We were able to generate cell lines with high expression levels of this protein-tag to allow efficient labeling with its substrate benzylguanine, or for CLIP benzylcytosine, respectively, with relatively low concentrations (i.e. μM range) within a few minutes. Furthermore, we made use of abundant free thiols on the cell membrane of cells, to immobilize these substrates globally on a second HEK293T cell population. We hypothesized that incubation of SNAP-expressing cells and BG-labeled cells would lead to the formation of a dense cell pellet that could no longer be dissociated. While this strong pellet formation could not be observed in any instance, we did notice a slight increase in doublet formation of cells and SNAP-BG interactions as seen through FACS analyses. In addition, we tested whether SNAP-expressing and CLIP-expressing cells could be covalently bound with each other using a double-functional BG-BC linker. However, in this scenario, we only observed a slight increase in cell doublet formation, rather than the generation of a dense non-dissociable cell pellet.

We then hypothesized that either the concentration ratio of SNAP-tag versus its substrate BG are too low to form such covalent artificial cell bonds or that the reaction site of the SNAP-tag towards the BG substrate is masked by other molecules present on cell membranes.

Thus, to investigate the concentration range of BG needed for efficient SNAP-tag binding on cells, we immobilized BG at different concentrations on PEG hydrogels. We observed that at concentrations above 5mM BG, SNAP-tag expressing HEK293T cells could efficiently attach to these surfaces. We also demonstrated that this interaction is indeed covalent and specific by showing that trypsinization does not lead to cell detachment as compared to RGD controls.

In order to systematically test the potential of covalent non-flat surface pairing, we used spherical PEG microgels to immobilize high concentrations of BG and SNAP-protein, maximizing then the availability of binding sites. Indeed by forcing the beads to come into close contact, we were able to observe stable clusters of SNAP-beads and BG-beads. As a result, we conclude that the concentrations of SNAP-tag and BG reached on the cell surface currently are insufficient to form enough covalent bonds between the cells to allow their long term pairing. Indeed also sterical hindrance of the two sites could be a cause for this concentration limitation, as present binding sites could simply not be physically available for the formation of covalent cell-cell bonds.

As detailed above, we optimized the expression of SNAP-tag and CLIP-tag under the short GPI anchor protein through the generation of high-expression level monoclonal cell lines. However, in the future, these tags could be fused to the end of longer surface receptors such as cell adhesion mediating CD proteins to ensure sufficient exposure of the tags.

In addition, BG functionalization of cells is currently limited by the stock concentration of this molecule in its solvent DMSO. Indeed benzylguanine is a strongly non-polar molecule and thus is only weakly soluble in water. This limitation could be resolved by generating BG linkers with long PEG chains in the center, a very common practice to enhance solubility of molecules especially in aqueous solutions. Furthermore to increase the local concentration of BG on cellular surfaces, one could imagine the use of branched multi-arm BG linkers, where one thiol on the cell membrane could lead to the exposure of multiple BG molecules.

In summary, we investigated whether SNAP technology can be used for artificially imitating cell-cell contact either with a substrate of interest or in between cells. We demonstrate that SNAP-BG interactions can be used for the generation of a universal cell substrate by binding SNAP-expressing cells to BG-functionalized PEG. The use of SNAP-technology is currently underdeveloped for use in direct cell-cell pairing, but we demonstrated that PEG-based microbeads could cluster through SNAP-protein immobilized on one bead population and BG-exposure on the other.

Conclusions

SNAP technology can thus far be used for the covalent attachment of a SNAP-tag expressing cell to any given substrate functionalized with its substrate BG. The generation of a universal substrate, as demonstrated in this work, is useful for the attachment of cells where long-term contact of cells with a surface is needed, i.e. for two-dimensional screenings where washing steps are associated with cell loss. Further this method could be used for the attachment of cells whose adhesion ligands are unknown. In order to use SNAP-tag technology for cell-cell pairing, that would add versatility to methods of cell tracking and isolation, further optimization is needed.

Acknowledgements

We thank Luc Reymond, Monica Rengifo Gonzalez and Kai Johnsson for their help and time for discussions and for generously providing SNAP-tag products. We also thank Simone Allazetta for generating the PEG microgels.

References

- [1] Bhatia, S.N., et al., *Effect of cell-cell interactions in preservation of cellular phenotype: cocultivation of hepatocytes and nonparenchymal cells*. FASEB J, 1999. **13**(14): p. 1883-900.
- [2] Bazzoni, G. and E. Dejana, *Endothelial cell-to-cell junctions: molecular organization and role in vascular homeostasis*. Physiol Rev, 2004. **84**(3): p. 869-901.
- [3] Nelson, C.M. and M.J. Bissell, *Of extracellular matrix, scaffolds, and signaling: tissue architecture regulates development, homeostasis, and cancer*. Annu Rev Cell Dev Biol, 2006. **22**: p. 287-309.
- [4] Do, D.V., et al., *The role of epithelial-mesenchymal interactions in tissue repair, fibrogenesis and carcinogenesis*. Current Signal Transduction Therapy, 2007. **2**(3): p. 214-220.
- [5] Lodish, H., et al., *Cell Interactions in Development*, in *Molecular Cell Biology 4th edition*, W.H. Freeman, Editor. 2000: New York.
- [6] Junqueira, L.C.U.a., J. Carneiro, and A.N. Contopoulos, *Basic histology*, in *A Concise medical library for practitioner and student* 1975, Lange Medical Publications: Los Altos, Calif. p. v.
- [7] Keppler, A., et al., *A general method for the covalent labeling of fusion proteins with small molecules in vivo*. Nat Biotechnol, 2003. **21**(1): p. 86-9.
- [8] Gautier, A., et al., *An engineered protein tag for multiprotein labeling in living cells*. Chem Biol, 2008. **15**(2): p. 128-36.
- [9] Provost, C.R. and L. Sun, *Fluorescent labeling of COS-7 expressing SNAP-tag fusion proteins for live cell imaging*. J Vis Exp, 2010(39).
- [10] Keppler, A., et al., *Labeling of fusion proteins with synthetic fluorophores in live cells*. Proc Natl Acad Sci U S A, 2004. **101**(27): p. 9955-9.
- [11] Keppler, A., et al., *Fluorophores for live cell imaging of AGT fusion proteins across the visible spectrum*. Biotechniques, 2006. **41**(2): p. 167-70, 172, 174-5.
- [12] Jansen, L.E., et al., *Propagation of centromeric chromatin requires exit from mitosis*. J Cell Biol, 2007. **176**(6): p. 795-805.
- [13] Maurel, D., et al., *Cell-surface protein-protein interaction analysis with time-resolved FRET and snap-tag technologies: application to GPCR oligomerization*. Nat Methods, 2008. **5**(6): p. 561-7.
- [14] Hein, B., et al., *Stimulated Emission Depletion Nanoscopy of Living Cells Using SNAP-Tag Fusion Proteins*. Biophysical Journal, 2010. **98**(1): p. 158-163.
- [15] Klein, T., et al., *Live-cell dSTORM with SNAP-tag fusion proteins*. Nat Methods, 2011. **8**(1): p. 7-9.
- [16] Bojkowska, K., et al., *Measuring in vivo protein half-life*. Chem Biol, 2011. **18**(6): p. 805-15.
- [17] Bodor, D.L., et al., *Analysis of protein turnover by quantitative SNAP-based pulse-chase imaging*. Curr Protoc Cell Biol, 2012. **Chapter 8**: p. Unit8 8.
- [18] Friedman, H.S., et al., *Phase I trial of O6-benzylguanine for patients undergoing surgery for malignant glioma*. J Clin Oncol, 1998. **16**(11): p. 3570-5.
- [19] Quinn, J.A., et al., *Phase II trial of temozolomide plus o6-benzylguanine in adults with recurrent, temozolomide-resistant malignant glioma*. J Clin Oncol, 2009. **27**(8): p. 1262-7.

- [20] Dolan, M.E., et al., *Metabolism of O6-benzylguanine, an inactivator of O6-alkylguanine-DNA alkyltransferase*. *Cancer Res*, 1994. **54**(19): p. 5123-30.
- [21] Chinnasamy, N., et al., *O6-benzylguanine potentiates the in vivo toxicity and clastogenicity of temozolomide and BCNU in mouse bone marrow*. *Blood*, 1997. **89**(5): p. 1566-73.
- [22] Wedge, S.R., J.K. Porteous, and E.S. Newlands, *Effect of single and multiple administration of an O6-benzylguanine/temozolomide combination: an evaluation in a human melanoma xenograft model*. *Cancer Chemother Pharmacol*, 1997. **40**(3): p. 266-72.
- [23] Fasman, G.D., *Handbook of biochemistry and molecular biology*. 3d ed. 1975, Cleveland: CRC Press.
- [24] Mendez-Ferrer, S., et al., *Mesenchymal and haematopoietic stem cells form a unique bone marrow niche*. *Nature*, 2010. **466**(7308): p. 829-34.
- [25] *Personal collaboration with the Frenette laboratory*. 2011.
- [26] Maurel, D., et al., *Photoactivatable and photoconvertible fluorescent probes for protein labeling*. *ACS Chem Biol*, 2010. **5**(5): p. 507-16.
- [27] Brun, M.A., et al., *Semisynthetic fluorescent sensor proteins based on self-labeling protein tags*. *J Am Chem Soc*, 2009. **131**(16): p. 5873-84.
- [28] Gronemeyer, T., et al., *Directed evolution of O6-alkylguanine-DNA alkyltransferase for applications in protein labeling*. *Protein Eng Des Sel*, 2006. **19**(7): p. 309-16.
- [29] Sahaf, B., et al., *Lymphocyte surface thiol levels*. *Proc Natl Acad Sci U S A*, 2003. **100**(7): p. 4001-5.
- [30] Stephan, M.T., et al., *Therapeutic cell engineering with surface-conjugated synthetic nanoparticles*. *Nat Med*, 2010. **16**(9): p. 1035-41.
- [31] Lutolf, M.P. and J.A. Hubbell, *Synthesis and physicochemical characterization of end-linked poly(ethylene glycol)-co-peptide hydrogels formed by Michael-type addition*. *Biomacromolecules*, 2003. **4**(3): p. 713-722.
- [32] Gobaa, S., et al., *Artificial niche microarrays for probing single stem cell fate in high throughput*. *Nat Methods*, 2011. **8**(11): p. 949-55.
- [33] Allazetta, S., T.C. Hausherr, and M.P. Lutolf, *Microfluidic synthesis of cell-type-specific artificial extracellular matrix hydrogels*. *Biomacromolecules*, 2013. **14**(4): p. 1122-31.
- [34] Sugiyama, T., et al., *Maintenance of the hematopoietic stem cell pool by CXCL12-CXCR4 chemokine signaling in bone marrow stromal cell niches*. *Immunity*, 2006. **25**(6): p. 977-88.
- [35] Nakamura, Y., et al., *Isolation and characterization of endosteal niche cell populations that regulate hematopoietic stem cells*. *Blood*, 2010. **116**(9): p. 1422-32.
- [36] Ding, L., et al., *Endothelial and perivascular cells maintain haematopoietic stem cells*. *Nature*, 2012. **481**(7382): p. 457-62.

CHAPTER VI

DISCUSSION AND PERSPECTIVES

Our study illustrates the power of bioengineering approaches as means to improve existing cell culture techniques, here in the field of stem cell research, in order to elucidate in depth biological mechanisms that cannot be sufficiently addressed with existing protocols.

To ultimately master stem cell behavior *in vitro*, we need to understand the intrinsic regulation the cell is exposed to inside the living organism: matrices, neighboring cells, biochemical factors, biophysical constraints – altogether comprised in the “niche” concept. We chose the bone marrow niche as a potent model system given its biological importance and immediate clinical relevance to the field of bone marrow and cord blood transplantation, which is currently the only sophisticated stem cell treatment explicitly approved by the FDA for use in the U.S. [1].

But the hematopoietic stem cell niche remains incompletely defined and plagued by questions about the molecular and cellular nature of its constituents in the bone marrow [2]. The role of mesenchymal stem cells (MSCs) as niche cells for hematopoietic stem cells (HSCs) added a new level of complexity to existing bone marrow microenvironment paradigms [3-5]. The field is dealing with a niche cell whose nature, identity, function, mode of isolation and experimental handling remain under fierce debate [6]. Conceptually an MSC is a single cell capable of differentiating along the three mesenchymal lineages to form bone, cartilage or adipose tissue *in vivo* [7]. Due to these characteristics, when transplanted, these cells are capable of organizing the hematopoietic microenvironment to generate an ossicle, a miniature bone marrow organ, which displays functional hematopoiesis [8].

Despite this physiological importance, mainly the differentiation capacities of these cells have been under investigation for translational approaches. Within these studies, the idea has been pursued that MSCs can even be used to regenerate a broad range of extra-skeletal tissues and also non-mesodermal lineages such as hepatic [9] and neural cells [10]. Many of these results can be traced back to the use of unorthodox chemically cued differentiation protocols together with inappropriate culture vessels. The field is ultimately flooded with reports about *in vitro* MSC differentiation capacities that display little to no *in vivo* relevance. Based on studies which demonstrate that mechanical stimuli of the microenvironment alone can trigger early fate decisions in MSCs [11], we aimed at generating *in vitro* screening methodologies to better recapitulate complex signaling found in native niches. Using our customizable cellular microarray platform, we were able to gain insight into how biochemical and biophysical signals converge to drive the adipogenic differentiation

of human mesenchymal stem cells. We mainly observed a dominant effect of substrate stiffness over molecular cues. However we could also identify combinations of biochemical signals that displayed synergistic pro-adipogenic interactions, as illustrated by the example of BMP2 and CCL2 on soft substrates. We strongly believe that combinatorial niche cues identified through such screenings can help to establish relevant *in vitro* differentiation protocols to direct stem cells to mature functional cell types. Nonetheless, the limitations of these screening platforms still restrict the scope of these endeavors. On the one hand, our screening setup relies on relevant and quantifiable readouts which are often lacking and that are sufficient to observe effects above the biological background noise. On the other, this screening platform is most powerful with prior knowledge in hand about what pool of signals to investigate. We are limited by the academic feasibility of large-scale screenings and for relevant high-content analyses such screening platforms need to be implemented in a fully automated fashion.

Despite offering the potential to screen multiple niche factors, such as mechanical cues and biochemical signals in combination, this platform still does not integrate sufficient complexity to truly recapitulate a native niche. While co-culture models of multiple cell types have been implemented on these microwells to add layers of complexity, the dimensionality of the platform is insufficient to model the cell-cell interactions and architectural organization of the *in vivo* microenvironment.

By adopting 3D culture systems established for the generation of *in vitro* organoid cultures, in Chapter 3 of this thesis, a novel high-throughput cell aggregation platform was presented. Importantly, compared to other state-of-the-art aggregation platforms [12], this array, composed of customizable micrometer-scale U-bottom shaped microwells, offers the potential to reproducibly generate large quantities of uniform spheroids at any given size. Additionally, the long-term culture of spheroids is ensured within the same platform through the use of hydrated cell-culture compatible substrates. Allowing their *in situ* manipulation through protein bioconjugation and microfluidic delivery, the platform offers versatility, multidimensionality and the generation of high-resolution information locally and temporally in a three-dimensional context. This level of control will enable the optimization of existing protocols to establish locally autonomous functional *in vitro* tissues, termed organoids. These organoids are envisioned useful for functional screenings *ex vivo* and to generate clinically relevant transplantable tissues. Only few have been described [13-15], hypothetically due to insufficient means to derive them, but they likely represent only the tip of an iceberg of possibilities that lie ahead.

Therefore, in Chapter 4 of this thesis, we have begun to elucidate the potential of forming a three-dimensional bone marrow organoid model *in vitro*. Using co-cultures of bone marrow niche and hematopoietic cells, we aim at understanding and ultimately recapitulating hematopoiesis-supportive processes. The establishment of hematopoiesis through ossicles formed from transplanted three-dimensional *in vitro* cultures of bone marrow niche cells has been impressively demonstrated [8]. These ossicles reproduced the architecture of native bones including a marrow cavity independent of instructive cues by exogenous scaffolds. Nonetheless, establishing a system to elucidate the role of the intrinsic bone marrow microenvironment that is completely free of *in vivo* manipulation is highly desirable to maximize the value of *in vivo* transplantations, to offer relevant *in vitro* screening opportunities and to eventually generate efficient *in vitro* HSC expansion protocols.

We conducted three-dimensional co-cultures of the hematopoiesis-supportive adipo-progenitor cell line OP9 together with HSCs. The 3D culture of mono-cultured OP9 induced a non-chemically cued adipogenic differentiation process within less than 5 days to produce manipulable adipocytic spheres, termed ‘lipospheres’. We believe this fast differentiation process occurs through the structural confinement of the cells, although the underlying mechanisms remain to be elucidated. Nonetheless, these liposphere structures offer the possibility to study adipocytic differentiation in a more manageable way, compared to standard two-dimensional cultures where forming adipocytes usually detach from the substrate, to float in the medium and be washed away during handling steps [16].

The 3D co-culture of OP9 together with primary HSCs was used to investigate the cellular interactions of the bone marrow niche. Importantly, compared to the 3D monocultures of OP9, bone marrow co-cultures lead to the nearly complete inhibition of the previously observed adipocytic differentiation process and an increased production of hematopoietic progenitors compared to conventional 2D cultures. We attribute this observation to interactions between the hematopoietic and the niche-like cells as supported by data investigating adipocytic conversion in the *in vivo* bone marrow microenvironment [17]. It remains to be shown that HSCs within these OP9 pellets self-organize in specific locations, such as the spheroid core. We hypothesize that generating niche cell spheroids of bigger sizes, would allow the generation of relatively hypoxic cores, to which HSCs would preferentially migrate [18]. The U-bottom microwell platform offers the potential to study such reorganization, given that co-cultures can be initiated at different time points, allowing distinct clustering of one cell type before addition of another in order to avoid biased observations of directly seeding multiple cell-types together.

Our work thus may support the future generation of *in vitro* 'bone marroids', functional bone marrow organoids. In order to achieve this goal, these organ-mimicking models need to be generated from primary tissue cells. Accordingly, we implemented an established spheroid culture of human CD105^{pos} CD146^{pos} mesenchymal stem cells that are hypothesized as the hematopoiesis-supportive niche population of the human bone marrow. Propagated as mesenspheres, these cells can be clonally expanded and retain their hematopoiesis-supportive ability. However, co-cultures with cord blood HSCs have demonstrated thus far, that this process is triggered through mainly soluble secreted factors. The underlying reason is that mesenspheres cannot be preserved throughout direct co-cultures, which leads to their attachment and ultimately to a phenotypic heterogeneity, which is associated with loss of HSC-support [19].

Using our U-bottom microwell platform, we were able to clonally derive primary human mesenspheres in high-throughput. Using the microwell separation, fusion of mesenspheres as observed in two-dimensional cultures, can be completely eliminated and medium switches can be performed without loss of morphologies.

Nonetheless, while being able to perform these co-cultures, we completely bypass the fact that the identity of niche cells remains strongly debated [20]. The phenotypic character of these cells remains to be clearly defined and the current technologies in place limit the identification of surface markers of such a rare population of cells that probably even undergo marker changes according to activation state or location.

In Chapter 5, we have therefore begun to investigate to identify putative niche cell candidates alternatively without a definition of marker panels. Using the self-labeling protein-tag SNAP-tag, which has been developed to track proteins in living cells [21], we investigated the potential of using this technology to target native cell-cell interactions. By expressing SNAP-tag fused and expressed universally to cell surface receptors on cellular membranes, we aimed at targeting SNAP through the covalent interaction formed with its substrate benzylguanine (BG). By immobilizing BG on PEG hydrogel surfaces, and then covalently linking SNAP-tag expressing HEK293T cells, we were able to demonstrate that this technology is useful for attaching a given cell expressing SNAP-tag to a given location. The generation of such a universal substrate can be useful for cell-types whose adhesion ligands are unknown [3] or to non-adherent cells that need to be immobilized to a substrate for handling reasons.

The key feature to enabling the same interaction between different cells to generate artificial cell-cell pairing is the immobilizing and availability of sufficient

amounts of either SNAP-tag or its substrate BG on cell membranes. Indeed, we hypothesize, based on our observations, that mainly the concentration of the SNAP-tag substrate was the reason we could not observe artificial cell-cell bonds. The main underlying reason is the solubility issue of this non-polar substrate, making it available only in DMSO solutions, which exhibit cytotoxicity at the high concentrations needed [22].

We validate that high concentrations of the substrate are means to enabling the suggested cell-cell pairing as demonstrated by the covalent aggregation of microbeads carrying SNAP-tag and BG at high concentrations. In conclusion, the biggest bottleneck is the structural composition of the SNAP-tag substrate. We therefore suggest the generation of multi-arm BG linkers with increased aqueous solubility, such as possible through incorporation of backbone PEG chains [23].

Collectively, the approaches described here are broadly applicable to gain deeper understanding of the intrinsic signaling and complexity found within a stem niche. Emerging new platforms that combine this knowledge will help to build powerful *in vitro* models of complex systems such as the human bone marrow. We envision the generation of niche-mimicking functional organoid cultures to enable means to recapitulate what nature has so perfectly constructed. These systems can be applied in various ways to revolutionize the current state of translational medicine. We build technologies in the journey towards personalized medicine, where the sampling and growing of human tissues *ex vivo* becomes a readily available health service.

References

- [1] FDA, *FDA Warns About Stem Cell Claims*. FDA Consumer Health Information, 2012. **January**.
- [2] Morrison, S.J. and D.T. Scadden, *The bone marrow niche for haematopoietic stem cells*. *Nature*, 2014. **505**(7483): p. 327-34.
- [3] Mendez-Ferrer, S., et al., *Mesenchymal and haematopoietic stem cells form a unique bone marrow niche*. *Nature*, 2010. **466**(7308): p. 829-34.
- [4] Nakamura, Y., et al., *Isolation and characterization of endosteal niche cell populations that regulate hematopoietic stem cells*. *Blood*, 2010. **116**(9): p. 1422-32.
- [5] Ding, L., et al., *Endothelial and perivascular cells maintain haematopoietic stem cells*. *Nature*, 2012. **481**(7382): p. 457-62.
- [6] Bianco, P., et al., *The meaning, the sense and the significance: translating the science of mesenchymal stem cells into medicine*. *Nat Med*, 2013. **19**(1): p. 35-42.
- [7] Pittenger, M.F., et al., *Multilineage potential of adult human mesenchymal stem cells*. *Science*, 1999. **284**(5411): p. 143-7.

- [8] Serafini, M., et al., *Establishment of bone marrow and hematopoietic niches in vivo by reversion of chondrocyte differentiation of human bone marrow stromal cells*. Stem Cell Res, 2014. **12**(3): p. 659-72.
- [9] Lee, K.D., et al., *In vitro hepatic differentiation of human mesenchymal stem cells*. Hepatology, 2004. **40**(6): p. 1275-84.
- [10] Woodbury, D., et al., *Adult rat and human bone marrow stromal cells differentiate into neurons*. J Neurosci Res, 2000. **61**(4): p. 364-70.
- [11] Engler, A.J., et al., *Matrix elasticity directs stem cell lineage specification*. Cell, 2006. **126**(4): p. 677-89.
- [12] Ungrin, M.D., et al., *Reproducible, ultra high-throughput formation of multicellular organization from single cell suspension-derived human embryonic stem cell aggregates*. PLoS One, 2008. **3**(2): p. e1565.
- [13] Eiraku, M., et al., *Self-organizing optic-cup morphogenesis in three-dimensional culture*. Nature, 2011. **472**(7341): p. 51-6.
- [14] Lancaster, M.A., et al., *Cerebral organoids model human brain development and microcephaly*. Nature, 2013. **501**(7467): p. 373-9.
- [15] Sato, T., et al., *Single Lgr5 stem cells build crypt-villus structures in vitro without a mesenchymal niche*. Nature, 2009. **459**(7244): p. 262-5.
- [16] Zhang, H.H., et al., *Ceiling culture of mature human adipocytes: use in studies of adipocyte functions*. J Endocrinol, 2000. **164**(2): p. 119-28.
- [17] Naveiras, O., et al., *Bone-marrow adipocytes as negative regulators of the haematopoietic microenvironment*. Nature, 2009. **460**(7252): p. 259-63.
- [18] Suda, T., K. Takubo, and G.L. Semenza, *Metabolic regulation of hematopoietic stem cells in the hypoxic niche*. Cell Stem Cell, 2011. **9**(4): p. 298-310.
- [19] Isern, J., et al., *Self-renewing human bone marrow mesospheres promote hematopoietic stem cell expansion*. Cell Rep, 2013. **3**(5): p. 1714-24.
- [20] Hanoun, M. and P.S. Frenette, *This niche is a maze; an amazing niche*. Cell Stem Cell, 2013. **12**(4): p. 391-2.
- [21] Gronemeyer, T., et al., *Directed evolution of O6-alkylguanine-DNA alkyltransferase for applications in protein labeling*. Protein Eng Des Sel, 2006. **19**(7): p. 309-16.
- [22] Da Violante, G., et al., *Evaluation of the cytotoxicity effect of dimethyl sulfoxide (DMSO) on Caco2/TC7 colon tumor cell cultures*. Biol Pharm Bull, 2002. **25**(12): p. 1600-3.
- [23] Veronese, F.M. and J.M. Harris, *Introduction and overview of peptide and protein pegylation*. Adv Drug Deliv Rev, 2002. **54**(4): p. 453-6.

APPENDIX A

List of proteins

Protein	Type	Mol wt/ kDa	Supplier
Wnt-3a	Human	37.4	R&D
Wnt-5a	Mouse	38	R&D
Dkk-1	Human	25.8	R&D
GDF-8	Mouse	24.8 (homodimer)	R&D
BMP-2	Human	26 (homodimer)	R&D
Dll4	Human	55.6	R&D
Jagged 1	Human	137	R&D
Dlk1 (Pref-1)	Human	32	Enzo Life Sciences
N-Cadherin	Human	89.2 (homodimer)	R&D
Laminin 1	Mouse	900	BD Biosciences
CCL2/MCP-1	Human	8.7	R&D
fibronectin	fragment	21	EPFL, LMRP

Protein combinations

Combi	Protein 1	Protein 2
C01	P1	
C02	P2	
C03	P3	
C04	P4	
C05	P5	
C06	P6	
C07	P7	
C08	P8	
C09	P9	
C10	P10	
C11	P11	
C12	P1	P2
C13	P1	P3
C14	P1	P4
C15	P1	P5
C16	P1	P6
C17	P1	P7
C18	P1	P8
C19	P1	P9
C20	P1	P10
C21	P1	P11
C22	P2	P3
C23	P2	P4
C24	P2	P5
C25	P2	P6
C26	P2	P7
C27	P2	P8
C28	P2	P9
C29	P2	P10
C30	P2	P11
C31	P3	P4
C32	P3	P5
C33	P3	P6
C34	P3	P7
C35	P3	P8
C36	P3	P9
C37	P3	P10
C38	P3	P11
C39	P4	P5
C40	P4	P6
C41	P4	P7

Combi	Protein 1	Protein 2
C42	P4	P8
C43	P4	P9
C44	P4	P10
C45	P4	P11
C46	P5	P6
C47	P5	P7
C48	P5	P8
C49	P5	P9
C50	P5	P10
C51	P5	P11
C52	P6	P7
C53	P6	P8
C54	P6	P9
C55	P6	P10
C56	P6	P11
C57	P7	P8
C58	P7	P9
C59	P7	P10
C60	P7	P11
C61	P8	P9
C62	P8	P10
C63	P8	P11
C64	P9	P10
C65	P9	P11
C66	P10	P11
C67	+ control: Fn	
C68	- control: BSA-Alx488	
C69	- control: BSA-Alx546	
C70	- control: Fc-Alx488	
C71	- control: PBS	
C72	- control: nothing	

Decrypter	
P1	Wnt3a
P2	Wnt5a
P3	DKK-1
P4	BMP2
P5	DLL4
P6	Jagged1
P7	DLK1
P8	N-Cadherin
P9	CCL2
P10	GDF8
P11	Laminin

Protein concentrations (before mixing)

Protein	m in µg	V _{reconst.} in µL	C _{reconst.} in µg/mL	C _{30% glyc.} in µg/mL	V _{30% glyc.} in µL	V _{min.} in µL	V _{array} in µL	C _{array} in µg/mL
Wnt5a	10	25	400	254,0	39,37	55	66,7	150
Wnt3a	10	25	400	253,6	39,42	55	66,7	150
Jagg	50	125	400	280,0	178,57	55	333,3	150
CCL2	10	25	400	262,4	38,11	55	66,7	150
GDF8	10	25	400	269,4	37,11	55	66,7	150
NCad	50	125	400	280,0	178,57	55	333,3	150
BMP2		50	400	269,9	74,10	55	133,3	150
DLL4	50	50	400	261,7	76,42	55	133,3	150
DLK1	10	25	400	280,0	35,71	55	66,7	150
DKK1	10	25	400	260,4	38,40	55	66,7	150
Lam	-	500	1790	1229,3	28,09	55	230,2	150
Fn	-	100	9000	3841,0	234,3	335	375,0	2400

APPENDIX B

CURRICULUM VITAE

SYLKE HOEHNEL

Current address: Avenue de Morges 17, 1004 Lausanne, Switzerland

Phone number: +41(0)78 662 15 04

Email address: sylke.hohnel@epfl.ch

Nationality: German

EDUCATION

2010-2014	PhD, Biotechnology and Bioengineering Ecole Polytechnique Federale de Lausanne (EPFL), Lausanne, Switzerland Laboratory of Stem Cell Bioengineering (Prof. Matthias Lutolf) PhD Thesis: Bioengineering approaches to emulate the stem cell niche
2008-2010	M.Sc, Biotechnology Eidgenössisch Technische Hochschule (ETH), Zürich, Switzerland Master thesis: Novel microengineered platform to assess stem cell fate in vitro Ecole Polytechnique Federale de Lausanne (EPFL), Lausanne, Switzerland
2004-2008	B.Sc, Biotechnology Eidgenössisch Technische Hochschule (ETH), Zürich, Switzerland Department of Chemistry & Applied Biosciences
1999-2004	Abitur, honors science program, Johannes-Kepler-Gymnasium Chemnitz, Germany
1995-1999	German School London (DSL), United Kingdom

ACADEMIC EXPERIENCES

2011	Summer research exchange at the Center for Medical System Innovation (CMSI) University of Tokyo, Japan Laboratory of Bioanalytical Chemistry (Prof. Takashi Funatsu) Internship project: Imaging of endogenous mRNAs in living cells using artificial nucleic acid antisense probes.
2007	International Genetically Engineered Machines (iGEM) competition Massachusetts Institute of Technology (MIT), Boston, United States
2004	Internship Life Science Learning Lab (Dr. Björn Maul) Leibniz Institute for Molecular Pharmacology (FMP), Berlin, Germany
2004	Jugend Forscht, Germany

NON-ACADEMIC EXPERIENCES

2006-2007	Board member of VeBiS (association of biology students), ETH Zürich, Switzerland
2001-2004	Member of the children and youth council (KJB), Chemnitz, Germany

PUBLICATIONS

Gobaa S, Hoehnel S, Roccio M, Negro A, Kobel S, Lutolf MP. Artificial niche microarrays for probing single stem cell fate in high throughput. *Nat Methods*. 2011 Oct 9;8(11):949-55.

Hoehnel S, Gobaa S, Lutolf MP. Substrate stiffness modulates the responsiveness of mesenchymal stem cells to commitment cues. *Integrative Biology*. Manuscript submitted.

Lienemann PS, Metzger S, Sala A, Kiveliö A, Milleret V, Papageorgiou P, Hoehnel S, Roch A, Naveiras O, Weber FE, Weber W, Lutolf MP, Ehrbar M. Biomimetic hydrogels for enhanced homing of endogenous Sca-1+ MPCs to bone fractures. Manuscript in preparation.

